Deutsches Rheuma-Forschungszentrum Berlin

Plasma Cell Homeostasis in the Tpo-retrogenic Mouse Model

von der Fakultät III - Prozesswissenschaften
der Technischen Universität Berlin
zur Erlangung des akademischen Grades
Doktor der Ingenieurwissenschaften
– Dr. Ing. –
genehmigte Dissertation

vorgelegt von
Dipl.-Ing. **Martin Szyska**

Promotionsausschuss:

Vorsitzender: Prof. Dr.-Ing. Vera Meyer
Berichter: Prof. Dr. rer. nat. Rudolf Manz
Berichter: Prof. Dr. rer. nat. Roland Lauster

Tag der wissenschaftlichen Aussprache: 03.06.2011

Berlin 2011

D83

Contents

1. Introduction

The immune system is a highly complex assembly of multiple lymphoid organs. It comprises a great host of different cell types and a dedicated system of vessels called the lymphatic system. Its main function is the protection of the body from the entirety of potentially pathogenic microorganisms, multicellular parasites and toxic substances as well as the clearance of defect and transformed cells that could result in tumors.
The immune system of higher vertebrates is one of the most evolved biological systems, matched in complexity of cell types and their interactions only by the central nervous system of higher mammals. Its flawless function is rooted in a fine-tuned balance. On the one hand, it effectively removes potentially harmful substances and cells from the body. On the other hand, the virtually unlimited number of tissues and cell types that make up a healthy individual are recognized as self and left unharmed.
Continuous evolutionary re-adjustment is required to maintain this balance on all levels of organization, as any deviation will tip the balance of immunity toward either immunodeficiency or autoimmunity. In the latter, the immune system fails to recognize certain host components as self and therefore attacks them, resulting in disease as displayed e.g. by systemic lupus erythematosus (SLE) (62).
The immune system can be broadly subdivided into innate (or unspecific) immunity and adaptive (or specific) immunity, the two of which contribute to the immune system in a predetermined order of events.

1.1 Innate Immunity

At first encounter with a pathogen[1], the mechanisms of innate immunity are initiated.

Steps of innate immunity

First, soluble factors in the serum called complement[2] factors initiate host protection by facilitating phagocytosis of microbes via opsonization and by direct killing via the membrane-attack complex.
Next, tissue-resident macrophages phagocytose encountered pathogens and secrete various cytokines and chemokines to attract monocytes, neutrophils, NK cells and later eosinophils and lymphocytes to the site of infection (40), all of which participate in various ways in host defense. Attracted monocytes differentiate into more macrophages

[1] Starting here, the word pathogen is used for any microorganism, transformed cell or substance, that display antigenic epitopes, recognizable as non-self

[2] The complement system is also called the humoral innate immunity

and dendritic cells that later present foreign antigens to cells of the adaptive immune system.
Both the cellular and the humoral innate immune system utilize pattern recognition receptors (PRRs) such as mannose-binding lectin or Toll-like receptors to register conserved and mostly repetitive patterns displayed by the pathogens called pathogen-associated molecular patterns (PAMPs). Examples are bacterial lipopolysaccharides (LPS) or viral non-methylated CG residues in DNA.
However, complement is also triggered by antibodies specifically binding to pathogen surfaces. Especially at re-encounter with the same pathogen, innate immunity is enhanced by specific antibodies provided by the humoral memory, as described later.

Soluble factors of the innate immune response

At encounter with pathogens, large amounts of cytokines and chemokines including interleucin (IL)-6, IL-1β, tumor necrosis factor (TNF)α and platelet-activating factor (PAF) are released mainly by macrophages, eosinophils and mast cells at the site of infection and cause inflammation. These soluble factors act locally by attracting more immune cells and result in vasodilatation, blood coagulation and massive changes in endothelial cells. At higher concentrations they can act systemically by initiating the acute-phase response.
The acute phase response (17) is triggered by systemic IL-6 and TNFα acting on hepatocytes in the liver (8, 132) and results in the induction of acute-phase proteins such as C-reactive protein, involved in host protection. Also, systemic thrombopoietin (TPO) production by hepatocytes is triggered by inflammatory IL-6 (70) produced at the site of inflammation, which results in re-compensatory platelet production.
The complement system also contributes with soluble mediators to inflammation. The proteolytic cleavage products of C3 and C5 called C3a and C5a are strong chemoattractants for phagocytes and cause their activation.
Usually, innate immunity suffices to clear an infection unnoticed by the host. However, if a permanent focus of infection is manifested by the pathogen, B and T cells are recruited to the site of infection. Dendritic cells that extensively display protein fragments of phagocytosed pathogens migrate to the secondary lymphoid organs to help initiate an adaptive immune response.

1.2 Adaptive Immunity

Adaptive immunity is induced by the innate immune system and provides highly specific and long-lasting protection against pathogens that have evaded phagocytosis and complement. Innate immunity relies on the recognition of conserved molecular pattern, whereas adaptive immunity provides protection against nearly any possible antigen via combinatoric diversity of the respective recognition receptors.

B and T lymphocytes are the cellular players of the adaptive immune response. Both cell types possess virtually unlimited heterogeneity in terms of antigen receptor specificity. Clonal expansion of few antigen-specific B and T cells and their differentiation into potent effector cells is the driving force of adaptive immunity, endowing it with the capacity to clear the body from most pathogens.
Humoral immunity, as part of the adaptive immune system, provides immunity via antibodies that direct a host of powerful effector functions directly to the pathogen. Antibodies are produced solely by terminally differentiated B cells called plasma cells that have lost B lineage commitment.
B and T cells also convey immunological memory allowing for rapid clearance of re-encountered pathogens.

1.2.1 B cell development

B cells express on their surface the B-cell receptor (BCR) which consists of a homodimer of two complexes of one immunoglobulin (Ig) light chain and one heavy chain respectively. The BCR differs from an antibody molecule only in the membrane-bound domain. B cells continuously originate from hematopoietic stem cells in the bone marrow where they mature and exit the bone marrow as naïve B cells.
During B cell maturation, somatic recombination of the immunoglobulin heavy and light chain loci results in a BCR of unique specificity for every developing B cell. The principle of its generation is the combinatoric assembly of two or three different types of gene segments for creating the DNA regions responsible for specificity of the Ig heavy (V, D and J segments) and light chain (V and J segments) (28). Every type of gene segments exists in 5 to 65 versions, the recombination of which results in about 10^{15} possible, highly overlapping specificities for the antigen receptor.
Because of this immensely high numbers of specificities, virtually any possible structure will be recognized by the adaptive immune system.
Nevertheless, not all possible recombined receptors will ultimately be expressed on a naïve B cell. Two distinct mechanisms restrict the diversity of antigen receptors, as will be shortly described here:

Positive Selection After completed recombination, the BCR is displayed on the cell surface (46). During this stage of development, B cells depend on survival signals provided by bone marrow stromal cells. However, these survival signals are only provided to B cells that express a correctly folded BCR. B cells that fail to do so are rapidly cleared from the immune system via apoptosis.

Negative Selection During this early stage of development, immature B cells are confronted with a great diversity of self antigens present in the bone marrow environment. Since somatic recombination generates entirely random specificities, many B cells are activated by their BCR recognizing self antigen. Activation at this stage of B

cell development results in apoptosis and thus all potentially self-reactive B cells that show affinity to self antigens are deleted from the B cell pool.
T cells develop in the thymus and generate specific T-cell receptors (TCRs) by comparable mechanisms.

B cell activation

Naïve B cells are short-lived in circulation and screen the organism for foreign antigens. A few of these cells succeed in entering B cell follicles of secondary lymphoid organs where they survive much longer than their circulating counterparts. Upon encounter with antigens that specifically bind to the BCR, B cells internalize, process and present fragments of that antigen held within an major histocompatibility complex (MHC)II-complex on the cell surface. They also alter their chemokine responsiveness, which causes them to migrate to the T-cell/B-cell interface of secondary lymphatic organs. Here, cognate T helper cells[3] that had previously been activated by antigen-presenting dendritic cells recognize the MHCII-peptide complex and stimulate the B cell to become activated. This stimulation involves both soluble factors such as IL-4 and membrane-bound factors like cluster of differentiation (CD)40 and CD80/86 that are transmitted via an immunological synapse to the corresponding receptors on B cells. In that process, T cells are in turn further activated by the B cells via distinct signaling pathways, which amplifies the immune reaction.

Extrafollicular response

Response to peptide antigens Most of the activated B cells migrate together with cognate T cells to the border of the T cell zone and the splenic red pulp[4] and form a primary focus of rapid clonal expansion. Proliferating B cells differentiate into short-lived plasmablasts that immediately initiate the production of large amounts of low affinity antibodies. This primary focus of plasma blasts rapidly declines after 3 to 7 days due to intrinsic apoptosis (139) and possibly by negative feedback from rising antibody titers via inhibitory Fcγ-receptor (FcγR)IIB (163).

Response to non-peptide antigens Different bacterial antigens can trigger a B cell response without the requirement for T-cell help. In this case, B cells are activated via the BCR in combination either with signals transduced by PRRs such as Toll-like receptors (TLRs) or via cross-linking of BCRs by repetitive structures such as bacterial polysaccharides.
This response incorporates only certain subsets of B cells (38) into a strictly extrafollicular response and results in short-lived plasma blasts of IgM isotype unless additional co-stimulation is provided by activated dendritic cells.

[3] T cells that recognize the same antigen in an MHCII-complex via its TCR that is recognized by a B cell via the BCR are referred to as their cognate T cells

[4] in lymph nodes, lymphocytes travel to the medullary cord

Germinal center reaction

A fraction of B cells is activated by peptide-specific T cells via CD40 and other co-stimulatory signals and enters the B-cell follicle of secondary lymphoid organs to form a secondary focus of rapid proliferation called germinal center (GC) (86,140). Proliferating B cells further modify their Ig heavy and light chains via somatic hypermutation (SHM) and class switch recombination (CSR).

Somatic hypermutation Affinity of BCRs to antigen is randomly changed by point mutations incorporated by SHM. B cells expressing high affinity BCRs are selected for survival by a yet poorly understood competitive mechanism called affinity maturation which involves a T-cell subset called T follicular helper cell (T_{FH}) and follicular dendritic cells (FDCs) (61,167).

Class switch recombination Additionally, B cells change the constant region of the Ig heavy chain by a process called class switch recombination, resulting in BCRs of different isotypes. Isotype switching allows the immune system to fine-tune effector functions depending on the individual pathogenic threat. Whereas IgA antibodies allow interaction of antibodies with mucosal surfaces, different IgG subclasses direct the focus on various aspects of systemic immunity such as complement activation, NK cell killing or neutralization.
After several rounds of cell divisions, a pool of B cells with high affinity for the pathogen emerges from the GC. These B cells bearing high affinity BCRs then further differentiate into plasma cells or memory B cells (27). There are indications that B cell fate is at least partly influenced by BCR affinity with high affinity receptors showing a propensity to cause plasma cell differentiation (14).

Plasma cell development

Plasma cells are terminally differentiated B cells stemming from primary foci or germinal center reactions. What determines whether a B cell takes the route towards plasma cell differentiation remains elusive but once taken, B cells start expressing Blimp-1. This plasma cell-specific transcription factor causes gradual down-regulation of the master transcription factor Pax5 that determines B cell commitment and represses plasma cell-specific gene expression (131).
Once repression by Pax5 is lifted, Xbp-1 and other genes cause dramatic changes in B cells leading to increased size and full dedication to antibody production as seen by greatly enlarged endoplasmic reticulum and the shift from membrane-bound BCR to the soluble form i.e. antibody. Cells in that stage are referred to as plasmablasts. Within the next few days, B cell-specific markers like BCR, CD19 or B220 are slowly down-regulated, cell division is eventually halted and plasmablasts either undergo apoptosis or become plasma cells.

Changes in chemokine responsiveness results in migration of plasma cells into mucosal or inflamed tissues or into the bone marrow via stromal cell-derived factor 1 (SDF-1) (48, 81).

Antibodies and half-life

Mature plasma cells secrete several thousand antibodies per second into the circulation where these fulfill their effector function depending on the isotype.
Antibodies of different isotypes also display varying half-lives as they are recognized by different Fc-receptors (FcRs) on different cell types (106). Consequently, antibody half-life is determined by a combination of affinity to and abundance of the respective FcR as well as by the consequence of that interaction, leading to half-lives ranging from 12 hours to 8 days in mice (156). Whereas most antibody-FcR interactions lead to internalization and proteolytic degradations of the complexes in vesicles, binding exclusively of IgG antibodies to the FcRn on endothelial cells leads to internalization and re-expression of the complex, a process coined as antibody recycling (11). This results in the comparably high serum half-life of IgG compared to IgM antibodies (65).

Termination of the immune response

When an infection is cleared from the body, stimulatory signals and antigen presentation decrease and the germinal center reaction starts to decline. Two additional mechanisms help terminate the germinal center reaction:

- Constant BCR signaling is a constant requirement for germinal center B cells in order to be rescued from apoptosis. High affinity antibodies produced by plasmablasts neutralize free antigen which favors B cell apoptosis.
- The germinal center reaction depends upon the constant provision of co-stimulatory signals by T_{FH} (158). Plasma cells can negatively regulate the germinal GC reaction by actively inhibiting T_{FH} function (116).

Thus, a large number of now redundant lymphocytes undergoes apoptosis and is cleared from the lymphatic organs by tingible body macrophages (137). Only memory B and T cells and long-lived plasma cells persist in order to provide protection against recurring infections (93), as explained below.

1.2.2 Immunological memory

After an immune reaction has subsided, a small number of highly specialized immune cells persist in order to allow the organism to quickly respond to re-encounter with the same pathogen. This is a crucial aspect of humoral immunity and is known as the immunological memory.

Memory B cells

One fraction of B cells exits the GC reaction and resides mainly in the splenic marginal zone as long-lived B cells. They are called memory B cells and are committed to preserving their high affinity BCR specificity for protection against recurring infections with the same pathogen (130, 145). At another re-encounter, memory B cells are activated without the need for further co-stimulatory signals and either differentiate into short-lived plasma cells secreting high affinity antibody (146) or re-initiate a germinal center reaction much more rapidly compared to a primary immune response (104). Although these memory B cells already possess high affinity antigen receptors, Ig heavy and light chain sequences are again subject to affinity maturation, resulting in BCRs of even higher affinity.

Long-lived plasma cells

Plasma cells are specialized in secreting large amounts of antibodies (several 10^4 per second). After clearance of the body from infection, some of them persist as long-lived plasma cells in niches in the bone marrow (88) in order to maintain long-lasting protective antibody titer[5], collectively coined as the humoral memory(see section 1.3). Pathogens that re-enter the host are immediately recognized by these protective antibodies in circulation and various effector mechanisms including complement and phagocytosis are triggered leading to rapid clearance or the initiation of an adaptive immune response.
In autoimmune settings (see below) these long-lived plasma cells can pose a severe challenge to conventional therapeutic approaches that target either proliferating cells or specifically B lineage cells. This therapy resistance is rooted in the fact that long-lived plasma cells are resting and gradually down-regulate B lineage-specific markers whereas most therapies specifically target proliferating cells or B lineage cells via e.g. anti-CD20 biologicals (33).
Unchallenged autoreactive long-lived plasma cells constitutively generate autoantibody titers that cause chronic tissue destruction and potentially re-initiate a full-blown immune response via one of the several antibody effector functions.

1.2.3 Break of tolerance

Normal function of the immune system depends on the strict distinction between self and potentially harmful. This dichotomy is maintained chiefly via depletion of T and B cells with undesired specificities of their corresponding receptors. The immune system is inherently "blind" to the difference between friend and foe as the combinatorically generated antigen receptors of B and T cells have an equal possibility to recognize self antigens or pathogenic epitopes. Additionally, somatic hypermutation of BCRs with

[5]These long-lasting antibody titers had previously been proposed to originate from continuous bystander activation (7) which was refuted later (90).

low affinity for pathogen also has a certain possibility to yield autoreactive B cells. Therefore, several crucial checkpoints are maintained in order to deplete these potentially harmful B and T cell clones. All of these checkpoints rely on a finetuned balance between pro-and anti-apoptotic signals transmitted to developing B or T cells. Disturbance of any of these checkpoints can lead to the eventual emergence of lymphocytes reacting against self antigens often followed by fatal autoimmune pathology.

Tolerance checkpoints

The main checkpoints preventing the generation of autoreactive B cell clones (42) are the following:

- **Negative selection** is the most crucial checkpoint for the depletion of self-reactive cells. In the bone marrow, pre-B cells that have re-arranged both Ig heavy and light chains express their BCR on the cell surface. BCR-signaling above a certain threshold indicates binding to any prevailing self-antigen and leads to immediate apoptosis. Any disturbance in this signaling results either in a limited B cell pool or an increased number of autoreactive B cells entering the circulation.

- In the GC reaction antigen, receptors of activated B cells undergo the process of **affinity maturation** which has been identified as an important tolerance checkpoint (154). A stringent competition between B cell subclones for survival signals provided by FDCs and T_{FH} leads to the depletion of cells with lower affinity to the presented antigen and of polyreactive cells (117). Aberrant regulation of survival signals in this situation can lead to the formation of autoreactive clones, as the contributing B cells are less restricted to increasing their affinity toward pathogenic epitopes. Additionally, low affinity self-reactive B cells can bind to their respective self antigen presented by FDCs and initiate affinity maturation toward that self epitope, resulting in high affinity self-reactive clones. Thus, pre-existing but dormant self-reactivity could be exacerbated, eventually resulting in the outbreak of autoimmune disease.

Autoreactivity

The result of the circulation of self-reactive B cells is mainly the production of antibodies targeting molecules expressed by the host. Host molecules attacked by autoantibodies can be marked for destruction by complement or for phagocytosis by macro-phages and granulocytes. Ultimately, the cells or tissues expressing the self antigen will be damaged or destroyed. Depending on the amount and isotype of produced autoantibody and type of self antigen that is being attacked, one of the many symptoms of autoimmunity will become manifested eventually.

In case of systemic lupus erythematosus (SLE), autoantibodies mainly directed against nuclear proteins and double-stranded deoxyribonucleic acid (DNA) initiate the gradual destruction of renal glomeruli via antibody deposition, which eventually leads to complete renal failure unless treated by potent therapeutics.

1.3 The Bone Marrow

The bone marrow does not only harbor long-lived plasma cells but is also the origin for all blood forming cells and an important organ of the lymphatic system

1.3.1 Structure of the bone marrow

Bone marrow is a densely packed tissue that occupies the medullary cavities of all skeletal bones (Fig. 1.1). Confined by the bone cortex, the bone marrow comprises a dense network of medullary vascular sinuses branching off from the central sinus and terminating as endosteal capillaries.
The border between bone and marrow is called the endosteum and is subject to continuous remodeling facilitated by osteoclasts and osteoblasts that cover this interface. Within vertebrae and the epiphyseal regions of long bones the marrow is increasingly interspersed with sponge-like bone material called cancellous or trabecular bone.
Bone marrow does not display any higher order structure like follicles. However, cells are loosely organized in relation to vascular sinuses, the endosteum and trabecular bone surfaces.

In humans, bone marrow can be subdivided into red marrow and yellow marrow. Whereas the red marrow is actively forming hematopoietic progenitors, the yellow marrow consists mainly of adipocytes. In young individuals, yellow bone marrow is essentially found in central sections of long bones but gradually takes over more marrow space with progression of age.

1.3.2 The cellular composition of the bone marrow

The bone marrow consists of highly heterogeneous cells of different lineages.
The endosteum is lined with osteoblasts of mesenchymal origin and myeloid osteoclasts. Osteoblasts that become trapped in the bone matrix are incorporated into the bone cortex as osteocytes. Quiescent hematopoietic stem cells (HSCs) are found in contact with subsets of osteoblasts (15, 166) and their progeny differentiates directionally towards vascular sinuses. These are composed of bone marrow endothelial cells (BMECs) that control cellular passage between marrow space and blood via tightly regulated expression of adhesion molecules. BMECs are surrounded by adventitial reticular cells. These cells share the same mesenchymal origin and might even be identical with reticular stromal cells which are characterized by their irregular shape with long cellular extensions, extracellular matrix expression and cell cycle arrest. Several subsets have

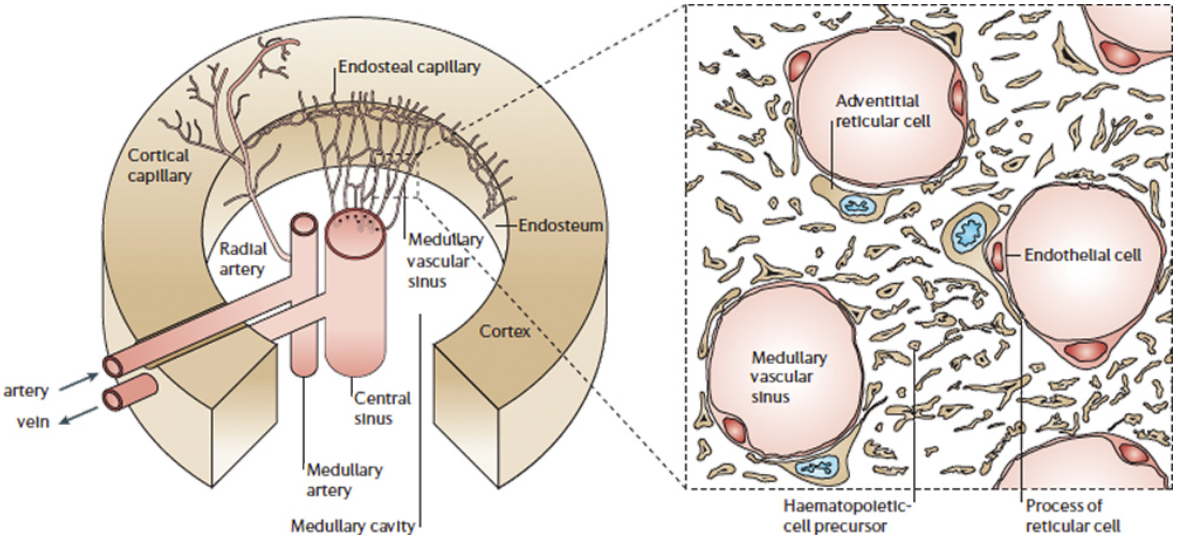

Figure 1.1: *The structure of the bone marrow*
Please see description in the text; figure taken from (102)

been proclaimed (151) according to marker expression although their etiology is still ill-defined. Mesenchymal stromal cells, osteoblasts and adipocytes together with BMECs are collectively referred to as bone marrow stroma.
Finally, the majority of cells in the bone marrow is comprised of hematopoietic cells either developing from their pluripotent progenitors or recirculating from other sources into the bone marrow.

Bone marrow is the major site for hematopoiesis

HSCs originate in the liver and migrate into the bone marrow at an early embryonic stage. Here, a small fraction of these cells remains pluripotent and quiescent in the endosteal HSC niche where they receive survival signals from specialized osteoblasts and possibly other cells such as endosteal vascular endothelial cells (15) . These quiescent HSCs maintain self-renewing capacity via asymmetric cell division that is dependent on and is regulated by cytokines like stem cell factor (SCF) and TPO. Recently, a second perivascular niche for mobilized HSCs was proposed to consist of SDF-1^{+}stromal cells (75, 150, 142), but is still highly debated (74).
After cell division one cell remains quiescent whereas the other starts to rapidly divide and to differentiate into one of the lineage-restricted progenitor cells called common lymphoid progenitor (CLP) and common myeloid progenitor (CMP). All lymphocytes stem from CLPs that later differentiate into either T or B cell progenitors. The CMP gives rise to all other hematopoietic cells including osteoclasts, eosinophils, granulocytes, monocytes, mast cells, megakaryocytes, and erythroblasts.

The bone marrow harbors recirculating cells

T cell progenitors leave the bone marrow at an early stage and to migrate into the thymus where they complete maturation. B cells, on the other hand, continue differentiation in the bone marrow before they enter the circulation as naïve B cells.
Recirculating B cells have been found to re-enter the bone marrow where they are supported by bone marrow dendritic cells in a perivascular niche (127). Furthermore, memory $CD4^+$ T cells have been shown to be maintained in the bone marrow by IL-7–producing mesenchymal stromal cells.

1.3.3 The plasma cell niche

The bone marrow has long been known to be the principal organ harboring the population of long-lived plasma cells and concomitant antibody production (94). Plasma cells generated in a GC reaction migrate into the bone marrow against a chemotactic gradient of SDF-1 via signaling through the cognate receptor CXCR4 (105, 48).
Survival of plasma cells strictly depends on a set of positive signals thought to be collectively provided by the plasma cell niche.

The niche concept

Here, the term niche is used in its ecological sense as a set of parameters necessary for the survival of the plasma cell (58)[6]. The so far undefined niche will be defined by a set of parameters including localization relative to superordinate structures, existence of accessory and competing cells as well as levels of soluble and membrane-bound survival factors, oxygen supply, and antibody levels. In that broader sense, the bone marrow plasma cell niche does not necessarily need to have a fixed position. The general lack of higher order structure would rather allow this set of parameters to prevail at different and changing absolute positions, depending on the flexible cellular composition of the bone marrow in response to the immune status.

Plasma cell survival factors

Plasma cells are intrinsically prone to undergo apoptosis due mainly to these two factors:

- Protein synthesis is an error-prone process leading to the gradual accumulation of misfolded proteins in the endoplasmic reticulum that need to be removed by the ubiquitin-proteasome system. Above a certain threshold of misfolded proteins, endoplasmic reticulum stress is detected by a regulatory network called the unfolded protein response (UPR) that inhibits translation and initiates transcription of chaperone and proteasomic genes (113). If these measures fail to reduce protein load, terminal UPR ultimately leads to apoptosis via the caspase

[6] pdf-version retrievable from here

cascade (77).
Massive antibody production in plasma cells poses a constant challenge for the UPR (35) involving a plethora of plasma cell-specific genes. This results in constant pro-apoptotic signals (115), which is exploited by novel therapeutic approaches using proteasome inhibitors (108, 95).

- One important negative feedback mechanism acts as a sensor for antibody titers via the inhibitory receptor FcγRIIB expressed by plasma cells (163). Excessive signaling through FcγRIIB transduces strong pro-apoptotic signals to plasma cells crucial for limiting the plasma cell niche and for preventing autoimmunity.

These and other pro-apoptotic signals greatly limit plasma cell half-life and can only be counteracted by sufficient anti-apoptotic signals provided by an appropriate survival niche. A number of soluble, matrix and cellular membrane factors have been found to partly provide these signals:

- The major inflammatory cytokine IL-6 has been shown both *in vivo* (141) and in culture (16) to be an important plasma cell survival factor.

- The TNF superfamily members B cell-activating factor belonging to the TNF family (BAFF) and a proliferation-inducing ligand (APRIL) have been found to be of paramount importance for various steps in B cell development.
BAFF was found to be crucial for GC-derived plasmablast differentiation and survival by signaling via transmembrane activator and CAML interactor (TACI) (2, 32). APRIL has been found to be important for the establishment and maintenance of long-lived plasma cells in the bone marrow via signals transduced by B cell maturation antigen (BCMA) (4, 109).
Furthermore, APRIL binds to heparan sulfate proteoglycans including syndecan (CD138) and can facilitate survival via that interaction (59, 50). In the mucosal lamina propria, syndecan highly expressed by plasma cells was shown to locally enrich APRIL that had been produced elsewhere (57) and to promote plasma cell survival. This could hold true also for long-lived plasma cells in the bone marrow.

- SDF-1 is a chemokine produced mainly in the bone marrow. Newly generated plasmablasts and plasma cells migrate against SDF-1 via the receptor CXCR4 (48). Several days after entering the bone marrow, plasma cells lose the capacity to migrate towards SDF-1. The receptor however remains expressed and SDF-1 promotes survival of plasma cells (16).

- TNF-α transduces signals mainly via the receptor TNF-R2 and triggers multiple myeloma (MM) cells to migrate into the bone marrow (64). In plasma cell culture systems, TNF-α was demonstrated to significantly prolong their half-live (16).

- The major plasma cells adhesion molecule is the integrin very late antigen 4 (VLA-4), which is highly expressed by these cells and facilitates adhesion to BMECs and stromal cells via vascular cell adhesion molecule 1 (VCAM-1). The interaction between VLA-4 and the extracellular matrix glycoprotein fibronectin has been shown to be crucial for terminal plasma cell differentiation and Ig production (124), which indicates a general role of VLA-4 signaling for plasma cell maintenance.

- Activation of the glycoprotein CD44 on plasma cells via its extracellular matrix ligand hyaluronic acid has been shown to greatly enhance plasma cell survival promoted by IL-6 (16), suggesting a more complex interplay between various external signals.

- Recently, the C-type lectin transmembrane receptor CD93 was identified as a plasma cell marker and could be shown to be required for plasma cell homeostasis (19).

It is still highly debated how intrinsic differences in plasma cells affect their survival. However, plasma cells that originate from B cells displaying high affinity BCR have been found to have an inherent advantage over low affinity plasma cells for entering the long-lived bone marrow niche (41). In view of the pro-apoptotic UPR in plasma cells (115), it is easily imaginable that competition in the plasma cell niche favors plasma cells with reduced antibody secretion (95).

Candidate cells for the plasma cell niche

Although several survival signals have been identified in the last years, no combination of these signals provides plasma cells with a half-life of more than a few days. Due to the great number of possibly involved genes and factors, the focus was put more on the cellular composition of the plasma cell survival niche.
Once a niche-forming cell were identified, possible survival factors could likely be found by expression analysis of this cell type. Additionally, this niche-forming cell could serve as a target for the depletion of long-lived plasma cells from the bone marrow.
Several bone marrow-resident cells have recently been implicated in the establishment or maintenance of plasma cells. In human cell co-culture systems, osteoclasts have been found to impact plasma cell survival (37) which has not been confirmed in mouse as of yet.
Further human data exist for the transformed plasma cell counterpart MM (95), clearly showing an interaction between MM and osteoclastogenesis ultimately resulting in osteolytic lesions (49). However, MM data has to be interpreted with caution as far as translation into normal plasma cell biology.
In mice, several cell types of different lineages have been associated with plasma cell generation or survival that suggests involvement in plasma cell niche formation.

- For many years, mesenchymal bone marrow cells collectively called stromal cells have been found in cell culture systems to provide survival signals to plasma cells including IL-6 (162). Also, the vast majority of plasma cells has been found in contact with a subset of stromal cells that produce the plasma cell chemoattractant and survival factor SDF-1 (150). Stromal cells also produce fibronectin (21), which allows adhesive interaction with plasma cells via CD44 and possibly promote survival (124).

- Granulocytes prevail in bone marrow in high numbers, are increased during inflammation and provide proliferation and differentiation signals via the production of large quantities of cytokines. Especially basophils (39) and eosinophils (20) have been found to impact plasma cell survival by varying degrees.

- Endothelial cells are the first bone marrow-resident cells encountered by plasma cells on route to their niche. They are highly sensitive to inflammatory signals and produce various cytokines that regulate the immune response. However, their impact on plasma cell homeostasis is proposed to be limited to regulation of their entrance into the medullary space.

- Dendritic cells have been implicated in plasmablast formation and survival in the spleen by secretion of BAFF and APRIL (23, 87). Their role is hence restricted to plasma cell generation.

- Megakaryocytes have been shown to be important for plasma cell homeostasis (161). More about megakaryocyte biology and their putative role in the plasma cell niche can be read in the next section 1.4 starting on page 15.

As more cell types emerge that seem to influence plasma cell survival, it becomes more probable that long-lived plasma cells are supported by a dynamic multicellular niche.

The plasma cell niche is a dynamic multicellular niche

With the advent of systems biology, the parameters of a putative plasma cell survival niche have been subjected to computational analysis. One of the main questions with regard to plasma cells was the apparent discrepancy between a niche of limited space and the preservation of a vast number of different antigen specificities.
This theoretical problem can easily and only be solved when the niche is considered as an open system in which every influx of new specificities is compensated by a similar efflux of minuscule fractions of pre-existing specificities (53). Whether this efflux in reality is accomplished by killing (121) or by mobilization of resident plasma cells (110) has not been fully established yet. Furthermore, the mechanism and responsible cell type has not yet been found.
A further implication of this model is the existence of a more refined, compartmentalized niche with different cell types responsible for one of the following possibly overlapping tasks:

- Entrance of plasma cells into the niche
- Selection of plasma cells for long-term survival by unknown mechanisms
- Maintenance of long-lived plasma cells by the provision of survival signals
- Regulation of plasma cell efflux during inflammation by killing or mobilization of resident plasma cells

The actual cell types fulfilling these proposed tasks might vary in different organs and under different conditions.

Plasma cell niches in other organs

Plasma cells have also been found to reside in other organs under certain conditions. The spleen has been found to harbor a small population of long-lived plasma cells that is thought to be derived from both primary foci and germinal centers and to reside in the splenic red pulp (144). Long-term plasma cell survival has also been detected in synovial GCs of arthritis patients (76) and human plasma cells are generally thought to find proper survival conditions in tertiary lymphoid organs of chronically inflamed tissues.

1.4 The Megakaryocyte

There are strong indications for a participation of megakaryocytes in plasma cell maintenance. They have recently been found co-localized with bone marrow plasma cells and to produce cytokines implicated in plasma cell survival. Furthermore, megakaryocyte frequency in bone marrow is with less than 1% similar to that of plasma cells and they have been demonstrated to produce the plasma cell survival factors IL-6, TNFα in human culture (63, 159). Recently, work performed in our lab has suggested a direct link between megakaryopoiesis and plasma cell homeostasis.

1.4.1 Function of megakaryocytes and platelets

Megakaryocytes are large polyploid cells of the hematopoietic lineage that develop in the bone marrow. Their main function is the production of platelets that are shed off into the blood stream and facilitate blood coagulation and wound healing.
During hemostasis, platelets are activated by von Willebrand factor and collagen released by injured endothelial cells and they bind to these collagen fibrils via adhesion between their membrane-bound glycoproteins including CD61 and collagen. Activated platelets become flat and stellate and release several molecules that tighten the binding between platelets and collagen and help initiate the coagulation cascade. Also, platelets release several chemokines and growth factors including PDGF and MIP-1α upon activation (78) and have been shown to directly trigger adaptive immunity via the expression of CD40L (29).

1.4.2 Megakaryocyte development

Megakaryocyte progenitors develop from HSCs in the bone marrow (Fig. 1.4.2). The major megakaryocyte growth factor TPO (73, 3) acting via the receptor c-Mpl (22) controls both HSC proliferation and differentiation of later stages of megakaryopoiesis. HSCs give rise to CMP that still has potential to differentiate into granulocyte, monocyte, erythrocyte or megakaryocyte. Commitment to the shared erythrocyte megakaryocyte lineage is regulated by transcription factors. Downregulation of PU.1 and upregulation of GATA-1 leads to differentiation into the MK-erythroid progenitor (MEP) (107, 112). CFU-Meg (called megakaryoblasts) are the first progenitors fully

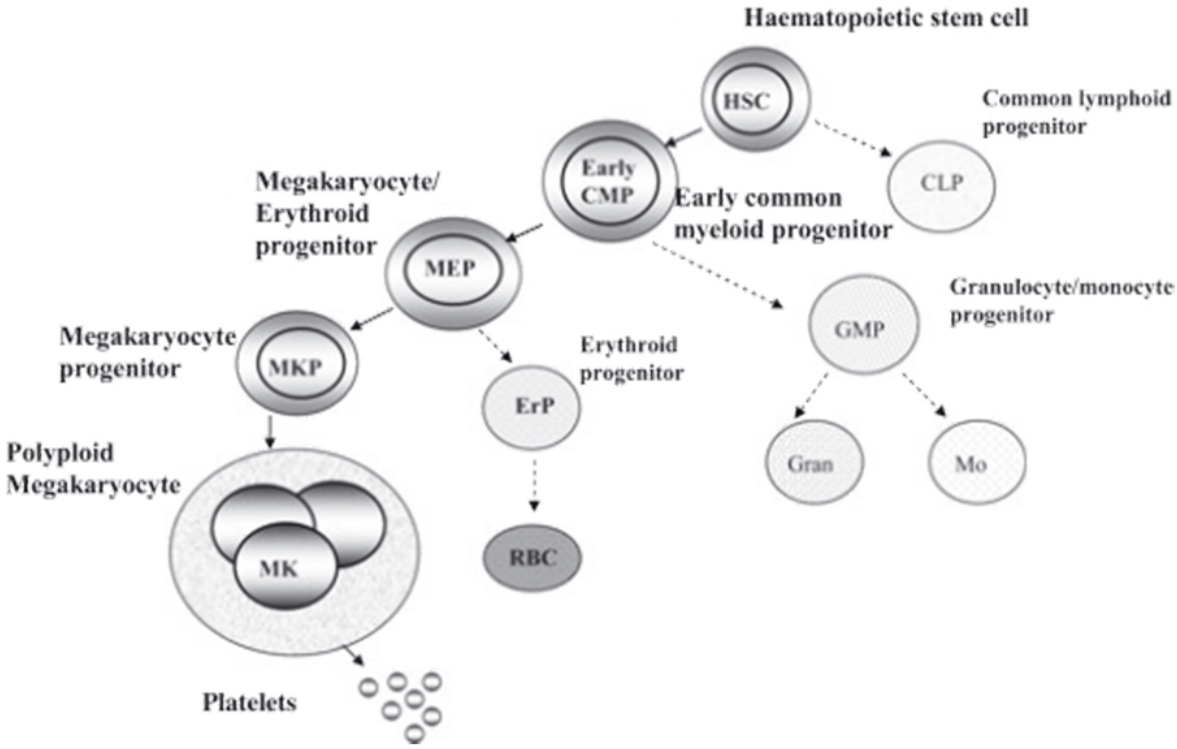

Figure 1.2: *Developmental pathway of megakaryopoiesis* Please see description in the text; figure taken from (26)

committed to megakaryocyte development, but the mechanism of separation from the erythroid lineage has not been elucidated yet. CFU-Meg already express the megakaryocyte marker CD41 and proliferate at stimulation with IL-3 and SCF. In combination with TPO and IL-6, proliferating CFU-Meg fully differentiate into megakaryocytes that arrest cell division and mature into polyploid megakaryocytes via mitosis without cytokinesis called abortive or endomitosis. Chromosomes are further duplicated and soon form large lobulated nuclei with DNA contents of up to 256N. This maturation is accompanied by expression and gradual upregulation of the characteristic surface markers CD9, CD41, and CD61, development of a cytoplasmic demarcation system

later involved in platelet generation and the accumulation of platelet organelles including the respective cytokines within the cytoplasm (112).
The final maturation step of megakaryocytes is the production of pro-platelets and ultimately the disintegration into nuclear bodies without cytoplasm.
Massive cytoplasmic fragmentation and expansion of the internal demarcation membrane results in the evagination of cytoplasmic extensions called proplatelets that protrude into the vasculature via transendothelial migration. In the blood stream, shear forces possibly mediate the shedding of smaller proplatelet units that further separate into platelets in circulation (66).

The level of megakaryocytes and platelets is strictly regulated

The level of megakaryopoiesis is finely attuned with circulatory platelet counts in a way that any drop in peripheral platelets by e.g. blood loss or clotting is rapidly compensated by new production of platelets from mature megakaryocytes. This is achieved by a negative feedback between platelet counts and levels of unbound TPO.
Both megakaryopoiesis and hematopoiesis are dependent on TPO-signals transduced by the TPO-receptor c-Mpl. The main producers of TPO are the liver and the kidney where this cytokine is constitutively produced and secreted into the blood stream. Here, most of the free TPO is taken up and internalized by platelets that highly express c-Mpl. Hence, the level of TPO arriving in the bone marrow is a function of platelet numbers.
By this feedback mechanism, peripheral platelet loss is rapidly registered in the bone marrow as increased TPO concentration. This results in increased progenitor proliferation, megakaryopoiesis and platelet production until equilibrium levels of free TPO and platelets are re-established.

Megakaryocytes, TPO and autoimmunity

In (New Zealand Black x New Zealand White)F1 (NZB/W) mice, a commonly used model for SLE, large numbers of megakaryocyte have been found in the spleen (100). Accordingly, elevated platelet counts have been reported in patients suffering from rheumatoid arthritis and SLE (31), suggesting a link between megakaryocytes and the establishment of autoimmunity. Whether increased megakaryopoiesis/ thrombopoiesis is a result of inflammation e.g. via elevated IL-6 levels or megakaryocytes and platelets indeed facilitated development or maintenance of autoimmunity remains to be elucidated.

1.5 Aim of this Work

The aim of this work was the in-depth analysis of increased megakaryocytes on humoral immunity. The impact on bone marrow and splenic plasma cell populations in response to elevated megakaryocyte numbers was investigated in detail.

1.5.1 Retrogenic mouse model

Increased megakaryopoiesis has previously been described. It was achieved either by injection of the growth factor TPO or by its transgenic overexpression (73, 165). As the injection of TPO only allows for a short-term inflation of the megakaryocyte compartment, a transgenic approach was pursued.
There are several methods available to generate mice transgenic for a certain gene. The most accurate but time consuming method is a gene knock-in, e.g. a targeted gene insertion into a predetermined locus. Additional Cre-specific recombination sites would allow for the specific expression of the inserted gene only by cell types expressing a specific transcription factor. This is facilitated by crossing the mice carrying the transgene containing the recombination sites with a mice expressing Cre-recombinase under the promoter that drives expression of the specific transcription factor.
An easier method is a simple transgenic mouse carrying the transgene in a random position. Special care is needed with this method as the inserted gene has to both be positioned in an open and accessible locus and not to interfere with existing genes and regulatory systems.
The advantage of both methods is the possibility to have mice containing the transgene in all cells and to transfer the transgene to the offspring. On the other hand, both of these methods requires the manipulation of oocytes followed by germ-line transmission of the desired gene, making these approaches very time-consuming.
Viral vectors for gene transfer have the advantage of requiring much less time and know-how compared to transgenic mouse or even a knock-in. Especially retroviruses are suited as gene vectors for stable expression, as they inserts as a provirus into the host genome. Once inserted, strong viral promoters allow for constitutive and high-level transcription of the gene of interest. Bone marrow from donor mice previously injected with 5-fluorouracil (5-FU) is a good source of mobilized hematopoietic stem cells (HSC), that can easily be transduced with retrovirus containing the respective gene of interest.

1.5.2 Microdissection

Megakaryocytes have previously been found to produce several factors associated with plasma cell survival or migration. However, the majority of data so far has been obtained in human cell culture systems from *in vitro* differentiated megakaryocytes derived from CD34. Although strongly hinting at an involvement of megakaryocytes in plasma cell maintenance in the bone marrow, cytokine production under physiological

conditions in the mouse bone marrow would reveal the potential impact of these cells on plasma cell survival. At that time, strong indications for a role of megakaryocytes in plasma cell biology came from preliminary and meanwhile published (161) histological analyzes performed by our lab.
Analyzing the location of antigen-specific plasma cells after secondary immunization with the T-cell dependent antigen ovalbumin (Ova), plasma cells displayed notable co-localization with mature megakaryocytes throughout the course of the entire immune reaction. Ova-specific plasma cells were found co-localized with mainly mature and highly polyploid megakaryocytes even after 130 days. Considering the relatively low frequency of both plasma cells and megakaryocytes (both between 0.1 and 0.5% of total cells), the measured co-localization of around 30% must be considered specific. Further investigating cytokine production of these co-localized megakaryocytes, expression of IL-6 and CD44, both important plasma cell survival factors, was found to be co-localized with cells expressing megakaryocyte markers.
The identification of megakaryocytes as producers of one or more of mentioned factors on the transcription level would give a first hint at their functional role for plasma cells and undermine their proposed importance for the plasma cell survival niche.
To further this investigation, mRNA-expression analysis of putative survival factors via gene expression profiling (GEP) or reverse transcription (RT)-PCR was performed in order to confirm the histological data and to identify additional factors not seen in histology. Isolation of mature megakaryocytes via fluorescence activated cell sorting (FACS) was not feasible, as the high pressure asserted on the sorted cells is very damaging to the very large and fragile polyploid mature megakaryocytes and resulting cells do not show the required purity of at least above 95%. Additionally, any cells obtained from that procedure are highly enriched for the less fragile small immature megakaryocytes. Hence, Laser Capture Microdissection (LCM) was applied in order to specifically isolate large multinucleate megakaryocytes.

2. Materials and Methods

2.1 Generation of TPO-retrogenic Mice

Retroviral transduction has been used for many years as an easy and reliable means of gene transfer (84). In this work, retroviral transduction was used for the manipulation of megakaryopoiesis in spleen and bone marrow in order to investigate the influence of megakaryocytes on plasma cell biology.
In the two-step protocol used (54), the first step was the generation of virus producer cell lines (92) that stably and safely produce high titers of retrovirus particles. By these means, retroviral transduction of murine cells was more reproducible since virus titers were not depending on transient expression in triple-transfected HEK 293 cells. In the first step, virus producer cell lines were generated that secrete high titers of retrovirus particles into the medium that was then utilized for transduction of murine target cells. By repeated transduction of the virus producer cells with the pantropic virus produced in HEK 293 cells, virus titers of the producer cells could be gradually increased (Fig. 3.2B). Selection for high titer clones containing multiple copies of the retroviral genome was greatly facilitated by fluorescence activated cell sorting (FACS), as virus titers correlated with the green fluorescent protein (GFP) expressed by the respective cells (data not shown). Virus producer cell lines retrogenic for thrombopoietin (TPO)(GP-TPO) with the highest GFP expression were sorted and expanded for further use.
In order to generate TPO-retrogenic mice, the following steps were performed:

1. Generation of retroviral expression vector
2. Generation of virus producer cell line
3. Transduction of hematopoietic stem cells of donor mice
4. Transfer of retrogenic stem cells into recipient mice

2.1.1 Generation of retroviral expression vector

Retroviruses present a perfect means for stable gene delivery into target cells. The minimal components for a virus to integrate into a host genome are the viral proteins gag, pol, and env, many of the eukaryotic host cell's biosynthetic molecules like dNTPs, ddNTPs and RNA-polymerase and the viral genome consisting of ss(+)RNA and containing two long terminal repeats (LTRs), a tRNA primer binding site and the

packaging sequence Ψ^+. Normally, gag, pol and env are genes encoded by the viral genome and expressed under the LTR-promoter. In order to prevent the generation of replication-competent retroviruses however, these genes are either coded by separate expression vectors or are stably integrated into the genome of virus producer cells. The viral genome is in turn modified to accommodate one or more target genes to be integrated into the infected cell.
Thus, the first step for retroviral gene transfer is the generation of a retroviral expression vector. Modern retroviral expression vectors contain components from different naturally occurring retroviruses in order to accomplish the desired target cell-specificity, stability and expression level. They are incorporated into a bacterial plasmid in order to allow propagation in E.coli.
Here, an MSCV vector was used that utilizes a modified LTR from the PCC4-cell-passaged myeloproliferative sarcoma virus (PCMV). It is derived from the moloney murine leukemia virus (MMLV) LTR but shows superior transcription activity and reduced transcriptional suppression in hematopoietic stem cells (HSCs). The plasmid backbone contains an E.coli origin of replication and the antibiotic resistance Amp^r. The retroviral sequence consists of the Ψ^+ sequence, a multiple cloning site (MSC) followed by an internal ribosome entry site (IRES) and the coding sequence for enhanced GFP (eGFP), all positioned between two LTRs. The entire sequence was inserted into the host genome upon infection with the virus.
Cloning of the target gene into the MCS allows for stable and bicistronic expression of both the target gene and eGFP under the control of the strong 5'-LTR promoter. Prior to inserting the target gene thrombopoietin (Thpo)[1] into the retroviral expression vector it was necessary to obtain the DNA for the coding sequence of TPO. The size limit for the ss(+)RNA to be packaged into a retrovirus particle is about 10 kb and in order for the packaging to occur with high efficiency the RNA should not be larger than 8 kb. This means that the sequence between 5'-LTR and 3'-LTR should be within this range. Genomic Thpo alone is larger than 10 kb, making it impossible to insert the entire gene into the expression vector along with the the Ψ^+ sequence, the MCS and the eGFP coding sequence.
Therefore, murine Thpo mRNA needed to be isolated, reverse transcribed into cDNA and validated via sequencing before being cloned into the MCS of the expression vector.

RNA-Isolation from murine liver

The liver is known as the primary site for the production of TPO. Therefore, the isolation of Thpo mRNA was performed using murine liver. Total RNA was isolated using the commercial RNeasy Mini-kit (QiaGen) following the kit's instruction. The principle of this RNA-isolation method is the use of a specialized silica-based membrane with selective RNA binding properties. Briefly, about 100mg of liver was homogenized

[1] Please note the difference between notation for the gene Thpo and the protein TPO expressed by the gene!

for 30 seconds using a rotor-stator device (*Ultra Turrox T25*, Janke Kunkel, Germany) and applied to columns provided by the kit. Subsequent steps were:a

1. Loading of RNA onto the column
2. Washing steps (high salt/low salt)
3. DNase treatment with the additional DNase-kit (Qiagen, Germany)
4. Washing steps
5. Elution of the RNA into 500 μl of molbiol-grade water (Invitrogen, Germany)

The DNase-step was included because previous experiments have shown an unsatisfactory contamination of the eluate with genomic DNA which would decrease efficiency of PCR.

2.1.2 Generation of retrovirus producer cell lines

Production of pantropic virus with HEK 293 cells

Pantropic MSCV virions are pseudo-typed with the envelope glycoprotein from the vesicular stomatitis virus (VSV-G) (30). Unlike other viral envelope proteins, VSV-G mediates viral entry through lipid binding and plasma membrane fusion (Emi et al., 1991). Stable expression of the VSV-G envelope protein is toxic; thus, the packaging cell line only contains the viral gag and pol genes. The pantropic virus is produced by transiently triple-transfecting a retroviral expression vector, the gag-pol plasmid, and the pantropic envelop plasmid pCAGGS-VSVg into HEK 293 cells.
All steps involving pantropic virus was performed under S2-conditions.

Transduction of GP+E86 with pantropic retrovirus

For transduction with pantropic retrovirus particles, medium of GP+E86 cells was substituted every 12 hours with supernatant from triple-transfected HEK 293 cells. Supernatant was filtered through 0.45 μm sterile filters (Millipore, Germany) and polybrene ((hexadimethrine bromide; Sigma Aldrich, Germany) was added at a final concentration of 120 μg/ml.

Determination of retrovirus titers using 3T3 cells

For determination of virus titers, the easily transducible 3T3 cell line was used.
Virus producer cells were adjusted to $2{\cdot}10^6$ cells/ml and cultured for 24h in conditioned DMEM (cDM) + 20% fetal calf serum (FCS). 20 hours later, 3T3 cells were adjusted to $1 \cdot 10^4$cells/ml in 500μl cDM + 10% FCS and cultured in 12-well plates. After another 4 hours, supernatant (SN) from GP cells was filtered through 45 μm sterile filters (Millipore, Germany) and diluted according to the following table:

Table 2.1: *Dilutions for 3T3 virus titer determination*

Dilution	**SN**	**cDM** +10% FCS	**Polybrene** (120 μg/ml)	**Factor**
1 : 50	20μl	380 μl	100μl	5000
3 : 50	60μl	340 μl	100μl	1880
1 : 5	200μl	200 μl	100μl	500

The 500 μl of diluted virus SN were added to the 3T3 cells and they were incubated for 40 h for transduction to take place. After that, cells were analyzed via flow cytometry for eGFP expression. Given a 100% transduction efficiency of the retrovirus on 3T3 cells, the obtained eGFP percentage multiplied with the respective factor from Table 2.1 yields the virus titer. For each individual SN, all three dilutions were tested in triplets and the dilution with percentages closest to 50% was used for mean titer calculation.

2.1.3 Generation of retrogenic mice via HSC transfer

Mice were treated according to approved animal experiment proposal **Reg0020/09**. First, donor Balb/c mice were injected with 5-fluorouracil (5-FU) (0.15 mg per g body weight) into donor mice. 5-FU is a potent antimetabolite widely used in chemotherapy. The rapid cell death of lymphocytes caused by the cytotoxicity of 5-FU leads to a mobilization of HSCs because the cell loss has to be re-compensated by newly formed hematopoietic progenitors. This mobilization facilitates transduction of the hematopoietic cell because retroviruses infect dividing cells with much greater efficiency than resting cells.
After two days, mice were sacrificed and whole bone marrow cells containing the mobilized HSC were harvested from bone marrow of femora, tibiae, spine, hip bones and forelegs[2] and cells were cultured for 48 hours in HSC expansion medium[3]. Afterwards, cells were harvested and co-cultured with adherent GP-GFP or GP-kTpo virus producer cells for another two days in HSC-medium.
Meanwhile, recipient mice were irradiated either lethally with 450 rad twice within 4 hours or sub-lethally with one dose of 400 rad. Retrovirally transduced bone marrow cells containing HSC were harvested from the virus producer cells and $\approx 2 \cdot 10^6$ cells were injected *i.v.* into recipient mice (control mice with cells grown on GP-GFP and TPO mice with cells grown on GP-kTpo).
Later, the protocol was modified in order to reduce transduction efficiency, as described in the respective Results section.

[2] Initial experiments showed that cell yield can be more than doubled when bone marrow harvest is extended beyond femur and tibia.

[3] see 2.3.3

Transduction of HSC using RetroNectin

As an alternative to culturing the HSCs directly on GP+E86 cells, HSCs were transduced by culturing with supernatant from GP+E86 cultures. However, because of extremely low transduction efficiencies, RetroNectin (TaKaRa Bio, USA) was used. RetroNectin is a fusion protein of three different fibronectin domains containing binding sites both for mammalian cells via VLA4/VLA5 and for retrovirus particles via heparin-binding domains. This facilitates co-localization of retrovirus particles and target cells.
6-well plates were loaded with 1 ml of RetroNectin in phosphate buffered saline (PBS) (20 μg/ml) and incubated for 2 hours at 37. Next, plates were washed with PBS and HSCs were added together with supernatant from GP+E86 cells.

2.2 Molecular Biology

2.2.1 Reverse transcription

The reverse transcription (RT) was performed with the SuperscriptIII-Kit (Invitrogen) using approximately 50ng of RNA. SuperscriptIII (Invitrogen) is a genetically modified enzyme derived from M-MLV reverse transcriptase with increased thermostability and decreased RNaseH activity. The reaction was performed as follows:

1. Preparation of the pre-mix **on ice!** containing [in μl] :

$(dT)_{20}$ Primer (50 μM)	1.0
dN_6 (50 ng/μl)	3.0
dNTP (25 mM)	0.4
RNA (10 pg - 1μg/μl)	5.0
H_2O	7.7
$\sum$	13.0

2. Incubation at 65 °C for 5 minutes

3. on ice for 1 minute

4. Addition of the enzyme mix containing [in μl]:

First strand buffer[4]	1.0
DTT (0.1 M)	1.0
RNaseOUT ^{TM} (40 U/μl)	1.0
SuperScriptIII^{TM}RT (200 U/μl)	1.0
$\sum$	7.0

[4]250 mM Tris-HCl (pH 7.5), 100 mM NaCl, 0.1 mM ethylenediaminetetraacetic acid (EDTA), 1mM DTT, 0,01%(v/v)
NP-40, 50%(v/) glycerol

5. Gentle mixing by pipetting up and down
6. Incubation at 50 °C[5] for 1 hour
7. Inactivation at 70 °C for 15 minutes

2.2.2 PCR

Primer-design

Primers were designed using Oligo 4.0 software (National Biosciences Inc., USA) which allows analysis of chosen primer combinations for intermolecular as well as intramolecular secondary structures like hairpins. Exclusion factors for primer pairs were:

- Annealing temperature below 55 °C
- Differences in annealing temperatures greater than 2K
- Free enthalpy (δT) of any secondary structure less than -5 kcal/mol
- Any putative secondary structure in the last three 3'-bases
- Less than two (G/C)bases in the last three 3'-bases
- Length of amplicon less than 100 bp

Total primer length was restricted between 10 and 30 bases. Ultimately, NCBI homology search was performed against the murine genome in order to rule out primers with ambiguous annealing potential, which would result in unspecific amplification.
A gradient polymerase chain reaction (PCR) was performed for determination of optimal annealing temperatures and, if necessary, $MgCl_2$ concentrations were adjusted, selecting for the conditions yielding the best compromise between amount of product and minimization of unspecific products like primer dimers.
For cloning purposes, it was necessary to introduce restriction sites into the amplicon 3'- as well as 5' to the actual sequence. This was performed via the use of adapter primers containing the desired restriction site at the 5'-end. An additional 5 bp-sequence of random nucleotides was added 5' to the restriction adapter in order to enable direct restriction of the PCR product, since restriction endonucleases can only cut internal restriction sites with high activity. Besides, a nucleotide overhang protects the primers from the DNA-polymerase's residual 5'-exonuclease activity.
For amplification with adapter primers, nested PCR was performed. In the first PCR, two outer primers annealing to a region surrounding the ultimately amplified sequence were used, effectively enriching the sequence to be amplified by the target (or *inner*) primers in the ensuing run. After gel extraction of the product from the first PCR, the second set of primers is used for amplification of the desired PCR product. Nested

[5] 55 °C were used for gene specific primers

PCR was used for proof-reading PCR with adaption primers, as direct PCR on whole cDNA using adapter primers resulted in suboptimal amplification. The respective outer primers were given the suffix "out".[6]
For validation of the quality of the sample DNA or RNA, a PCR was performed using β-actin-PCR primers. The 41,7 kDa protein β-actin is constitutively and highly expressed as a subunit of the cytosceletal structure in virtually all cell types. As a typical housekeeping gene it is expressed at approximately constant levels, making it suitable for quality control of a PCR.
All Primers used throughout the experiments were ordered from *TibMol-Biol*, Germany and are listed in Tables 2.3 and 2.4.

Analytical PCR

In many cases, a PCR was used entirely for validating the existence of a DNA-fragment. In that case, an analytical end-point PCR was performed using Fast-Start PCR (Roche Applied Science, Germany), consisting of the following steps:

1. Preparation of PCR-Mix: [in μl]

10xPCR-Buffer[7]	2.0
dNTP-Mix (25 mM each)	0.4
Primer Mix (10 mM each)	1.0
HotStart Taq-Polymerase	0.4
H_2O	16.2
$\sum$	**19.5**

2. Addition of 0,5 μl DNA sample (up to 500 ng of plasmid DNA, cDNA, genomic DNA, or a trace of an E.coli-culture)

3. Running of the following PCR-program in a thermocycler:

$95\,^{\circ}C$	1	minute	
$95\,^{\circ}C$	1	minute	$\}\times 35$
$xx\,^{\circ}C$[8]	1	minute	$\}\times 35$
$72\,^{\circ}C$	1	minute	$\}\times 35$
$72\,^{\circ}C$	10	minutes	
$4\,^{\circ}C$	∞		

4. Applying the content of the PCR-reaction directly onto an agarose for gel electrophoresis (2.2.2)

[6] see Primer Table at pages 33 and 34
[7] containing $MgCl_2$ (25 mM)
[8] 55-65°C, depending on the optimal annealing temperature of respective primer according to results from gradient PCR

For semiquantitative analyses, as performed for megakaryocyte expression analysis, 5-fold dilutions of the cDNA sample were used for the amplification which facilitated rough comparison of the expression levels of respective genes.

Proof-reading PCR

Single point mutations introduced during the PCR potentially result in non-functional proteins or even no expression at all if an introduced stop codon leads to premature termination of protein synthesis. Hence, for cloning purposes proof-reading PCR was performed using the Hotstart proofreading *AccuPrime-PCR* kit[9] (Invitrogen, USA), following this scheme:

1. Preparation of the PCR-Mix: [in μl]

PCR-Buffer (10x)	5.0
Enzyme Mix	0.4
Primer Mix (10 mM each)	1.5
H_2O	42.6
$\sum$	49.5

2. Addition of 0,5 μl DNA sample like plasmid DNA, cDNA, genomic DNA

3. Running of the following PCR-program in a conventional thermocycler:

$95\,^{\circ}C$	2	minutes	
$95\,^{\circ}C$	15	seconds	$\times 32$
x[10] $^{\circ}C$	30	seconds	
$68\,^{\circ}C$	90	minute	
$68\,^{\circ}C$	2	minutes	
$4\,^{\circ}C$	∞		

4. Storage in the refrigerator at 4 °C for a maximum of 24 hours or directly applying the content of the PCR-reaction directly onto an agarose gel for subsequent gel purification.

Gel electrophoresis

Agarose gels were prepared using 1,5% agarose in tris-acetate-EDTA (TAE) buffer heated in a microwave (Siemens, Germany) with ethidium bromide (BioRad, USA) in a plastic shaper with appropriate spacer combs (all PeqLab, UK). The gel was run in a gel chamber (PeqLab, UK) connected to an electric charger (Power Pack 300, BioRad) for $\approx$ 45 minutes at 130 V. Gel pictures were captured using an ImageQuant 350 with the accompanying software ImageQuant Capture (all from GE Healthcare, USA)

[9] containing DNA polymerase from Thermococcus *species KOD*

[10] annealing temperature depending on primers used

DNA-purification from agarose gel

Gel Extraction was performed via the *JetSorb* Gel extraction kit (Genomed, Germany)[11] according to the protocol's description.

2.2.3 Cloning procedures

The cloning strategy for the generation of both pMSCV-Thpo and pMSCV-cMpl is described in the respective Results sections (3.1.1 and 3.1.3).

Restriction and ligation

A list of employed restriction enzymes is provided in Table 2.2:

Table 2.2: *Restriction Enzymes used for cloning with recognition sequences*

Restriction Enzyme (Origin)	**Restriction sequence (including cutting sites)**	**supplied from** Company
Bgl II (Bacterium *glaucomycotis*)	5'...A$^{\blacktriangledown}$GATC–T...3' 3'...T–CTAG$_{\blacktriangle}$T...5'	New England BioLabs, Germany
EcoR I (E. *coli*)	5'...G$^{\blacktriangledown}$AATT–C...3' 3'...C–TTAA$_{\blacktriangle}$G...5'	New England BioLabs, Germany
Xho I (E. *coli*)	5'...GAT$^{\blacktriangledown}$ATC...3' 3'...CTA$_{\blacktriangle}$TAG...5'	New England BioLabs, Germany

Restriction was performed following this general scheme:

1. Preparation of the reaction mix on ice containing:
   - PCR-grade water for a final reaction volume of 50 μl
   - 1 μg of plasmid DNA (or DNA purified from a clear band on an agarose gel)
   - 5 μl of restriction buffer (10x)[12]
   - 1 μl of each required restriction enzyme
2. Gentle vortexing the mix after addition of the restriction enzyme
3. Incubation at 50 °C for at least 2 hours

[11] alternatively, the *QiaQuick* Gel Extraction kit (QiaGen, Germany) was used

[12] For the type of buffer used, especially when performing double digestions, please refer to the respective charts in the NEB catalogue

4. Calf intestinal alkaline phosphatase (CIP, New England BioLabs, Germany) was added to the mix after one hour
5. Stopping the reaction via heat inactivation at 65 °C for 20 minutes
6. Applying the mix directly onto an agarose gel for analysis or gel excision following gel electrophoresis

Ligation The reaction of a typical ligation is performed following this scheme:

1. Thawing of aliquoted[13] ligation buffer and re-suspending of any precipitated ATP
2. Preparation of the ligation mix containing:
   - Restricted DNA with optimal molar ratio of 1:1
   - 1 μl T4 DNA Ligase (New England BioLabs, Germany)
   - 2 μl 10× ligation buffer containing ATP
   - PCR-grade water to a final volume of 20 μl
3. Carefully and **very gently** mixing by slowly pipetting up and down
4. Incubation at room temperature for at least 2 hours or at 4 °C for at least 12 hours

The ligation mix can then directly be used for cloning into E.coli (2.2.3).

Preparation of agar plates

The agar plates were created as follows:

1. Add 5 LB-capsules and 3 g Agar *agar* (both from Roth, Germany) to 200 ml bidest water
2. Heat sterilization
3. When cooled down to 55 °C, addition of antibiotics (10 mg kanamycin or 20 mg ampicillin)
4. Spread 5 ml of warm Agar over the inner surface of a plastic petri-dish
5. Let solidify and store upside down at 4 °C

[13] recommended because of the ATP's high susceptibility to repeated freeze-thaw cycles

Chemical transformation

The principle of chemical transformation relies on a special chemical pretreatment of the bacterial culture that destabilizes the cell membrane, making the cells highly susceptible to uptake of foreign DNA compared to non-treated bacteria. They are called to be *competent*. A heat shock for a short time reversibly disrupts the cell membrane, allowing the influx of plasmid DNA into the cells.
Transformation throughout the experiments was performed using the TOP10 chemically competent E.*coli*[14] provided with the PCRII-Blunt-TOPO® cloning-kit (Invitrogen, USA). The transformation of TOP10 E.*coli* was performed adhering to the following scheme:

1. Preparation of the cloning reaction
2. Providing the following items for the ensuing steps:
   - 1 vial of TOP10 chemically competent cells (50 μl) thawed **on ice**
   - Heating block preheated to 42 °C containing water in the required slots
   - LB agar plates containing the appropriate selective antibiotic (two for each transformation) pre-warmed to 37 °C in an incubator
3. Adding of 2 μl of the TOPO reaction or the entire volume (20 μl of the restriction-ligation reaction) to the provided vial of freshly thawed competent cells[15] followed by gently shaking the cells
4. Incubation on ice for 30 minutes
5. Heat-shocking the cells for 30 seconds at 42 °C and immediately returning the vials to ice
6. Adding 250 μl of room temperature SOC-medium
7. Shaking the tubes for 1 hour at 37 °C in an incubator with shaker set to 200 rpm, allowing the genes for antibiotic resistance to become expressed
8. Spreading 10 μl and 50 μl of the cell suspension on two separate selective plates, respectively, using glass pearls
9. Incubation at 37 °C for at least 8 hours[16]

[14] F$^-$ ***mcr***A Δ(***mrr-hsd***RMS-***mcr***BC) Φ80***lac***ZΔM15 Δ***lac***X74 ***rec***A1 ***ara***D139 Δ(***ara-leu***)7697 ***gal***U ***gal***K ***rps***L (Str^R) ***end***A1 ***nup***G

[15] alternatively one vial of cells was split into two separate 25 μl samples

[16] with the plates upside down in order to prevent evaporation and undesired drying out of the plate's surface

Subsequent analysis and selection of positive clones regarding their inserts was performed by picking 5-10 clearly separated colonies and growth in 6 ml LB-Medium containing the appropriate antibiotic.[17] in a shaker incubator at 37 °C over night.
The suspension cultures were then applied to the plasmid purification procedure, as will be described in the next section.

Plasmid preparation

The used spin-column based plasmid preparation relies on the length-dependent precipitation characteristics that differs between plasmids (1-5 kb) and the E.*coli*-genome (4.6 Mb).
In these experiments, the *NucleoSpin*® plasmid preparation kit (Macherey-Nagel, Germany) was used, strictly following the manual's working scheme, which can be broadly separated into three basic steps:

- Cell lysis under alkaline conditions
- Clearing of the lysate
- DNA adsorption onto the column's membrane
- Washing and elution of plasmid DNA

For DNA sequencing, plasmid DNA was further purified using a classic **ethanol precipitation** protocol listed here:

1. Adding 2 μg of plasmid DNA in 90 μl PCR-grade water
2. Adding 10 μl of $CH_3COO^+Na^-$ (3 M, pH 4.6)
3. Adding 250 μl ethanol (100%)
4. Centrifuging at 13000 rpm for 20 minutes
5. Removing the supernatant and resuspending in 500 μl ethanol (70%)
6. Centrifuging at 13000 rpm for another 15 minutes
7. Removing the supernatant and drying the pellet for 15 minutes in a heating block set to 50 °C

Plasmid yield was subsequently validated via a photometer (NanoDrop 2000 from ThermoScientific, USA).

[17] 50 μg/ml LB Medium of Kanamycin for transformation with PCRII-Blunt-TOPO® or 100μg/ml of Ampicillin

DNA-sequencing

For validation of the correct direction and sequence of inserted sequences, plasmids were sent to AGOWA genomics (now LCG Genomics, Germany) for commercial sequencing. Obtained sequences were analyzed with *VectorNTI 9.0 Advance* from Invitrogen, USA.

2.3 Cell Culture

All cell culture was performed under sterile conditions in a laboratory hood (*HERA safe*; Heraeus, Germany). Cells were incubated in tissue culture flasks or plates (all from Greiner bio-one, Germany) at 37°C and 5 % CO_2 in a *Heraeus 6000* incubator (Heraeus, Germany).

2.3.1 Cells for virus production

HEK 293 is a cell line derived from human embryonic kidney (43) that has been used for long as a cell line with low maintenance that can easily be transfected.
Cells were cultured in cDM + 10% FCS to full confluence and passaged every 3 days using Trypsine-EDTA (1x; Fischer, Germany). cDM was prepared with the following:

- DMEM + 2 mM Glutamax (Gibco, UK)
- 1 mM sodium pyruvate (Sigma-Aldrich, Germany)
- 100 mM MEM non-essential amino acids (Sigma-Aldrich, Germany)
- 5 mM HEPES (Sigma-Aldrich, Germany)
- $1.1 \cdot 10^3$ U/ml β-mercaptoethanol (Sigma-Aldrich, Germany)
- 100 U/ml Penicillin (Sigma-Aldrich, Germany)
- 100 mg/ml Streptavidine (Sigma-Aldrich, Germany)

3T3 is a fibroblast cell line derived from mouse embryonic tissue (149). Here they were used for analysis of retrovirus titers[18] because of their ease of transduction.
Cells were cultured in cDM + 10% FCS to 90 % confluence and passaged every 4 to 5 days using Trypsine-EDTA.

[18] see 2.1.2

Table 2.3: *List of primers used for mRNA expression analysis of megakaryocytes* Q+ means that the addition of Q-solution was necessary

Primer	**Sequence**
mApril – 179 bp 58°C Q+	
mApril-fwd	5'-GAAGGACAAGGGAGAAGAG-3'
mApril-rev	5'-AATGTTCCATGCGGAGAAAG-3'
mBaff – 357bp 63°C	
mBaff-fwd	5'-AATAGTGGTGAGGCAAACAGG-3'
mBaff-rev	5'-GGAGGTACAGAGAAGACGAGG-3'
mCD11b – 425bp 60°C	
mCD11b-fwd	5'-TTCAATGACTTCAAGAGAAACCC-3'
mCD11b-rev	5'-TACTTCCTGTCTGCGTGCC-3'
mCD41 –224bp 62°C	
mCD41-fwd	5'-CCGTTTACGCAGAGAGTTTTCGC-3'
mCD41-rev	5'-TGGGTTGCTGTTGTCGTAGGTG-3'
mSDF-1 – 105bp 61°C	
mSDF-1-fwd	5'-GAGCCACATCGCCAGAGCC-3'
mSDF-1-rev	5'-CACACTTGTCTGTTGTTGTTCTTC-3'
mTNFa – 335bp 67°C Q+	
mTNFa-fwd	5'-AATAGTGGTGAGGCAAACAGG-3'
mTNFa-rev	5'-GGAGGTACAGAGAAGACGAGG-3'
mIL6 – 279bp 58°C Q+	
mIL6-fwd	5'-CAAAGAAATGATGGATGCTACC-3'
mIL6-rev	5'-CCTTAGCCACTCCTTCTGTGAC-3'
mβ-actin – 270bp 62°C	
mβ-actin-fwd	5'-CTCAGCTGTGGTGGTGAAGC-3'
mβ-actin-rev	5'-CGTGAAAAGATGACCCAGAT-3'
mHPRT – 249bp 62°C Q+/-	
mHPRT-fwd	5'-GCTGGTGAAAAGGACCTCT-3'
mHPRT-rev	5'-CACAGGACTAGAACACCTGC-3'
mBaff – 357bp 63 °C	
mBaff-fwd	5'-AATAGTGGTGAGGCAAACAGG-3'
mBaff-rev	5'-GGAGGTACAGAGAAGACGAGG'
mBaff – 357bp 63°C	
mBaff-fwd	5'-AATAGTGGTGAGGCAAACAGG-3'
mBaff-rev	5'-GGAGGTACAGAGAAGACGAGG-3'

Table 2.4: *List of primers used for cloning and analysis of TPO- and cMpl-retrovirus vector* The restriction motifs of adapter primers are highlighted and Kozak-sequence is boxed

Primer	**Sequence**
Outer Primers for nested PCR – **mTpo**	
mTpO-out1-fwd	5'-ACCTCTCTCCCACCCGACTCT-3'
mTpO-out2-fwd	5'-CATACAGGGAGCCACTTCAGTTAG-3'
mTpO-out1-rev	5'-TCCAGTGCTGTGTATCCCTTCC-3'
mTpO-out2-rev	5'-GAAAGCAGAACATCTGGAGCAG-3'
Primers for Cloning containing restriction adapters – **mTpo**	
mTpO-k-fwd	5'-GAC-A^GATCT-GCCACC ATGGAGCTGACTGATTTGC-3' (BglII)
mTpO-fwd	5'-GAC-A^GATCC-ATGGAGCTGACTGATTTGC-3' (BglII)
mTpO-rev	5'-GTC-C^TCGAG-CTATGTTTCCTGAGACAAATTCC-3' (XhoI)
Outer Primers for nested PCR – **mcMpl**	
mcMpl-out1-fwd	5'-CAGTGCCGGAGAAGATGCC-3'
mcMpl-out2-fwd	5'-GGAGAAGATGCCCTCTTGG-3'
mcMpl-out1-rev	5'-AGGTAGTGTGTAGGAATGTATAGGTC-3'
mcMpl-out2-rev	5'-TTGAGGATGGATAAGGTAGTGTGTAG-3'
Primers for Cloning (with restriction adapters) – **mcMpl**	
mcMpl-k-fwd	5'-ACA-A^GATCT-GCCACC ATGGCCTCTTGGGCCCT-3' (BglII)
mcMpl-fwd	5'-CCG-A^GATCC-ATGCCCTCTTGGGCCCT-3' (BglII)
mMpl-rev	5'-GGA-C^TCGAG-TCAGGGCTGCTGCCAAT-3' (XhoI)
Inner Primers for PCR-validation of insert **mcMpl**	
mcMpl-in-fwd	5'-CTCCATTTCTGACAGTGAAG-3'
mcMpl-in-rev	5'-AGCCTGGTGGATCCAAAAAG-3'
Primers for Sequencing of pMSCV	
IRES-up	5'-ATGCTCGTCAAGAAGACAGG-3'
MSCV-MSC-5	5'-CGTTCGACCCCGCCTCGATCC-3'

Table 2.5: *Material and Instruments used for Molecular Biology*

Name	**Content**	**Origin**
Photometer *UV 1202*		Shimadzu, Japan)
PCR cycler *Mastercycler personal*		Eppendorf, Germany
Gradient cycler *PTC-200*		MJ Research
Block thermostat TCR-200		Roth, Germany
RNase-free water		Invitrogen, USA
DEPC water	DEPC	Sigma-Aldrich; Germany
PCR-grade Reaction Tubes (0.2/0.5 ml)	Polypropylene, coated	Eppendorf, Germany
Round Bottom Test Tubes (13ml)		Greiner Bio-One, Germany
Plastic Petri Dishes		Greiner Bio-One, Germany
$MgCl_2$	(25 mM)	Merck, Germany
PCR-grade Reaction Tubes (0.2/0.5 ml)	Polypropylene, coated	Eppendorf, Germany
dNTPs	(100 mM)	Biomol, UK
PCR-Buffer (10x)	TrisHCl (670 mM, pH 8.8) $(NH_4)_2SO_4$ (160 mM) Tween20 ($0{,}1\%_{v/v}$)	Sigma-Aldrich, Germany
Taq Polymerase	(5 U/μl)	DRFZ (expressed in E.coli)
RNaseOUT^{TM}	(40 U/μl)	Invitrogen, USA
DNA Molecular Weight Marker	*Gene Ruler*	Fermentas, Germany
Pipet tips	with Filters	Nerbe, Germany
Pipets	Eppendorf *Reference*	Eppendorf, Germany
LB-Medium-capsules	5 capsules in 1 l water	Q-Biogene, USA
SOC-Medium		Invitrogen, USA
Kanamycin	10 mg/ml	Gibco, USA
Ampicillin	10 mg/ml	Gibco, USA
Agarose (Broad Band)		Roth, Germany
50×TAE-Buffer	57.1 ml/l conc. acetic acid 242 g/l Tris 100 ml/l EDTA(0.5 M, pH 8)	Sigma, Germany

GP+E86 cells are derived from the 3T3 cell line that had been transfected with plasmids containing *gag*, *pol* and *env* proviral DNA from Moloney murine leukemia virus (MMLV) (92). When transfected with a plasmid containing the packaging signal Ψ^+, ecotropic retrovirus particles are produced.
Cells were cultured in cDM+20% FCS to 90 % confluence and passaged every 4 to 5 days using Trypsine-EDTA.
After FACS, cells were cultured for one passage with cDM + Gentamycin (50μg/ml; Sigma-Aldrich, Germany) to avoid contamination.
For co-culture with HSCs, $8 \cdot 10^6$ GP+E86 were cultured in 19 ml cDM+20% FCS and cultured for 12 hours before the co-culture.

2.3.2 32D cells – TPO assay

32D is an immortalized myoblast-like cell line derived from interleucin (IL)-3-treated murine bone marrow cell preparations. The subline 32D clone 3 used in these experiments was obtained from ATCC (CRL-11346) and propagated in 32R medium consisting of:

- RPMI (Gibco, UK)
- 10% FCS
- 10mM HEPES
- 1 mM sodium pyruvate
- 4.5 g/L glucose (Sigma-Aldrich, Germany)
- 1.5 g/L sodium bicarbonate (Sigma-Aldrich)

As an IL-3 source, either IL-3 medium supplement (WEHI-3B conditioned medium; from BD Biosciences, USA) or 1ng/ml of recombinant IL-3 (Peprotech, Germany) was used.

Generation of c-Mpl-retrogenic 32D

For generating the c-Mpl-retrogenic TPO-dependent 32D cell line, 32D cells were adjusted to 10^4 cells/ml in 10ml DMEM32 medium containing IL-3 and were cultured for 12 hours. For the following 3 days, medium was exchanged every 12 hours with filtered supernatant from HEK 293 cells triple-transfected with pMSCV-Mpl or pMSCV and the accessory plasmids (see section 3.2) supplemented with IL-3. After the rounds of transduction, 32D cells were kept in culture for an additional two days before GFP^+cells were sorted to high purity and expanded in IL-3-containing medium. We obtained c-Mpl-retrogenic 32D cells called 32D-Mpl and 32D transduced with pMSCV called 32D-GFP. Both cell lines grew well in DMEM32+IL-3, did not proliferate in serum-free medium (SFM) and were GFP^+.

Selection TPO-dependent 32D clones

For selection for TPO-dependent subclones, serum-free media (STEMPRO-34 SFM complete medium; Invitrogen, Germany) + 2 mM glutamin (Sigma-Aldrich, Germany) was used. Recombinant TPO (Peprotech, Germany) was initially used at 100 ng/ml and then gradually reduced to 1 ng/ml for selection of highly sensitive sub-clones.
These TPO-selected 32D-Mpl cells were expanded in SFM+10 ng/ml TPO for further use in the ensuing functional assays.

Detection of functional TPO with 32D-Mpl

For detection of TPO-levels in medium, 32D-Mpl cells were cultured at 1000 cells/200μl in 96-well plates in 90% acSFM + 10% sample medium. As a control, 32D-GFP cells were cultured in same media to account for proliferation attributable to IL-3.
For detection of TPO production by GP+E86 cells, the supernatant of GP+E86 cells was removed from respective cells cultured at a density of $2{\cdot}10^4$/ml in SFM and filtered through a pore size of 20 μm, which retrained both retrovirus and GP+E86 cells. The supernatant was added in serial dilution to 32D-Mpl cells as before. After 4 days of culture along with 32D-Mpl cells cultured on serial dilutions of defined amounts of recombinant TPO, 32D-Mpl cells were harvested and viable cells were counted with flow cytometry.

2.3.3 HSC-culture

Bone marrow cells were cultured at $2 \cdot 10^6$ cells/ml in cDM+20% FCS supplemented with IL-3 (20 ng/ml), IL-6 (50 ng/ml) and stem cell factor (SCF) (50 ng/ml; all Peprotech, Germany) for HSC expansion.
For co-culture with virus-producer cells or growth on virus supernatant, HSCs were harvested as the non-adherent fraction after 48 hours in culture, washed in PBS+0.5% bovine serum albumin (BSA)(=PBS/BSA) and resuspended at $2{\cdot}10^7$ cells/ml in cDM +20% FCS supplemented with 20-fold concentration of cytokines (IL-3, 400 ng/ml; IL-6, 1 μg/ml and SCF, 1 μg/ml) and polybrene (120 μg/ml). Next, 1 ml of HSCs was applied to 19 ml virus producer cells or virus supernatant and cultured for 48 h prior to transfer.

Table 2.6: *Material for Cell Culture*

Equipment		
Name	**Features**	**Origin**
Glass Bottels	0.2/0.5/1.0 l	Schott, Germany
Reaction tube	0.5/1.5/2.0 ml	Eppendorf, Germany
Falcon tubes	15/50 ml	Greiner Bio-One, Austria
Tissue Culture Flasks	50/250/550 ml	Greiner Bio-One, Austria
Cell Culture Multiwell plates	12/24 well	Greiner Bio-One, Austria
Cell Culture MicroPlates	96 well	Greiner Bio-One, Austria
Pipet Tips	10/200/1000 μl	Corning Costar, USA
Plastic Pipets	5/10/20 ml	Corning Costar, USA
Cryo-Tubes	1 ml	Nalge-Nunc, Sweden
Glass Pipets	5/10/25 ml	Schott, Germany
Plastic Syringe *Norm-Ject*	20 ml	Henke-Sass-Wolf, Germany
Buffers and Media		
	Content	
PBS	137 mM NaCl	Roth, Germany
	2.7 mM KCl 8.1 mM Na_2HPO_4 1.5 mM KH_2PO_4 (pH 7.2)	Sigma Aldrich, Germany
PBS/BSA	PBS + 0.5 $\%_{m/v}$ BSA	Biomol, Germany
RPMI 1640	???	Life Technologies, UK
RPMI Plus	RPMI 1640	Life Technologies, UK
	10% FCS 10 mM L-Glutamate 100 U/ml Penicillin 100 μg/ml Streptomycin 20 μM 2-β-mercapto-ethanole	Invitrogen, USA
Aqua dest.		DRFZ

2.4 Flow Cytometry—Analyzing Cell Populations

For flow cytometric analyses, single cell suspensions of spleen, bone marrow and blood were prepared and stained as described below. All data was acquired on LSRII or Canto flow cytometer with FACSDiva software (all BD Biosciences, USA) for most analyses except for platelet counts and 32D assays. The latter two required absolute cell counts which were performed on a MACSQuant (Miltenyi, Germany). Data was analyzed with FlowJo for Mac and PC (Tree Star Inc., USA).

2.4.1 Preparation of single cell suspensions

Blood was collected in reaction tubes coated with heparin (Sigma, Germany) and erythrocyte lysis was performed using *Pharm Lyse* buffer (BD Biosciences, Germany) and incubating for 5 min prior to centrifugation at 300g.
Next, supernatant was discarded and cells were resuspended in PBS/BSA.

Bone marrow Femora and tibie were excised from surrounding tissue and thoroughly cleaned. Next, epiphyses were removed with scissors and the bone marrow was flushed with PBS/BSAusing 5 ml syringes and .45 gauge needles. Obtained bone marrow was filtered through a cell strainer and washed in excess PBS/BSA.
Next, supernatant was discarded and cells were resuspended in PBS/BSA.

Spleen was excised and suspended through a cell strainer and washed twice with excess PBS/BSA. After the first washing step, tissue conglomerates were carefully removed.
Next, supernatant was discarded and cells were resuspended in PBS/BSA.

2.4.2 Staining of cell suspensions

Surface staining Single Cell suspensions were adjusted to 0.5-5$\cdot 10^6$ cells/100μl and nonspecific binding between staining antibodies and Fc-receptors (FcRs) was blocked with antibodies against FcR (1 μg/ml) in PBS/BSA. Next, cells were incubated for 10-15 min with surface antibodies (0.5-2 μg/ml).
For exclusion of dead cells, the samples were incubated with 4',6-diamidino-2-phenylindole (DAPI) 2 min before analysis.

Intracellular staining For intracellular staining after surface staining, cells were fixed and permeabilized using the *Cytofix-Perm* kit from BD Biosciences, Germany according to the manufacturer's description. Briefly, pelleted cells were incubated with *Cytofix-Perm* buffer for 15 min on ice followed by washing and staining with antibodies directed against intracellular markers for 20 min on ice.
DAPI was not used after intracellular staining.

BrdU-staining Occasionally, 5-bromodeoxyuridine (BrdU) was used for discrimination between dividing and resting plasma cells. For that, the BrdU-staining kit (BD Biosciences, Germany) was used which is based on the *Cytofix-Perm* kit from the same company. Briefly, cells were fixed and cell membrane was permeabilized after surface staining as described above. Subsequently, nuclear membranes were permeabilized with *Cytoperm Plus* buffer provided by the kit followed by a quick re-permeabilization of the cell membrane. Next, DNA was degraded by incubation with DNase for 1 hour at 37°C to make BrdU residues accessible. Finally, cells were stained with antibodies against BrdU and further intracellular epitopes.

Ova-specific staining For detection of plasma cells producing antibodies specific for ovalbumin (Ova)-peptide, cells were stained intracellularly with Ova that had been chemically coupled to Alexa700 (Ova-Alexa700).

GC B-cells Germinal center cells were identified via their binding of peanut agglutinin (PNA) (125) in combination with additional markers. The PNA used in these experiments was coupled to biotin (DRFZ, Germany).

2.4.3 Analyzing platelet numbers

Platelets are small cell fragments of 2-3 μm in diameter prevailing in very high numbers in the blood ($0.2-1 \cdot 10^9$/ml)
In order to analyze peripheral platelet counts, 20 μl of blood were diluted in 480 μl PBS+1% EDTA (PBE) and centrifuged for 2 min at room temperature (rt) and 170 g to pellet lymphocytes. Next, 50 μl of the platelet-eniched supernatant were further diluted in 250 μl PBE and stained with α-CD61-PE. Finally, platelets were counted with a MACS*Quant* Analyzer (Miltenyi, Germany) in 96-well format via gating on the distinct population in FSC/SSC and the $CD61^+$fraction.
Prior control experiments with staining for the erythrocyte marker Ter119 showed a clear separation between platelets and erythrocytes both in the light scatter and in CD61 and Ter119 expression (data not shown).

2.4.4 Analyzing megakaryocyte ploidy

Megakaryocytes of different states of maturity can be distinguished via their ploidy, as they perform abortive mitosis and gradually increase their ploidy. The ploidy state can be measured with DNA-intercalating dyes resulting in characteristic peaks of fluorescence intensity that correlate with ploidy[20]. Ploidy states are based on the leftmost TO-PRO-3 peak representing 2n ploidy state. In order to properly detect intranuclear DNA with TO-PRO3 (Invitrogen, UK), cells need to be fixed with ethanol and cellular

[19]Biotin is recognized by streptavidin coupled to fluorochromes
[20]see Fig. 3.14A

Table 2.7: *Antibodies Used for Flow Cytometry*

Epitope	Fluorochrome	**Origin**
B220	Pacific Blue	BD Pharmingen, Germany
	APC-Cy7	BD Biosciences, Germany
	Alexa405	DRFZ, Germany
	Biotin	DRFZ, Germany
IgM	Alexa700	DRFZ, Germany
IgD	Cy5	DRFZ, Germany
	Biotin	DRFZ, Germany
	Pacific Blue	DRFZ, Germany
CD138	PE	BD Biosciences, Germany
MHCII	FITC	DRFZ, Germany
CD4	PE	DRFZ, Germany
	Alexa700	DRFZ, Germany
	Alexa405	DRFZ, Germany
CD8	Cy5	DRFZ, Germany
Gr-1	Alexa405	DRFZ, Germany
	Biotin	DRFZ, Germany
CD11b	Alexa405	DRFZ, Germany
Ter119	PE	BD Biosciences, Germany
PNA	Biotin	DRFZ, Germany
CD61	PE	BD Biosciences, Germany
CD41	Biotin	, Germany
BrdU	APC	BD Biosciences, Germany
Ig κ	Pacific Orange	DRFZ, Germany
	Cy5	DRFZ, Germany
Biotin[19]	PerCP	BD Pharmingen, Germany
	PE	DRFZ, Germany
	PeCy7	DRFZ, Germany

RNA has to be degraded.
The staining method was performed as follows:

1. wash cells in cold PBS
2. wash again in PBS/BSA+2mM EDTA
3. fix cells with ice-cold mix of 80% EtOH and 20% PBS+2mM EDTA
4. wash with *Wash/Perm* buffer (BD Biosciences, Germany)
5. incubate with RNase (50μg/ml in PBS; Sigma-Aldrich, Germany) at 37°C for 30 min

6. wash again with *Wash/Perm* buffer
7. stain with αCD61-PE and TO-PRO3 (2μM) in *Wash/Perm* buffer
8. wash 2x in cold PBS/BSAdirectly prior to analysis

2.4.5 Channels and compensation

The analysis of multicolor flow cytometry data as performed within these experiments required several pre-considerations as far as color compensation was concerned[21]. Extensive pre-testing with different markers, fluorochromes and respective filter com-

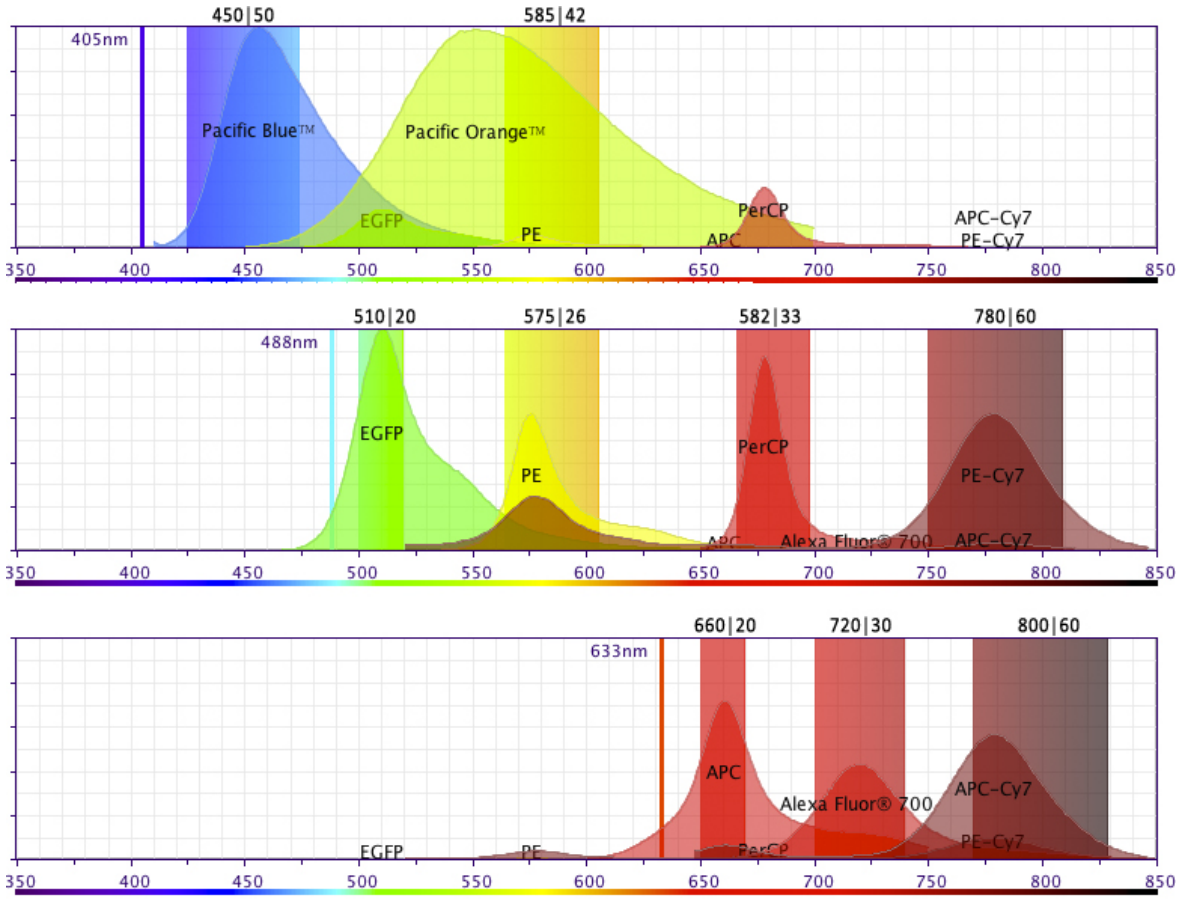

Figure 2.1:
Overview of the Fluorochromes and the Filters used for Flow Cytometry
From top to bottom, the settings for the three lasers (405nm, 488nm and 633nm) used at this LSRII are shown. Emission spectra are shown in each graph for all fluorochromes used. The band-pass filters used for emission with the respective laser are shown as colored bars.

[21] read more about color compensation in (123, 51) and this excellent Flow Cytometry Guide

binations was undertaken for the establishment of the staining panels at the LSRII cytometer.
In Fig. 2.1, the used channels with the respective filter settings are shown. Single staining controls, fluorescence-minus-one (FMO) and isotype controls were used throughout the experiments when applicable and color compensation was performed for all individual experiments using single staining controls.

2.5 ELISA

The general principle of the enzyme-linked immunosorbent assay (ELISA)is fixing the antigen onto a surface previously coated with respective antibodies (coating antibody) followed by detection of the captured antigen with a secondary antibody (detection antibody) specific for the same antigen. Here, the antigen itself was antibody that was captured either by goat antibodies specific for mouse antibody isotype (total immunoglobulin (Ig)M/IgG titers) or by coating with Ova (Sigma-Aldrich, Germany) (Ova-specific titers). For detection, biotinylated isotype-specific antibodies were used (all antibodies from Southern Biotech, USA).
Different ELISA-methods vary in the way the detection step is amplified and converted into a measurable signal. Here, biotinylated detection antibodies were used. This detection signal was amplified with streptavidine coupled to alkaline phospatase (SA-AP) (Roche Applied Science, Germany) and converted via the enzyme and ALP (ALP kit from Roche/Hitachi cobasas, Japan) as a substrate into a yellow product. The amount of signal is measured at an ELISA reader at 405 nm wave length.

Here, the ELISA was performed as follows (per well):

- Coating
    1. Application of 50 μl unlabeled coating antibody well (5 μg/ml in PBS) or with Ova (20 μg/ml) to 96-well flat-bottom high-binding plates (Corning, USA)
    2. Incubation over night at 4 °C
    3. Washing with 250 μl PBS
- Blocking:
    1. Application of 100 μl PBS+3% BSA
    2. Incubation for 1 hour at 37 °C
    3. Washing with 250μl PBS/BSA
- Serum samples were diluted to 1:5000 in PBS/BSAfor total titers and to 1:200 for Ova-specific titers

- Incubation with serum (3-fold dilution series):
    1. Application of 50 μ PBS/BSAto all wells except for the top row of the 96-well plate
    2. Application of 75 μ diluted samples and standard in duplicates into the first row
    3. Transferring of 25 μl from the wells in the row containing the diluted serum samples to the row below using a multichannel pipet (Eppendorf, Germany)
    4. Continuing dilution by transferring 25 μl from each row to the one below
    5. Discarding 25 μl from the last row
    6. Incubation at 4 °C over night or for 1 hour at rt
    7. Washing 3× with PBS
- Labeling with detection antibody:
    1. Incubation with 50 μl of biotin-coupled detection antibodies (2 μg/ml in PBS/BSA) at 4 °C over night or for 1 hour at rt
    2. Excessive washing under running bidest water
- Development
    1. Incubation with 50 μl of SA-AP (0.3 U/μl in PBS/BSA) at rt for 20 min
    2. Careful and repeated washing under running bidest water
    3. Addition of 4.1 ml buffer ALP1 to 935 μl ALP2 per plate
    4. Immediate incubation of wells with 50 μl at rt
    5. Development for 20-120 min
    6. Measurement of optical density (OD) in a 96-well photometric detector at the wavelength of 405 nm.

Samples were applied in duplicates and blank-subtracted OD-values were used for calculation of concentrations. For 4-parameter curve fitting and as a global reference commercial Ig-standard (Bethyl Laboratories, Inc., USA) or pooled serum samples were used for total and Ova-specific antibodies, respectively. Data was analyzed with Softmax (Molecular Devices, USA) and EXCEL (Microsoft, USA).

2.6 ELISPOT

The enzyme-linked immunosorbent spot (ELISPOT) is a method closely related to ELISA with one important difference. Cells are immobilized onto a cellulose membrane allowing for detection of locally limited secretion of antigens associated with individual cells. Here, plasma cells immobilized on MultiScreen$_{\text{HTS}}$ IP-96well-plates (Millipore, Germany) were detected via their secretion of antibodies.
Coating and detection reagents and concentrations were similar to the ones used for ELISA (2.5). As a development substrate, BCIP/NBT (GeneTex Inc., USA) was used. ELISPOT was performed as follows:

- Coating
  1. Pre-wet each well with 15 μl EtOH (35 % in PBS) for 1 min
  2. Rinse wells 3x with 150 μl PBS to dilute EtOH
  3. Coat wells with 50 μl unlabeled coating antibody (5 μg/ml in PBS) or Ova (20 μg/ml)
  4. Incubation over night at 4 °C
  5. Wash 2x with 150 μl PBS
- Blocking:
  1. Block membrane with 200 μl medium (RPMI+10% FCS) for 2 hour at 37 °C
  2. Washing with 250μl PBS/BSA
- Preparation of cell suspension
  1. Obtain single cell suspension from spleen or bone marrow (2.4.1)
  2. Adjust cells to approx. $3 \cdot 10^6$/ml
  3. Wash in large volume of cold medium to minimize background by antibodies secreted into the medium
  4. Resuspend cells in 100 μl medium per well
- Incubation with cells
  1. Pre-fill all wells except for the bottom row with 200 μl medium and 100 μl to the bottom row
  2. Apply 100 μl of cell suspensions in duplicates into the first row of the plate
  3. Transfer 100 μl from the wells in the row containing the cells to the row below using a multichannel pipet (Eppendorf, Germany)
  4. Continue dilution by transferring 100 μl from each row to the one below
  5. Discard no cells from last row!

6. Incubate for 2 hours at 37 °C and 5% CO_2 in an incubator
7. Decant cells and wash 4x intensely with PBS+0.1% Tween-20 (Carl Roth, Germany)

- Labeling with detection antibody

1. Incubation with 100 μl of biotin-coupled detection antibodies (2 μg/ml in PBS/BSA+Tween-20) at 4 °C over night
2. Wash plates 3x under running bidest water

- Development

1. Incubate with 50 μl of SA-AP (0.3 U/μl in PBS/BSA) at rt for 20-30 min
2. Wash plates 3x under running bidest water
3. Apply 25 μl of BCIP/NBT to wells and incubate at rt for 5-10 min until faint spots become visible
4. Stop the reaction by pulling off plastic cover from plate and rinsing with running water from both sides
5. Let dry for at least 4 hours at 37 °C or over night at rt
6. Acquire well images at ELISPOT reader (ImmunoSpot S5; Cellular Technology Ltd., USA)

Spots were analyzed on a PC with ImmunoQuant Analysis Software (Cellular Technology Ltd. USA) and spot numbers were calculated back to total organ antibody secreting cell (ASC) numbers.

2.7 Histology

2.7.1 Freezing of organs

Freezing of lymphoid organs

For histological analyses, two different methods were used depending on the organ to be analyzed. For spleen and lymph node, respective organs were isolated from mice, cleaned and, if needed, sectioned into appropriately sized pieces and placed into cryomolds containing O.C.T. freezing medium. Initial experiments have shown that integrity of tissues was optimal when freezing was performed as slow as possible.
Therefore, a plastic beaker filled with hexane was placed into a slurry of dry ice mixed with acetone. After 5 min, tissues were slowly dipped into the isopentane until O.C.T. had become white. Subsequently, tissues were frozen and stored in −20°C or −80°C or immediately sectioned.

Fixation and freezing of bone marrow

In order for the delicate and fragile cellular structure of the bone marrow to remain intact, the bone marrow has to be fixed with a mild fixing agent and the water content needs to be minimized, as ice crystals generated during the freezing procedure would destroy the three-dimensional cellular structure of bone marrow. Also, decalcification was foregone, as this procedure can be harmful to structures and hardened blades were used. Hence, a special freezing protocol was adapted using **fresh**, methanol-free paraformaldehyde (PFA) as fixing agent and sucrose for water removal, as follows:

- Bone marrow was cut from mice, femur and tibia were carefully disconnected and attached tissue removed with a paper cloth.
- Whole bone was fixed with 4% PFA in phosphate buffered saline (PBS) for 4 hours on a shaker at 4°C
- Fixing agent was removed, bones are cleaned with PBS and placed on 10% sucrose in PBS for 8 hours on a shaker at 4°C
- Bones are incubated in 20% sucrose in PBS for 8 hours on a shaker at 4°C
- Bones are incubated in 30% sucrose in PBS for 8 hours on a shaker at 4°C

Subsequently, bones were dried with a paper cloth and placed in an embedding container filled with embedding medium and the tissue was slowly frozen as described for lymphoid organs. Frozen bones were wrapped in saran wrap and aluminum foil to prevent the embedding medium from drying and to ensure constant temperature.

2.7.2 Sectioning of organs

Sectioning of spleen

Frozen spleens were sectioned at −20°C in a microtome using standard blades. Sections of 7-9 μm thickness were flattened onto the microtome's work area using precision brushes and attached to a glass microscope slide pre-cooled to −20°C by gently warming the glass slide on the flip side of the tissue section. All sections from lymphoid organs were fixed with acetone prior to storing or staining. The microscope slides were dried at rt for 20 min before being placed on acetone at −20°C for 5 min. Next, slides were completely dried for at least an hour before being either stored at −20°C or −80°C or directly stained (2.7.3).

Sectioning of bone marrow

The structure of fixed bone marrow is preserved well when the above protocol was performed. However, thin bone marrow sections have the tendency to be brittle, because,

unlike most organs, bone marrow lacks collagenous fibers for stability. Therefore, sectioning was performed using special adhesive tape. An appropriately sized piece of this tape was placed onto the section to be cut and thoroughly adhered using a fitting tool. Next, the tissue was cut and the tape containing the section was released from the tissue in the process. Then, the tape was placed on a microscope slide, tissue facing away from the glass, and fixed via conventional adhesive tape to the slide. Bone marrow samples were kept at −20°C or at −80°C for longer storage in a dry container.

Table 2.8: *Material and Instruments used for Histology*

Name	**Origin**
Microtome *Microm HM560*	ThermoScientific, Germany
Microtome Blades *Edge-Rite*	Richard-Allen Scientific, USA
Confocal Microscope *DM IRE2*	Leica, Germany
Confocal Microscope *FV 1100*	Olympus, Japan
Transmission Microscope *M021*	Olympus, Japan
O.C.T. Compound*Tissue-Tek*	Sakura Finetek, Netherlands
Precision (acrylic) Brushes *artisti*	Boesner, Germany
Microscope Slides *Superfrost Ultra Plus*	Menzel Gläser, Germany
Cover Slip (24 x 60/25x25 mm	Menzel Gläser, Germany
Cryomold, different sizes	Sakura Finetek, Japan
Fluoromount-G	Southern Biotech, USA
Wax pen emphDako pen	Dako, Denmark
Paraformaldehyde, methanol-free (16% in ampoules)	Electron Microscopy Sciences, USA
Acetone	Sigma-Aldrich, Germany
Cryofilm (adhesive tape)	Section Lab, Japan
Sectioning Set (Cryofilm fitting tool, wooden stage, strainer, embedding container)	Section Lab, Japan
SCEM embedding medium (containing 4% carboxymethylcellulose)	Section Lab, Japan
Sucrose, biograde	Sigma-Aldrich, Germany

2.7.3 Staining of tissue sections

All staining steps were performed with antibodies diluted in PBS/BSA(PBS containing 5% bovine serum albumin (BSA)) unless indicated otherwise. First, tissue sections were rehydrated by carefully flushing the slides twice with PBS/EDTA (PBS containing 2mM ethylenediaminetetraacetic acid (EDTA)). The embedding medium surrounding the section was mostly removed during this procedure. Next, the staining area was circumscribed using a Dako pen and the wax was allowed to dry for 30 min. After that, sections were blocked with Fc-Block ($F_C\gamma R$) for 15 min and afterwards washed with PBS/BSA. Next, sections were incubated with the antibody solution for 10 - 20 min

at rt or at 4°C over night prior to another washing step. Depending on the antibodies used, sections could be incubated next with secondary antibodies or streptavidine-coupled fluorochromes followed by another washing step. Finally after removal of excess PBS/BSA, a few drops of mounting medium were applied to the slides, cover slips were placed on the sections and all air bubbles were removed between slide and cover slip. After drying of the microscope slides over night in the dark, they were ready for microscopy.

Table 2.9: *Antibodies used for Immunohistochemistry*

Antigen – Fluorochrome	**Dilution for Usage**	**Origin**
Fc-Block ($F_C\gamma$-R)	1:250	DRFZ, Germany
Streptavidine – Alexa546	1:250	BD Pharmingen, Germany
B220-FITC	1:50	BD Pharmingen, Germany
CD138-PE	1:100	BD Pharmingen, Germany
CD41-Bio	1:250	Southern Biotech, USA
CD61-FITC	1:100	BD Pharmingen, Germany
Biotin-PerCP[22]	1:200	BD Pharmingen, Germany

2.8 Laser Capture Microdissection

Laser capture microdissection (LCM) is a relatively young and easy method developed for the isolation of specific fragments or even individual cells of histological sections. The method employs a low-power infrared laser to activate a special hyperthermoplastic membrane placed immediately over the desired cell or tissue. The instantly liquified transfer film forms a depression in the membrane plain and adheres to the cells that are located within the laser beam diameter. The laser focus is directed to the membrane and thus does not compromise the quality of proteins or nucleic acids or structure within the sample. In the ArcturusXT Microdissection Instrument (Instrument and all accessory equipment and kits from MDS Analytical Devices, USA) used for these experiments, specially designed *CapSure HS* laser capture microdissection (LCM) Caps that are coated with the thermoplastic film are guided via the instrument and the associated software onto the region of interest. The instrument focusses a laser pulse onto the membrane to liquify the film towards the selected cells. Optimally, the cells adhere to the cap surface when it is lifted from the tissue section while the surrounding tissue remains intact on the slide. The captured material can be examined, and the cap can then be placed directly into a microcentrifuge tube for extracting DNA, RNA or protein. The material adherent to the cap's membrane was then extracted into a reaction tube using the manufacturer's *PicoPure* RNA Isolation kit for ensuing RNA expression analysis, as described in section 2.8.4 on page 51.

Precautions for RNA preparations

Throughout all steps of LCM special care was taken in order to minimize RNA degradation and contamination with DNA. RNA is rapidly degraded by both intracellular endo- and exonucleases and by the abundance of RNases from skin and mucosa. Degradation by intracellular RNases can be minimized by quickly freezing samples after preparation and keeping the samples at $-20°C$ or on ice at all times. For minimizing the impact of exogenous RNase and contamination with DNA, gloves were worn at all times and workspaces were regularly cleaned with RNase AWAY (Invitrogen Life Technologies, Germany). During tissue sectioning, the work area and the blades of the microtome were regularly cleaned with 100% ethanol. Components of RT and RT-PCR kits were aliquoted to small volumes and upon suspected contamination, every component was exchanged by a new one. Additionally, all RNA work and PCR setup was performed in the Ultraviolet Sterilizing PCR Workstation (Peqlab Biotechnologie GmbH). The used water and the buffers used were either DEPC-treated

2.8.1 Preparation of sections for LCM

For obtaining bone marrow tissue sections for LCM, mice were sacrificed and tibie were isolated from the mice. The bones were cleaned with tissue cloth (Kimwipe, Kimberley Clark, USA) and both the tibial plateau (*caput tibiae*) and the ankle were excised to reveal the bone marrow. Carefully, the intact bone marrow was flushed out with a 0.45 gauge syringe and transferred onto a cryomold containing mildly prefrozen O.C.T. using a blunted syringe tip. The tissue was then completely covered with O.C.T. and subjected to slow freezing as described in 2.7.1. Subsequently, tissues were cut into 8μm sections in a microtome (Microm HM560, ThermoScientific, Germany) set to $-20°C$ and fixed to the microscope slide (2.7.2). The microscope slides were then placed on dry ice until commencing of the fixing/staining procedure.

2.8.2 Fixing and staining of sections for LCM

Tissues used in LCM need to be devoid of residual water in order for the dissected tissue to optimally adhere to the thermoplastic membrane. Hence, a special *HistoGene* LCM Immunofluorescence Staining Kit was used, as briefly described here:

- Sections were removed from dry ice and condensate dried off for 1 min
- Sections were placed in acetone precooled to $4°C$ for 2 min
- Sections were placed on a $4°C$ ice block and dried for 1 min
- Sections were incubated with staining solution provided with the kit for 2 min
- Sections were drained with a paper and incubated with antibody solution for 3 min

- Sections were drained and rinsed with 200 μl staining solution
- Sections were drained with a paper towel and subjected to dehydration steps
- Sections were placed in 70% ethanol for 30 sec
- Sections were placed in 95% ethanol for another 30 sec
- Sections were placed in freshly prepared (absolutely H_2O-free) 100% ethanol for another 30 sec
- Sections were placed in xylol for 5 min and subsequently dried in a fume hood for 5 min

LCM was performed immediately after the dehydration protocol, in order to minimize rehydration and RNA degredation.

2.8.3 LCM – procedure

As seen in Fig. 2.2, megakaryocytes were easily identified via a combination of morphological information obtained from the transmission view and immunofluorescent staining against the megakaryocyte marker CD61 with a FITC-coupled antibody (BD Pharmingen, Germany). Thus identified megakaryocytes were selected for the laser capture run and the cap was placed above desired stretch of tissue. After the intensity and pulse length of the laser was adjusted to result in optimally shaped membrane indentions, cells were captured onto a cap. If possible, one cap was used for several rounds of capturing by placing the cap's free areas on consecutive tissue stretches.
When sufficient numbers of megakaryocytes were captured on the membrane, the cap was moved by the instrument into the quality control position for acquisition of several microscopic pictures of the picked material. The finalized caps were immediately removed from the LCM device and RNA extraction was performed, as described in the following section. Due to the process being very time-consuming, the assessment of these pictures for occurrence of contaminating cell material was performed after RNA extraction and prior to RNA expression analysis. In addition to capturing megakaryocytes, areas of the tissue devoid of megakaryocytes were also captured onto respective caps, in order to obtain negative control samples.

2.8.4 Isolation of RNA from microdissected megakaryocytes

Extraction of megakaryocytes and purification of RNA was performed using the PicoPure RNA isolation kit from lifeTechnologies (former Arcturus).

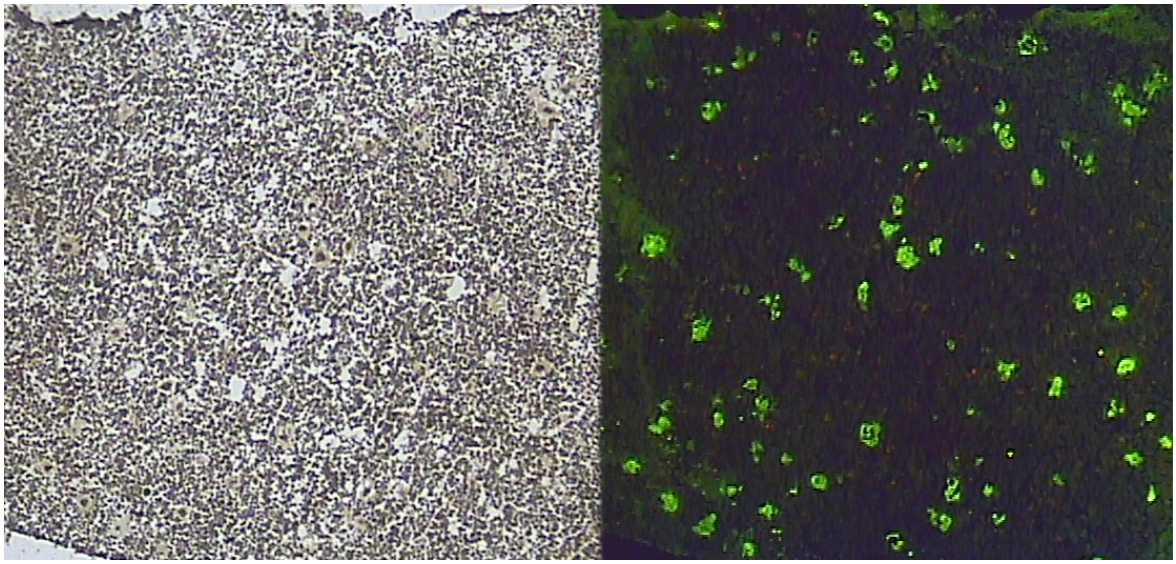

Figure 2.2: *Identification of megakaryocytes during LCM*
Left The dehydrated tissue section of a murine femur shows a densely packed cellular structure with rare larger cells evenly distributed throughout the marrow.
Right Staining with FITC-coupled antibodies against CD61 clearly identifies most of the large cells as megakaryocytes and greatly facilitates LCM procedure.

Extraction and isolation of megakaryocytes from LCM caps

Briefly, CapSure HS LMC Caps were placed on an alignment tray and 10 μl extraction buffer were applied into the buffer well of the cap. In later attempts, 0.5 μl of yeast rRNA (500 ng/μl) were added to the extraction buffer to protect isolated RNA. An 0.5 ml reaction tube was placed on the cap and the reaction was incubated at 42°C for 30 min. Afterwards, extracted material was spun into the reaction tube and collected material was stored for further use at −80°C.

RNA isolation

RNA isolation was performed as described in the kit's manual using a spin column. No DNase treatment was performed because of its background RNA-exonuclease activity. RNA was eluted in 15 μl elution buffer and subjected to quality assessment.

Validation of RNA

RNA quality after the procedure was measured with the Bioanalyser instrument (*Agilent 2100*, Agilent Technologies, Germany). RNA preparation are separated via gel chromatography according to size and amount of degradation are analyzed via the height and separation of the peaks of 18S– and the 28S–rRNA.

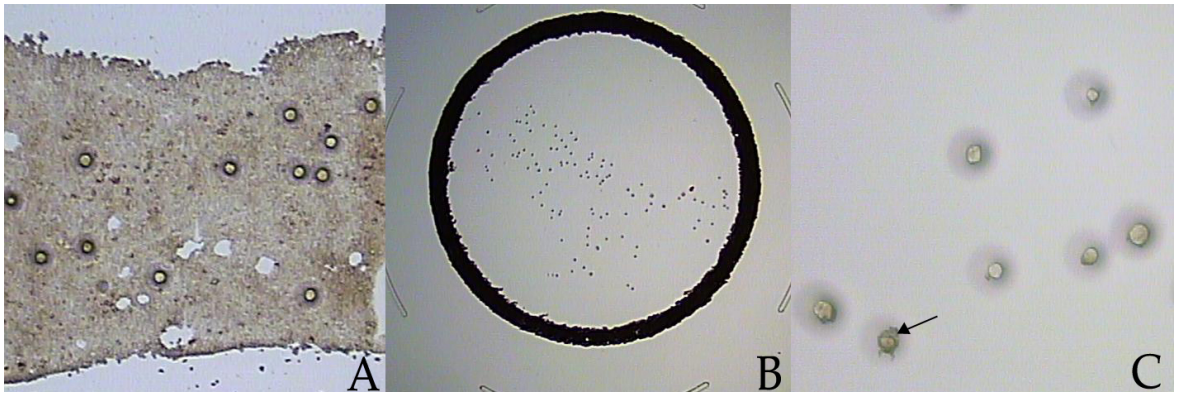

Figure 2.3: *Laser capture microdissection of a set of individual megakaryocytes from femur* **A** View of a previously microdissected tissue section of the bone marrow of a murine femur as displayed by the instrument's microscopic view. Clearly visible are the gaps in the tissue caused by the capturing of cellular material. **B** Ensuing quality check shows several individual cells adherent to the invisible thermoplastic membrane of the cap. **C** Quality check in larger magnification shows several pure dissected megakaryocytes and one potential contamination with undesired cell material (see arrow).

2.9 Analysis software and graphic presentation

All data was acquired with the respective equipment, exported to and stored in Excel (Microsoft, USA). Data was subsequently analyzed for statistical significance with Prism (Graph Pad Software, USA) using unpaired two-tailed t-test and the following notation:

$*$	significant ($P \leqslant 0.05$)
$**$	very significant ($P \leqslant 0.01$)
$***$	extremely significant ($P \leqslant 0.001$)

Scientific data and schemes were arranged and visualized using Prism, Powerpoint (Microsoft, USA) and Photoshop (Adobe, USA) on Mac and PC.

2.10 General Items

Name	Origin
Tissue Preparation Utensils	FST Medizintechnik, Germany
Reaction Tubes (0.5/1.5/2.0 ml)	Sarstedt, Germany & Eppendorf, Germany
PP Test Tubes (15/50 ml)	Greiner Bio-One, Austria
Glass Bottles (500 ml)	Schott, Germany
Glass Pipettes (5/10/25 ml)	Hirschmann, Germany
Round-bottom FACS tubes (5 ml)	Becton Dickinson, USA
Glass pipettes (5/10/25 ml)	Hirschmann, Germany
Pipetboy *Pipetus*	Hirschmann, Germany
EppiBox	NeoLab, Germany
Precision Pipet Set (10/20/100/200/1000 μl)	Gilson, USA
Pipet Tips	Corning Costar, USA
Pasteur Pipets	n.a.
Parafilm	American National Can, USA
Minishaker *MS-1*	Faust, Germany
Vortexer *IKA Minishaker*	IKA Works Inc., USA
Vortexer *Vortex-Genie2*	Scientific Industries, USA
CASY Cell-Counter & Analyzer, Model TT	Schärfe System, Germany
Biofuge *fresco* Desk Centrifuge	Heraeus, Germany
Megafuge *1.0*	Heraeus, Germany
Sterile Hood *HeraSafe*	Heraeus, Germany
Aspiration Device	Neuberger, Germany
Incubator with Shaker	GFL, Germany
Refrigerator and $-20\,^{\circ}$C Freezer	Liebherr, Germany

3. Results

3.1 Generation of TPO-retrogenic mice

Previously, megakaryocytes were demonstrated to have an impact on plasma cell biology (161). Histological analyses show co-localization between both cell types and megakaryocytes seem to produce several plasma cell survival factors.
In mentioned publication, the effect of increased megakaryocyte numbers on the development and maintenance of plasma cells was addressed by injection of recombinant thrombopoietin (TPO). However, this was greatly hampered by the feedback between TPO and platelet numbers as explained in section 1.4.2. Thus, TPO-injection resulted in a merely transient increase in megakaryocyte numbers in the bone marrow, which severely impeded the analysis of the long-term maintenance of plasma cells. Consequently, in order to investigate the effects of stably increased megakaryocyte numbers, TPO-transgenic mice were generated that express TPO in hematopoietic cells mainly resident in the bone marrow and thereby circumvent the physiological route of TPO through the blood stream in which the feedback regulation occurs.

3.1.1 Cloning of retroviral TPO expression vector

In the first step of the generation of TPO-retrogenic mice, the retrovirus vector containing the coding sequence of Thpo was generated[1]. An overview of the cloning strategy can be seen in Fig. 3.1. The retrovirus transfer vector contains one XhoI and two unique BglII restriction sites directly adjacent to each other which were employed for the insertion of the Thpo-sequence. A PCR fragment containing the full length coding sequence of Thpo and introduced restriction sites for BglII and XhoI was generated from total cDNA reverse transcribed from murine liver RNA[2]. After ligation and transformation into chemically competent E.*coli*, 17 out of 24 clones showed an insert of the expected 1085±5 bp, when digested with XhoI and BglII. Full range two-directional sequencing of 4 of these clones showed fully intact Thpo-sequences in 3 of the 4 clones. Common to all was a silent ($G^{28}\rightarrow T$)mutation that would not interfere with the functionality of the translated protein.

[1]Please note the difference between notation for the gene Thpo and the protein TPO expressed by the gene!

[2]Please see a complete list of all primers used for this work in Table 2.4 on page 34

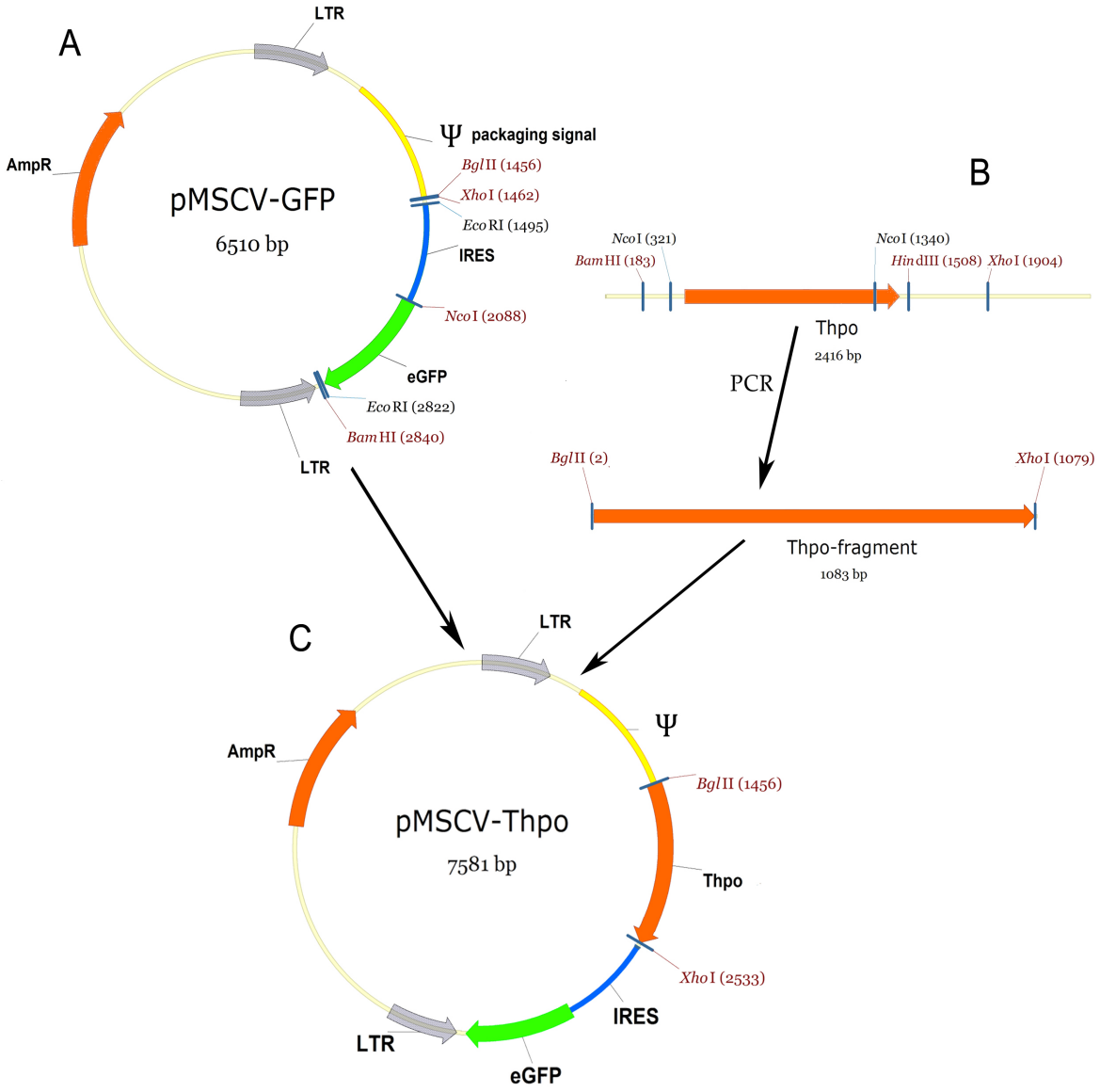

Figure 3.1: *Cloning strategy for the Generation of retroviral Thpo expression vector*
A The retroviral transfer vector pMSCV contains an ampicillin resistance gene (Amp^r) and two long-terminal repeats (LTR) encompassing the provirus. These LCMs serve as viral promoters and are necessary for stable insertion into the genome of the host cell. The viral genome contains the viral packaging signal Ψ^+, a multiple cloning site upstream of an internal ribosomal entry site (IRES) and the eGFP gene.
B The whole murine Thpo mRNA sequence is depicted on top. The cDNA fragment containing the entire Thpo coding sequence (Thpo CDS) and the restriction sequences specific for the enzymes *BglII* and *XhoI* was generated by RT and PCR using adaptor primers .
C The retroviral expression vector pMSCV-Thpo was created by digestion of pMSCV and the PCR fragment of Thpo with *BglII* and *XhoI* and ligation. It comprises the Thpo CDS under the control of the LCM promoter upstream of an IRES-GFP cassette.

3.1.2 Generation of Thpo retrovirus packaging cell line

Three retrovirus expression vectors were generated for the production of virus, as explained above:

- pMSCV – the empty expression vector only containing the CDS of enhanced green fluorescent protein (eGFP) downstream of an IRES sequence
- pMSCV-Thpo – pMSCV with the entire CDS of the protein TPO followed by IRES-eGFP
- pMSCV-kThpo – pMSCV with the entire CDS of TPO directly downstream of a Kozak sequence for possibly augmented translation efficiency (79, 80)

Mice retrovirally transduced with the empty vector pMSCV served as control group to account for immunological changes due to the overall procedure (irradiation, injection of exogenous cells, possible immunogenicity caused by eGFP, etc.). In order to ensure the most potent retrogenic TPO-production, the two related vectors pMSCV-Thpo and pMSCV-kThpo were compared in the functional 32D-assay for efficacy in mediating TPO-production in transduced cells (3.1.3).
The three packaging cell lines were generated in a two-step fashion (Fig. 3.2A):

1. Generation of a pantropic retrovirus containing the Thpo CDS in HEK 293 cells
2. Generation of an ecotropic Thpo retrovirus producer cell line by repeated infection of a retrovirus packaging cell line with the pantropic retrovirus

For production of pantropic retrovirus, HEK 293 cells were triple-transfected with the respective retrovirus expression vector and the two accessory plasmids pCAGGS-VSVg and pEQ-Pam3(-E) (see 2.1.2). Initial experiments showed a drop in virus titers after three to four days under our culture conditions probably due to toxicity of the VSV gene product and to declining vitality of HEK 293 cells after transfection. Therefore, continuous transduction of the packaging cell line was made possible by triple-transfecting a new charge of HEK 293 cells every 56 hours throughout the transduction period (Fig. 3.2A).

Repeated transduction of the ecotropic retrovirus packaging cell line GP+E86 with supernatant from triple-transfected HEK 293 cells led to a gradual increase in both the frequency of $eGFP^+$ cells and their respective mean fluorescence intensities (Fig. 3.2B). After up to 10 rounds of transduction with supernatant from the HEK 293 cells, GFP^+ GP+E86 cells were sorted via fluorescence activated cell sorting (FACS). These were resorted after an additional week in culture for the 20% highest GFP expressers[3], yielding virus producer cell lines with a purity of 100%.

[3]Because GFP is downstream of the Thpo sequence under regulation of the same viral promoter in the virus genome, GFP expression was expected to correlate with expression of TPO

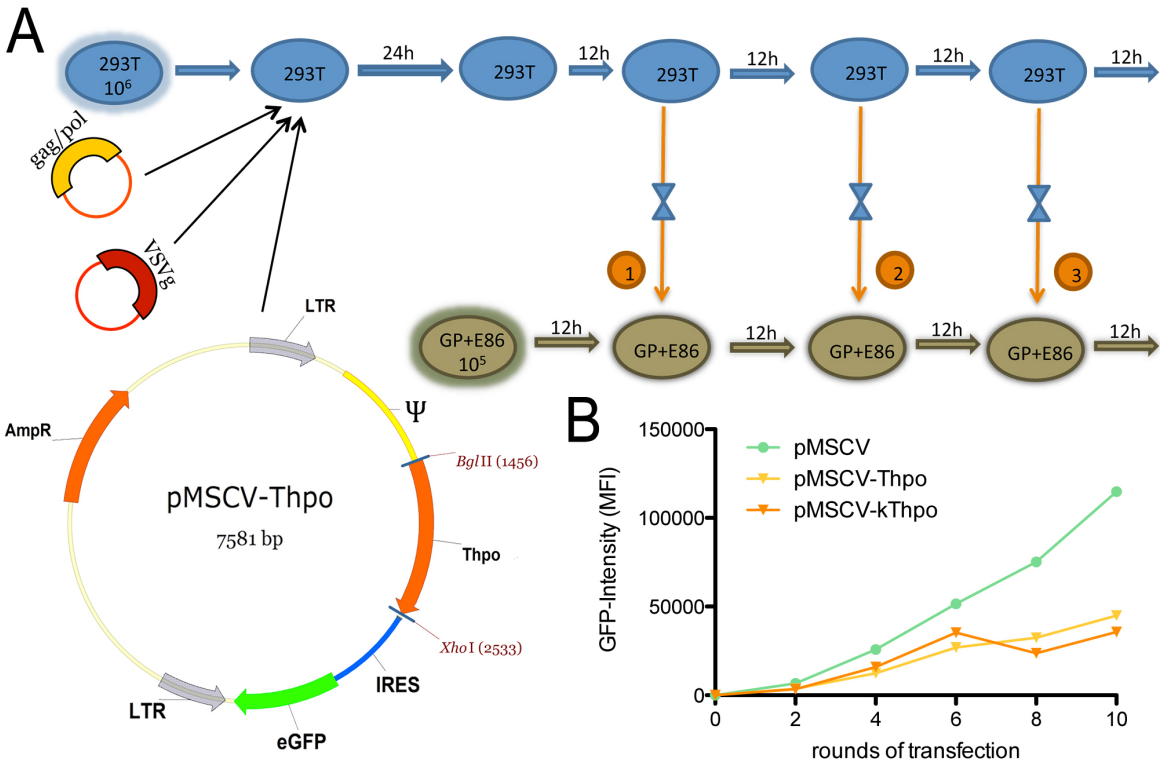

Figure 3.2: *Generation of Retrovirus Producer Cell Lines*
This experiment scheme shows the generation of retrovirus producer cell lines from packaging cell line GP+E86 and retrovirus produced by triple-transfected HEK 293 cells. This is exemplified for pMSCV-Thpo and analogous for the other two retrovirus expression vectors.
A HEK 293 cells were triple-transfected with the retrovirus expression vector and the two accessory plasmids pCAGGS-VSVg and pEQ-Pam3(-E) containing the CDS for gag and pol and supernatant was repeatedly (up to ten times) transferred to the GP+E86 packaging cell line.
B Flow cytometry analysis was performed with the transduced GP+E86 cells every two hours for determination of GFP MFI, showing a gradual increase in GFP-intensity throughout the transduction period. MFI are of the GFP^+ GP+E86 cells only. Frequency of GFP^+ producer cells ranged from 0.1 to 1.9%.
MFI, mean fluorescence intensity

Repeated rounds of transduction lead to an increase in virus titers (as measured by the 3T3 assay described in section 2.1.2) of 900±60 after the first supernatant transfer to $5.5\pm1 \cdot 10^4$ after the 10^{th} round. GFP intensities in GP cells were increased from 3400-6700 to 35,000-115,000 (MFI). Significant difference was observed neither in the virus titers nor in the GFP MFI between virus generated from pMSCV-Thpo (MSCV-Thpo) and virus from pMSCV-kThpo (MSCV-kThpo), showing no impact of the Kozak-sequence on protein synthesis. This is probably due to the very strong LCM-promoter that already causes maximum transcription.
Thus, three producer cell lines derived from GP+E86 were generated and named after the retrovirus expression vector used for virus production. GP-GFP for pMSCV (containing GFP downstream of IRES), GP-TPO for pMSCV-Thpo, and GP-kTpo for pMSCV-kThpo. Both GP-TPO and GP-kTpo constitutively produce ecotropic retrovirus able to transduce the CDS for TPO:IRES:GFP into a murine target cell and synthesize GFP and TPO protein.

3.1.3 Generation of TPO-dependent 32D cells

A TPO-dependent cell line was generated in order to confirm production of functional TPO by the virus producer cell lines GP-TPO and GP-kTpo.
For this purpose, the widely used 32D cell line was selected. The growth of 32D cells is strictly dependent on interleucin (IL)-3. 32D cells transgenic for other cytokine receptors acquire growth dependence for the respective cytokine. Hence, TPO-dependent 32D cells were generated by ectopic expression of the TPO-receptor c-Mpl. Initial attempts with the retroviral approach revealed a high susceptibility of 32D cells for retroviral transduction. Thus, the now well-established method of retroviral transduction was used for the generation of a cMpl-bearing 32D cell line. However, it was not necessary to generate retrovirus producer cell lines as an intermediate source for constitutive virus titers because 32D cells are a transformed cell line that, once transduced, keeps the retroviral genes stably in its genome.

Cloning of retroviral c-mpl expression vector

The full length CDS of c-Mpl (1890bp) including the 5-terminal signal sequence directly following the ATG start codon was amplified from bone marrow cDNA and restriction sites BglII and XhoI for cloning into pMSCV were introduced using adaptor primers[4]. Subsequently, both pMSCV and the extracted c-Mpl amplicon were digested, ligated and transformed into E.*coli*. 18 of 21 picked clones contained the right insert according to PCR using primers annealing to sequences inside the c-Mpl CDS. This was confirmed for two of these clones with digestion of their isolated plasmids with BglII and XhoI. Subsequently, purified plasmids were sequenced, showing both plasmids to contain the full length CDS of c-Mpl transcription variant 1. Transcription variant 1 is the

[4]Please see a complete list of all primers used for this work in Table 2.4 on page 34

predominant form of c-Mpl that occurs in murine cells.
The resulting plasmid was called pMSCV-Mpl and used for transfection of HEK 293 cells.

Selection of TPO-dependent 32D cells

Initial tests showed that 32D cells proliferate well in medium containing fetal calf serum (FCS), indicating that this serum contains homologous IL-3 or another compensatory factor in sufficient amounts. Thus, any TPO-dependency of the 32D-Mpl cells would have been masked by IL-3-driven proliferation. Therefore, 32D-Mpl cells were selected for sensitivity to TPO by prolonged culture in serum-free medium (SFM) supplemented with gradually decreased amounts of TPO. Non-retrogenic 32D and 32D-GFP did not grow in TPO-containing SFM, whereas 32D-Mpl cells expanded in SFM containing concentrations of TPO as low as 2 ng/ml. At lower TPO concentrations, cells did not divide anymore and became resting. At TPO levels below ≈0.5 ng/ml cell numbers started to decrease (data not shown).

Functionality of retrovirally produced TPO

The generated 32D-Mpl cells were cultured in SFM over a serial dilution of TPO (between 90 ng and 40 pg/ml). After 4 days, the cells were harvested and the number of GFP^+ 4',6-diamidino-2-phenylindole $(DAPI)^-$ 32D cells as identified by scatter (Fig. 3.3A) were counted with a flow cytometer. When TPO concentration was plotted against the number of 32D cells in log-log scale, a striking correlation became apparent (Fig. 3.3B). This correlation appeared to follow a function closely resembling Michaelis-Menten kinetics (97): The formula for Michaelis-Menten kinetics is as follows:

$$V = \frac{V_{max} \times c}{K_m + c}$$

When V was substituted with the cell number N and c would be the concentration of TPO in the medium, the function reads as:

$$N \approx \frac{88,8 \times c}{177 + c}; R^2 = 0.997$$

Next, this assay was used for the measurement of functional TPO secreted by GP-TPO and GP-kTpo cells (see 2.3.2). As can be seen in Fig. 3.3C, 32D-Mpl clearly proliferated in a concentration-dependent manner, albeit not as strictly following above mentioned correlation. As there are no reports about the production of IL-3 or TPO by GP+E86 cells, this proliferation is most likely caused by the secretion of retrovirally transgenic TPO by the GP+E86 cells. The observed decline in the correlation slope at higher medium concentrations is possibly caused by inhibitory factors produced by the GP+E86 cells reaching threshold levels at these medium concentrations.

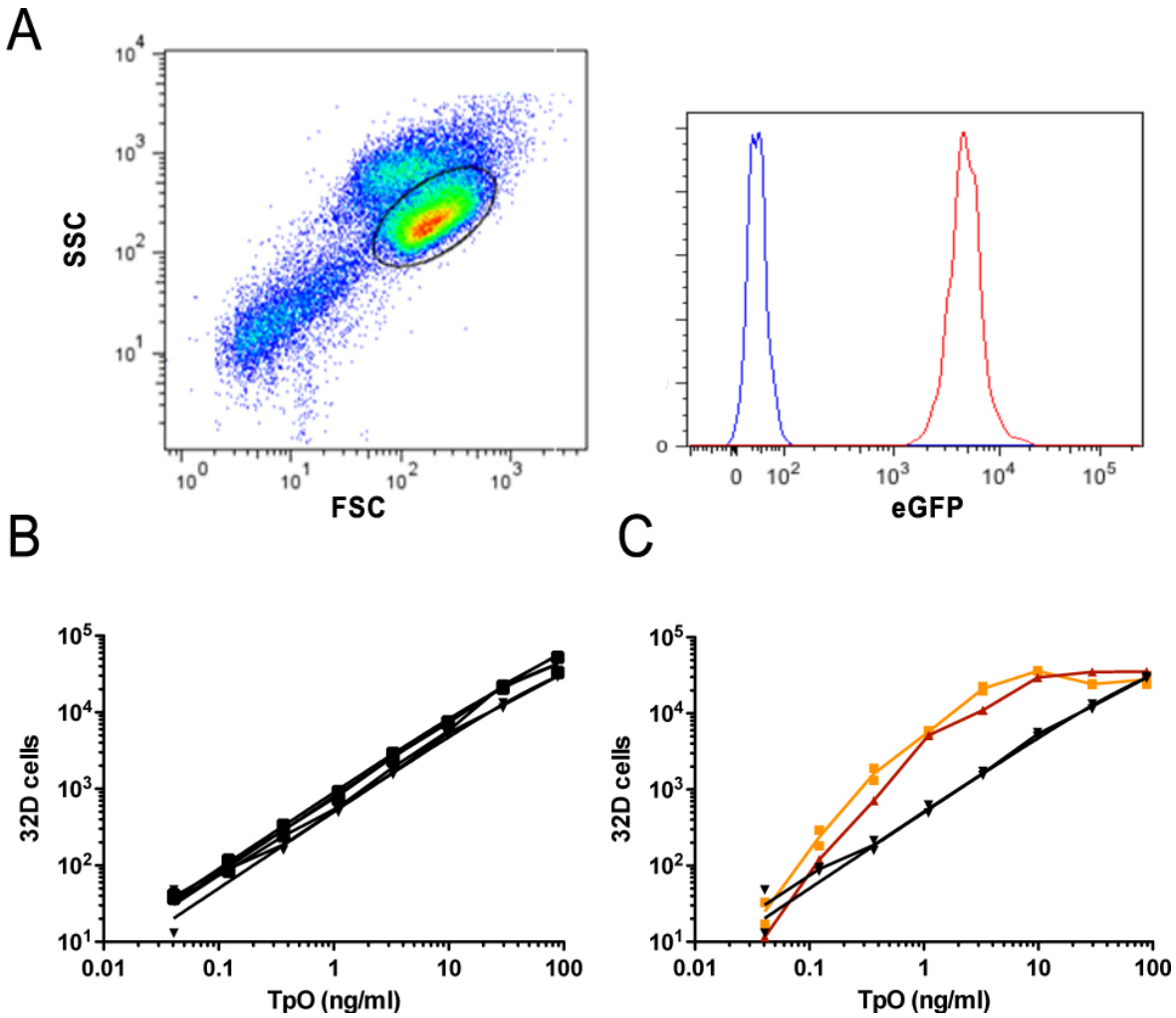

Figure 3.3: *Thpo-dependency of c-mpl retrogenic 32D cell line*
A 32D-Mpl cells were grown in SFM with TPO and cultured for 4 d. Gating for cell count is shown. 32D cells were gated on viable population as seen in the scatter-plot (left). In the histogram (right), GFP-expression of gated populations from 32D-Mpl (red) and non-transgenic (blue) 32D-cells is shown. **B** 32D-Mpl cells were grown in SFM with a serial dilution of TPO cultured for 4 days and analyzed via flow cytometry as shown in (A). TPO concentrations are plotted against cell numbers on log-scale. Experiments were performed in triplets. **C** 32D cells were grown in serial dilutions of Thpo (black) or conditioned medium from GP-TPO (orange) and GP-kTpo (red). The x-axis indicates concentration of TPO or dilution of GP-TPO conditioned medium in percent.

Then, TPO concentrations were calculated based on the computed correlation between TPO and cell number. For GP-TPO and GP-kTpo. Determined TPO levels in culture supernatant were ≈ 650 and 950 ng/ml, respectively. When omitting the values for highest medium concentrations, the calculated concentrations increased to 0.85 and 1.34 μg/ml for GP-TPO and GP-kTpo, respectively.
Thus, it was shown that retroviral transduction with MSCV-Thpo and MSCV-kThpo leads to production and secretion of high amounts of soluble and biologically functional TPO into the extracellular space. The increased transcription strength mediated by the additional Kozak consensus sequence in pMSCV-kThpo leads to an increase in TPO secretion by approximately 50%. Therefore, the virus producer cell line GP-kTpo was chosen for efficient retroviral transduction of murine bone marrow cells.

3.1.4 Generation of TPO retrogenic mice via HSC-transfer

In the previous sections, the generation of a virus producer cell line was described that constitutively secretes high titers of the ecotropic retrovirus MSCV-kThpo. Murine cells infected with this virus (e.g. GP+E86) integrated the virally transduced Thpo::IRES::eGFP CDS into their own genome, became GFP-positive and stably secreted large amounts of TPO into the medium. Next, this virus producer cell line was used to generate mice retrovirally transgenic for TPO (short: TPO-retrogenic). Fig. 3.4A shows a schematic overview of the entire procedure as described in section 2.1.3.
For an initial experiment, recipient mice were lethally irradiated. Unfortunately, two of the control mice died from septic shock shortly after transfer of retrogenic HSCs, which was probably caused by contaminating GP-GFP cells in the HSC preparation. These cells are very immunogenic due to high titer virus production. This event made the initial investigations rather descriptive.
Analysis of remaining harvested HSC revealed an initial GFP^+percentage between 1.9 and 6.5% (data not shown), showing that the transduction of HSC was at least partially successful.
Following the injection of retrogenic HSCs, both control and TPO mice gradually increased GFP percentage of blood lymphocytes to reach levels between 28.7 and 60.6% after 5 weeks.
Thus, retrogenic HSC transfer leads to a stably retrogenic hematopoietic population in tested mice since the measured amount of GFP^+cells can only result from a constant pool of retrogenic HSCs as transferred retrogenic lymphocytes have a much smaller half-life and thus cannot account for these ratios.

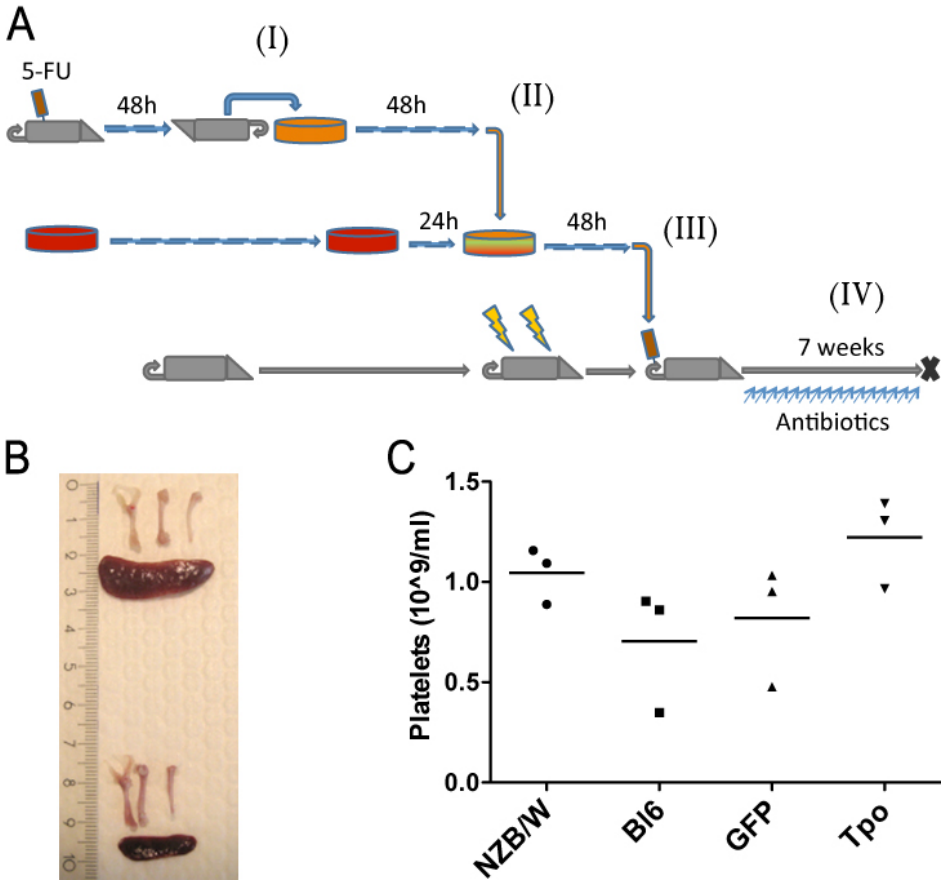

Figure 3.4: *Generation and general features of Thpo-retrogenic mice.*
A Scheme for the generation of retrogenic mice. **(I)** Mice previously fed with 5-FU were sacrificed and bone marrow cells were harvested and expanded in culture with appropriate cytokines (section 2.3.3) for two days. **(II)** Expanded bone marrow cells were than co-cultured with adherent virus-producer cells and cytokines for another two days, allowing the retrovirus carrying the genes for Thpo and GFP to infect HSC. **(III)** HSC were harvested from the virus-producer cells and directly injected into previously irradiated recipient mice. **(IV)** Mice were fed with antibiotics for another 3 to 7 weeks and are analyzed as early as 7 weeks depending on the experiment
B TPO-retrogenic and GFP-retrogenic BALB/c mice were generated as described in (A) and sacrificed after 7 weeks. Spleen and bone marrow (from left to right: hip bone, femur, and tibia) from Thpo-retrogenic (top) and GFP-retrogenic (bottom) mice are shown. Retrogenic mice display enlarged spleens and pale bone marrow.
C Blood from different mouse strains was taken at 12 weeks of age (NZB/W and Bl6) or 7 weeks after transfer of either empty vector retrogenic cells (GFP) or Thpo-retrogenic cells (Thpo) into BALB/c mice and platelet counts were measured via flow cytometry. n=3

3.1.5 General features of TPO-retrogenic mice

Organ comparison between TPO and control mice

Following the course of the experiment, all mice appeared healthy as compared with wild type BALB/c mice. The TPO-group, however, showed a slight decline in body weight (20.1±1.5 g in the TPO group compared to 22.5±0.9 g in controls). 7 weeks after HSC transfer mice were sacrificed and striking differences were observed between both groups regarding both bone marrow and spleen. Spleens in TPO mice were greatly enlarged which was reflected in a weight gain of this organ (452±100 mg in the TPO group compared to 132 mg in controls; Fig. 3.4B). Spleens from TPO mice appeared very firm and fibrotic and follicles were not macroscopically visible as is usually the case.
Bone marrow of TPO retrogenic mice appeared very pale and lacked the deep crimson color usual for bone marrow. Furthermore, bone marrow space was greatly reduced in TPO mice due to bone ingrowth which made it very difficult to obtain bone marrow material.
The cells obtained from bone marrow and spleen were counted and as expected from the difficult accessibility bone marrow from the TPO mice only yielded about 6-26% of control mice ($0.7\text{-}3.2 \cdot 10^6$ in TPO vs. $1.2 \cdot 10^7$ in control). Total cell counts were also decreased in the spleens of TPO animals despite the greatly increased size and weight, although to much lesser extent as in the bone marrow ($0.5\text{-}1.2 \cdot 10^8$ in TPO mice compared to $1.5 \cdot 10^8$ in the control mouse)

Platelet count in blood

Prior to sacrificing the mice, blood was drawn from control and TPO mice as well as from untreated, non-irradiated mice and platelet count was determined as described in 2.4.3. Untreated mice had $1100\pm40 \cdot 10^9$ platelets/ml whereas the control mouse had only 555[5]. This reduced platelet count was possible due to the fact that the hematopoietic system had not entirely recovered from the massive depletion of cells caused by the irradiation procedure. In contrast, TPO mice showed elevated platelet counts ranging from 1470 to 2580, clearly showing the effect of the transgenic TPO on the thrombopoietic system.
This increase in platelet counts in TPO mice could be reproduced in retrogenic mice generated under much less harsh conditions. In those mice, control animals had platelet counts comparable to wild type and the fewer retrogenic cells in TPO-retrogenic mice were nevertheless sufficient to cause the platelet increase. In Fig. 3.4C, this is shown for mildly retrogenic animals showing again an increased platelet count in TPO retrogenic animals compared to GFP control mice. Platelet counts of the two mouse strains (New Zealand Black x New Zealand White)F1 (NZB/W) and BALB/c were included into the experiment, which shows the variance in platelet counts between different strains.

[5]Platelet counts always in 10^9 platelets/ml

Analysis of splenic megakaryocytes

Histological sections of frozen spleens from both TPO-retrogenic and GFP-retrogenic mice were stained for plasma cells and megakaryocytes and analyzed via confocal microscopy (Fig. 3.5). Megakaryocytes are seen only very rarely and evenly spread throughout the tissue in GFP-retrogenic control mice. Contrastingly, spleens of TPO mice displayed many megakaryocytes and megakaryocyte progenitors some of which display unconventional shapes, making the distinction between individual cells rather difficult.
The analysis of bone marrow of TPO-retrogenic animals, however, was not possible in histology. Due to the greatly increased brittleness of TPO-retrogenic bone marrow, no continuous tissue sections could be obtained. Therefore, the analysis of megakaryocyte numbers in bone marrow was performed via flow cytometry if deemed necessary.

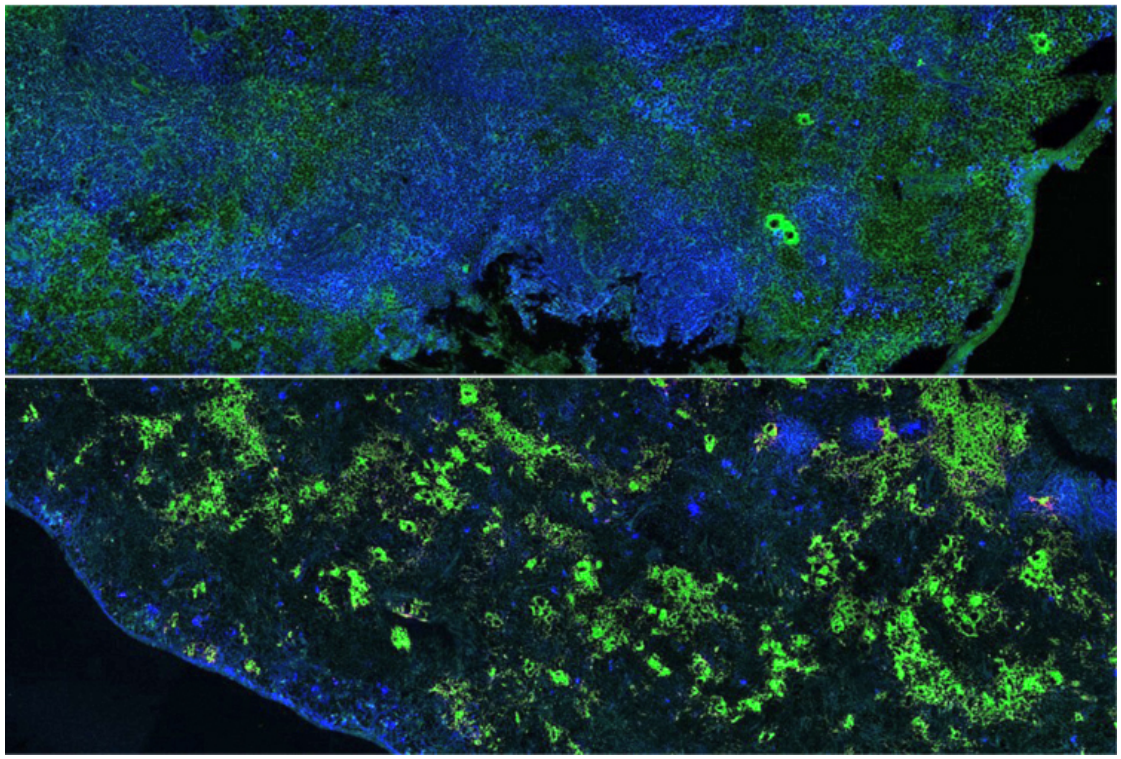

Figure 3.5: *Histological analysis of spleens from retrogenic mice.*
Spleens of mice retrogenic for empty vector (top) and Thpo-retrogenic mice were sectioned, stained with antibodies against Ig κ-light chain (blue) and CD61 (green), and analyzed via confocal microscopy. Megakaryocytes (in green) are very rare in control mice but their numbers are highly increased in TPO-retrogenic spleens. The picture of the Thpo-retrogenic spleen is representative of mice from early experiments that established between 26 and 61% retrogenic cells in their hematopoietic cells. Later experiments were deliberately performed with less efficiency, as described in the text.

3.2 Analysis of the Plasma Cell Compartment in TPO-retrogenic Mice

Retroviral transduction with TPO leads to increased platelet counts and massive increase of megakaryocyte numbers in the spleen and most likely in bone marrow. The following questions were addressed with this model:

- Megakaryocytes in the bone marrow are co-localized with plasma cells and seem to specifically favor survival of newly generated plasma cells. How does an increase in megakaryocyte numbers/turn-over influence the establishment and maintenance of an ovalbumin (Ova)-specific plasma cell memory after secondary immunization?

- The spleen has limited potential to harbor long-lived plasma cells from both primary and secondary foci (144). However, increased splenic megakaryocyte numbers are accompanied by hypergammaglobulinemia and elevated plasma cell numbers in lupus-prone NZB/W mice (100, 56), raising the question whether increased megakaryocyte numbers in spleen can cause hypergammaglobulinemia?

One problem is posed by the side effects observed in initial experiments that might hamper analysis of the results. Therefore, different approaches were attempted in the following experiments to decrease the efficiency of the retrogenic HSC transfer in order to decrease side effects without losing the increase in megakaryocytes in bone marrow and possibly in the spleen, as explained in the respective sections. Plasma cells and antibody titers were analyzed in TPO-retrogenic mice in comparison with mice retrogenic for GFP. Antibody titers were determined with standard enzyme-linked immunosorbent assay (ELISA)[6]. Plasma cell numbers and frequencies were measured via enzyme-linked immunosorbent spot (ELISPOT)[7] or via flow cytometry[8]. In flow cytometry, plasma cells were identified by staining for CD138 (syndecan) (83,90), B220 (CD45R) and intracellularly with Ig κ (Fig. 3.6A). The Ig κ light chain is one possible heterodimer of an antibody molecule[9] and can be used to identify plasma cells as they contain large numbers of antibody molecules produced for secretion.
In order to follow plasma cell development and the cellular fate following an immune reaction, the widely used model for T-dependent immunization using the protein antigen Ova was chosen (90). For detection of Ova-specific plasma cells, in flow cytometry, Ova chemically coupled to a fluorochrome was used. Plasma cells that produce antibodies specific for Ova bind fluorochrome-coupled Ova intracellularly (Fig. 3.6B). However, flow cytometric analysis was only feasible when sufficient cells were available as Ova-specific plasma cells exist at very low frequencies ($< 0.1\%$). Alternatively, Ova-specific

[6] see Materials and Methods section 2.5 on page 43
[7] section 2.6 on page 45
[8] section 2.4 on page 39
[9] 95% of murine antibodies including those raised against Ova employ the Ig κ-light chain, which makes the staining of λ-light chains unnecessary

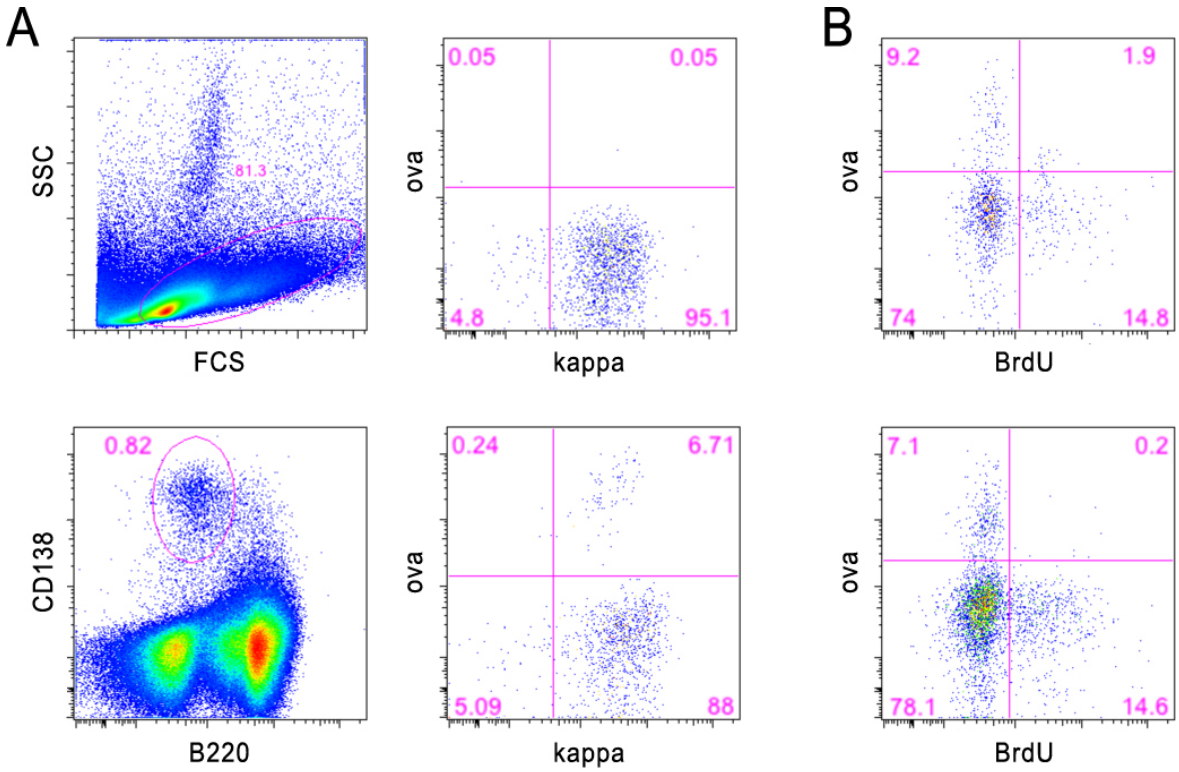

Figure 3.6: *Identification of plasma cells via flow cytometry.*
Flow cytometry analysis of total spleen cells stained on the cell surface with antibodies specific for B220 and CD138 and intracellularly with antibodies against Ig κ, Ova and BrdU. **A** Total cells were preselected for further analysis with a gate excluding granulocytes and debris (upper left). Plasma cells were identified in flow cytometry as $B220^{-/lo}CD138^{++}$ (lower left). Splenic plasma cells of mice immunized with the adjuvant alum only (top middle) or boost-immunized with Ova in alum (bottom middle) are mainly Ig κ^{++}, as indicated by the gates. Only mice immunized with Ova peptide show the Ova-specific staining (bottom middle). **B** Mice were primed with Ova and simultaneously fed with BrdU for two weeks. 5 weeks later, mice were boosted with Ova and analyzed 5 days later with flow cytometry. Plasma cells from bone marrow (top right) and spleen (bottom right) were gated as in **A**. Most Ova^{+} plasma cells are $BrdU^{-}$ and therefore stem from the secondary immunization.

ELISPOT was used.
We used the DNA analogue 5-bromodeoxy uracil (BrdU) for differentiation between proliferating plasma blasts and plasma cells that did not proliferate during the 3 week period of BrdU feeding. BrdU becomes integrated into the genome of proliferating cells (56) whereas resting (and therefore by definition long-lived) plasma cells do not accumulate it. The incorporation can be measured by staining with antibodies specific for BrdU, as seen in Fig. 3.6.

3.2.1 Immunization of TPO-retrogenic mice

The TPO-retrogenic mouse as a model for increased megakaryopoiesis was then used to investigate the effect of elevated megakaryocyte numbers both on steady state antibody titers as well as on the establishment and the outcome of an immune response. At the same time, the influence of elevated thrombopoietin levels on additional lymphocyte populations was examined. For this purpose, TPO-retrogenic mice and control mice were generated as described in the previous section with minor modifications.
In order to decrease mortality of mice after HSC transfer and to ameliorate mentioned side effects, HSCs were not co-cultured anymore with the virus producer cells. Instead, the supernatant of GP-TPO or GP-GFP was used for transduction of HSC on RetroNectin-coated plates[10]. Also, only 25% of the initial HSC number ($5 \cdot 10^5$) was injected into lethally irradiated recipient mice. As expected, none of the 20 mice that received the modified HSC transfer died before analysis.
The ensuing immunization experiment is shown schematically in Fig. 3.7A. Two weeks after HSC transfer, retrogenic mice were Ova-immunized to prime the immune system for the Ova peptide. 5 weeks later, mice were boost-immunized again with Ova. In between the two immunizations, blood was taken at two time points and analyzed with flow cytometry for monitoring the establishment of the retrogenic cell compartment and development of the immune system (Fig. 3.7B+C). Initially high frequencies of retrogenic lymphocytes (up to 52.4% as measured by GFP expression) decline over the course of the experiment to 5.9 to 14.7% in the TPO-retrogenic mice and even lower frequencies in control mice (between 0.1 and 12.1%).
Mice were then allocated into two groups such that distribution of GFP percentages was comparable among the mice of both groups. The mice of the first group were sacrificed at day 6 after boost in order to investigate plasma cell development at the peak of secondary immunization (48). The second group was analyzed at day 21 after boost in order to see the influence of increased megakaryopoiesis on the maintenance of plasma cells in both bone marrow and spleen after termination of the immune reaction.

[10] see Materials and Methods section 2.1.3 on page 24

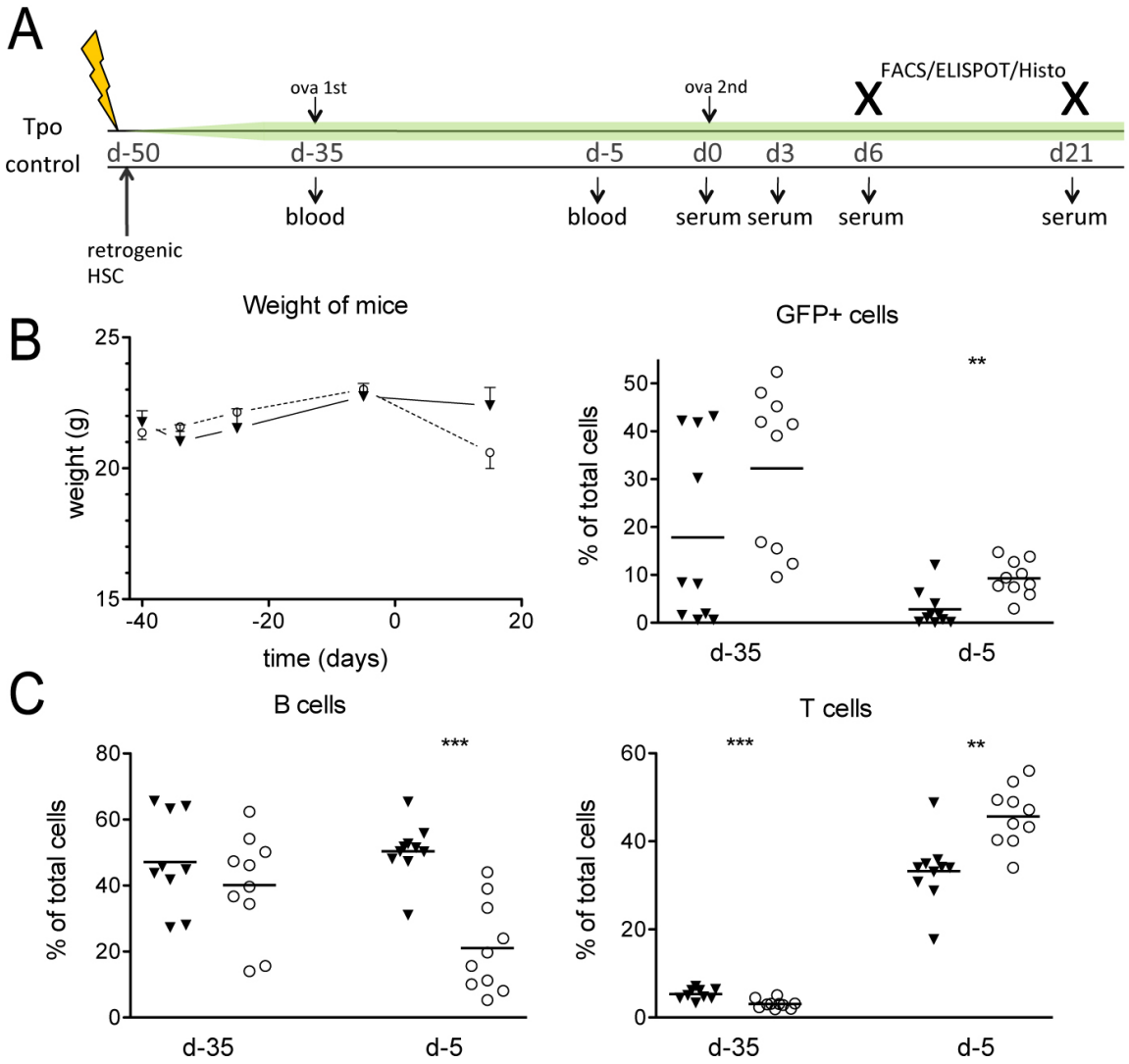

Figure 3.7: *Immunization experiment of TPO retrogenic mice.*
A Experimental scheme for the immunization experiment. Mice where lethally irradiated followed by *i.v.* transfer of hematopoietic donor cells (HSC) made retrogenic with virus containing the coding sequence for either GFP (control) or TPO and GFP (Tpo). Mice were immunized twice with Ova alum *i.p.* at the time points denoted with *ova 1st* for primary and *ova 2nd* for secondary immunization. Blood was taken at different time points to analyze retrogenic efficiency and re-establishment of the immune system (see **B** and **C**). Serum was taken before and after boost immunization as depicted and mice were sacrificed at day 6 and day 21 after boost immunization (**X**).
B Weight of mice was observed at different time points for evaluation of mouse health status (left). Percentages of GFP^+cells in the blood were analyzed at different time points before immunization via flow cytometry. **C** Blood taken at different time points was analyzed via flow cytometry for GFP-expressing cells (left), $B220^+CD4^-$ B cells (left) and $B220^-$ $CD4^+$T cells (right). n=10; GFP-control(▾); TPO retrogenic(○)

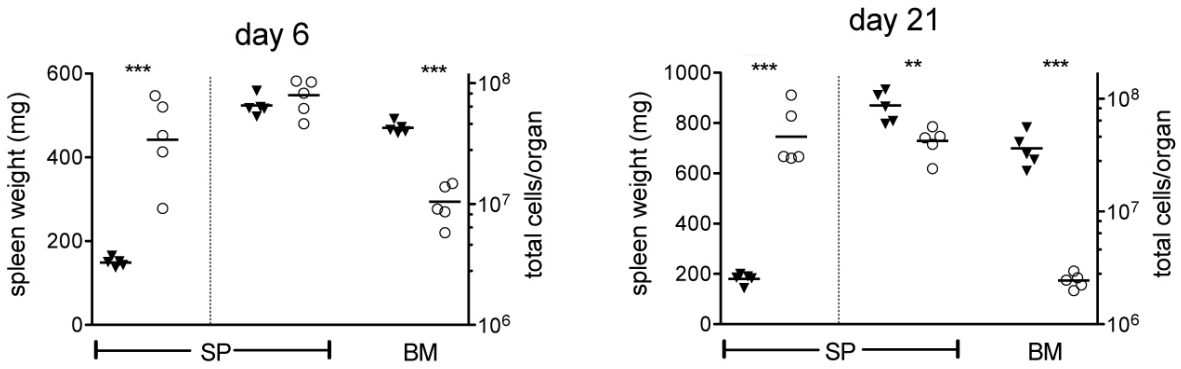

Figure 3.8: *Organ Development in TPO-retrogenic mice*
Mice were made retrogenic and subsequently immunized as explained in the text and outlined schematically in Figure 3.7. Mice were analyzed for spleen weight and cell numbers in spleen and bone marrow at day 6 (middle) and 21 (right) after boost.
n=5; GFP-control(▾); TPO retrogenic(○); SP, Spleen; BM, Bone marrow

Development of lymphocyte populations in retrogenic mice

Peripheral blood B cells frequencies significantly decreased in TPO mice compared to control (21% and 54.3%, respectively), whereas T cells became significantly more abundant in TPO retrogenic animals (33.2% in TPO mice and 45.7% in control; Fig. 3.7C). Therefore, TPO levels have an effect on the establishment of B and T cell compartments in the tested mice.
All mice appeared healthy throughout the experiment. Routine measurement of body weight showed only a slight drop in average body weight in the TPO-retrogenic animals at the latest time point 9 weeks after HSC transfer (Fig. 3.7B).
After sacrificing the mice, however, it became clear that the applied modifications to the HSC transfer did not abolish the effects observed in the previous experiments. As seen in Fig. 3.8, spleens of TPO-retrogenic mice were greatly enlarged. Indeed, spleens from TPO-mice killed at day 21 after boost immunization displayed even bigger size and weight than at day 5 and contained less cells. This shows that the observed effect is time-dependent and becomes more pronounced over time. Similar behavior was observed for bone marrow of TPO-mice. At both time points, bone marrow of TPO-retrogenic mice appeared very pale with decreased medullary space due to greatly increased trabecular bone volume. Total cell numbers were decreased to 30% of control at day 6 and further declined to ≈10% of control counts at day 10 (Fig. 3.8).

Plasma cell numbers after immunization

After sacrificing the mice, total plasma cell numbers in both spleen and bone marrow were analyzed with flow cytometry (Fig. 3.9A). Whereas splenic plasma cell counts were comparable between the two groups at day 6, they rapidly declined to almost

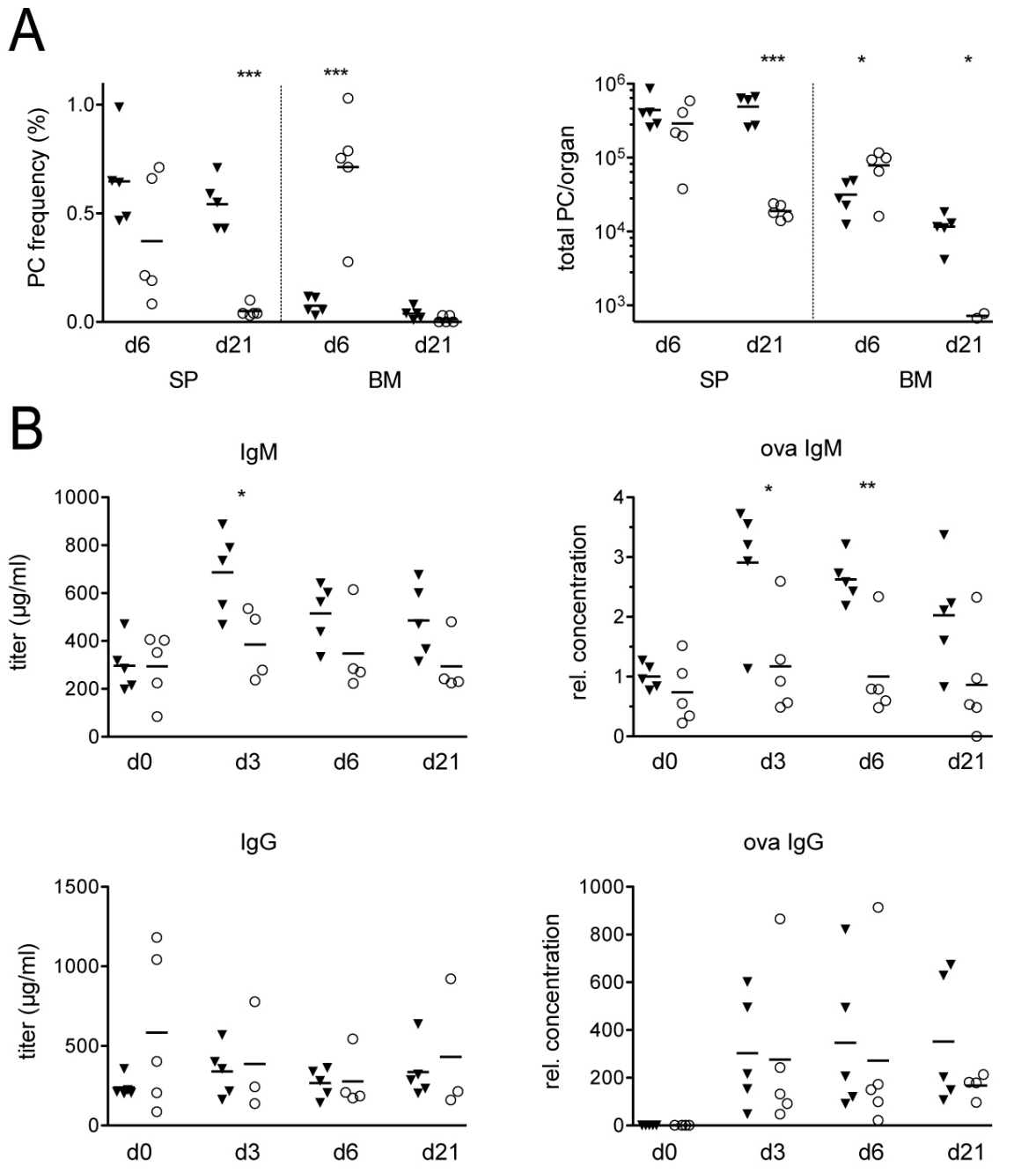

Figure 3.9: *Plasma cell analysis and antibody titers in Ova-immunized TPO-retrogenic mice* BALB/c mice were immunized as described in the text and depicted in **Fig. 3.7**.
A Mice were sacrificed at day 6 or day 21 after secondary Ova-immunization and bone marrow and splenic cells were analyzed via flow cytometry. Plasma cells were identified, as previously described, as $B220^{-/lo}CD138^{++}$and total plasma cell frequencies (left) and numbers (right) were determined via total cell counts.
B Serum was taken from mice throughout the course of the secondary Ova-immunization as depicted in the experiment scheme (**Fig. 3.7**) and analyzed via ELISA for total (left panels) and Ova-specific antibody titers (right panels) of the principal isotypes IgM (upper panels) and IgG (lower panels).
n=3-5; GFP-control(▾); TPO retrogenic(○); SP, Spleen; BM, Bone marrow

undetectable levels in TPO-mice at day 21.
Interestingly, bone marrow plasma cells were slightly but significantly increased in TPO-mice at day 6 despite the lower total cell count. Consequently, this plasma cell increase became very pronounced and highly significant when regarded in frequencies. However, plasma cells were hardly detectable in bone marrow of TPO-mice at day 21 whereas plasma cell numbers in control mice declined by only about 50% as would be expected at the end of an immune reaction.

Antibody titers after immunization of retrogenic mice

Serum samples taken from the mice at different time points along the immune response were analyzed with ELISA for total and antigen-specific antibody titers of IgM and IgG isotypes. IgG antibodies usually stem from plasma cells that have performed isotype switching and affinity maturation within a germinal center (GC) reaction. These IgG^+plasma cells have a greater tendency than IgM-secreting plasma cells to become long-lived and to enter the bone marrow survival niche (93).
As seen in Fig. 3.9B, IgM titers were comparable at boost immunization in both groups but failed to notably rise in the TPO mice after Ova-boost. Similar results were obtained for Ova-specific antibody titers which again stayed constant in the TPO-retrogenic animals whereas Ova IgM levels clearly increased in the control animals following immunization.
IgG titers were hardly affected by the immunization in either group. Initially, total mean IgG titers were slightly increased in the TPO mice but declined to similarly low levels as observed in the GFP-retrogenic animals. Ova IgG antibodies were not detectable at the beginning of the secondary immunization but rose after day 3 to comparable levels in both groups of mice.
Thus, serum antibody titers obviously developed differently depending on the antibody isotype. Whereas IgM levels were comparable at boost immunization and later only developed in the control mice, the levels of IgG were elevated in the TPO group at day 0 and no difference was seen at later time points.

IgM and IgG antibody secreting cells (ASCs)s in bone marrow and spleen

To further investigate the distribution of plasma cells in the bone marrow and spleen, ELISPOT analysis was performed because of its higher sensitivity compared to flow cytometry. In Fig. 3.10, the results are shown for both organs at day 6 and day 21 after boost immunization.
At day 6 after immunization, frequencies of both total and Ova-specific IgM-secreting plasma cells were significantly decreased in spleens of TPO-retrogenic mice compared to control mice. This difference became even more pronounced at day 21 after immunization.
In contrast, total splenic IgG plasma cells were increased in TPO-retrogenic mice at day 6 after immunization but were reduced to 30% compared to control mice at day

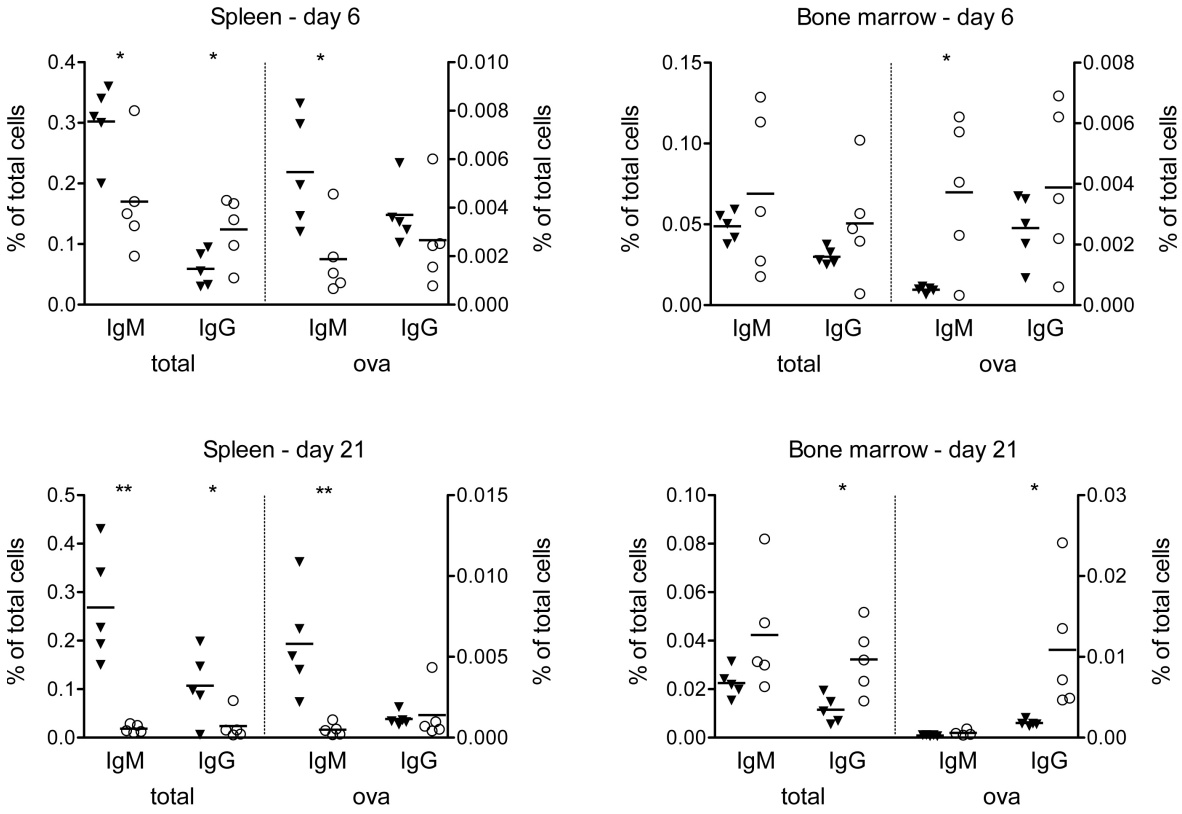

Figure 3.10: *ELISPOT analysis of Ova-immunized TPO-retrogenic mice.*
BALB/c mice were immunized as described in the text and depicted in **Fig. 3.7**. Mice were sacrificed at day 6 or day 21 after secondary Ova-immunization. Splenic (top panels) and bone marrow cells (bottom panels) were analyzed via ELISPOT for ASCs secreting total and Ova-specific IgM and IgG antibodies. Frequencies were calculated based on total cell numbers, as determined previously. n=5; GFP-control(▾); TPO retrogenic(○)

21 in TPO mice compared to control. Ova-specific IgG plasma cells were comparable in spleen at both time-points, indicating a selective advantage of antigen-specific IgG plasma cells generated in the immune response over total IgG-specific plasma cells in TPO mice.
In bone marrow, total plasma cells were greatly decreased in the TPO-retrogenic animals (data not shown) due to an overall decrease in total cell numbers at both time-points as seen above in Fig. 3.7. However, total plasma cell frequencies of both isotypes were comparable in both groups at both time points (Figure 3.10). Frequencies for Ova-specific IgM^+ plasma cells were significantly increased in the TPO-retrogenic group at day 6 but were virtually undetectable in either group at day 21. Ova-specific plasma cells of IgG isotype became significantly increased at day 21 in the TPO mice. Again, there appeared to be a selective advantage of antigen-specific plasma cells in the mouse model for increased megakaryopoiesis.

3.2.2 Transfer of antigen-specific cells into TPO-retrogenic mice

In the last section, TPO-retrogenic mice were shown to feature increased IgG titers, most likely due to increased plasma cell numbers in spleen and possibly bone marrow, depending on the degree of degradation of medullary space leading to minimized total cell counts in this organ. After immunization, splenic plasma cells gradually decreased in frequencies and numbers. Notably, plasma cell frequencies in bone marrow, especially of the the IgG isotype remained higher in the TPO-retrogenic animals until day 21 after immunization.
This indicates a decisive impact of the megakaryopoietic system on plasma cell maintenance. However, also plasma cell generation seemed to be greatly affected by increased TPO-levels, as seen by a disrupted T-cell/B-cell ratio and impaired follicular structure in spleen, as observed by confocal microscopy. Therefore, the data was hard to interpret with regard to maintenance versus generation of plasma cells.
Furthermore, the low levels of Ova-specific IgG after the boost immunization indicate that the primary immunization of recently irradiated mice might be very inefficient and the boost immunization more or less resembled a primary immunization. However, longer waiting periods after irradiation would have been hardly advisable as the degradation of bone marrow in the TPO-retrogenic mice seemed to be progressive and the time frame for analysis, especially of bone marrow plasma cells was limited.
For circumventing above mentioned complications, non-retrogenic mice were immunized with Ova and boosted three weeks later before transferring total spleen cells of these animals into retrogenic animals. By doing so, any differences in plasma cell generation as well as insufficient strength of secondary immunization in irradiated animals were prevented by uncoupling these two steps.
Fig. 3.11A outlines the experimental strategy. First, two groups of mice were made retrogenic for GFP or for TPO, respectively. To achieve this, HSCs were transduced with retroviral supernatant on RetroNectin-coated plates[11] and injected into sublethally irradiated mice[12]. Meanwhile, donor mice were injected with Ova peptide for primary immunization before boost immunization 11 or 5 days prior to transfer of total splenic cells into the retrogenic recipients. By means of two different boost time points of donor mice, transfer of cells derived from an ongoing immune reaction at two different stages was achieved. Day 5 spleen cells contain proliferating GC B cells and other activated immune cells including dendritic cells, T_{FH}-cells and T_h-cells as well as Ova peptide in presented fashion, all necessary for an ongoing immune reaction. On the other hand, day 11 spleen contains above mentioned cells and Ova-peptide in reduced

[11] see Materials and Methods section 2.1.3 on page 24

[12] Although reduced retrogenic HSCs had been used in the immunization experiment of TPO-retrogenic mice, as explained in the previous section 3.2.1, massive and undesirable effects were observed in both spleen and bone marrow. Therefore, efficiency of the retrogenic approach was further reduced, as ratios of retrogenic cells in the hematopoietic department below 10% still proved more than sufficient at impacting megakaryopoietic regulation. Thus, irradiation intensity was reduced to a sublethal dose of 450 rad, in hope to greatly hamper seeding of retrogenic HSC in a less affected bone marrow environment of recipient mice.

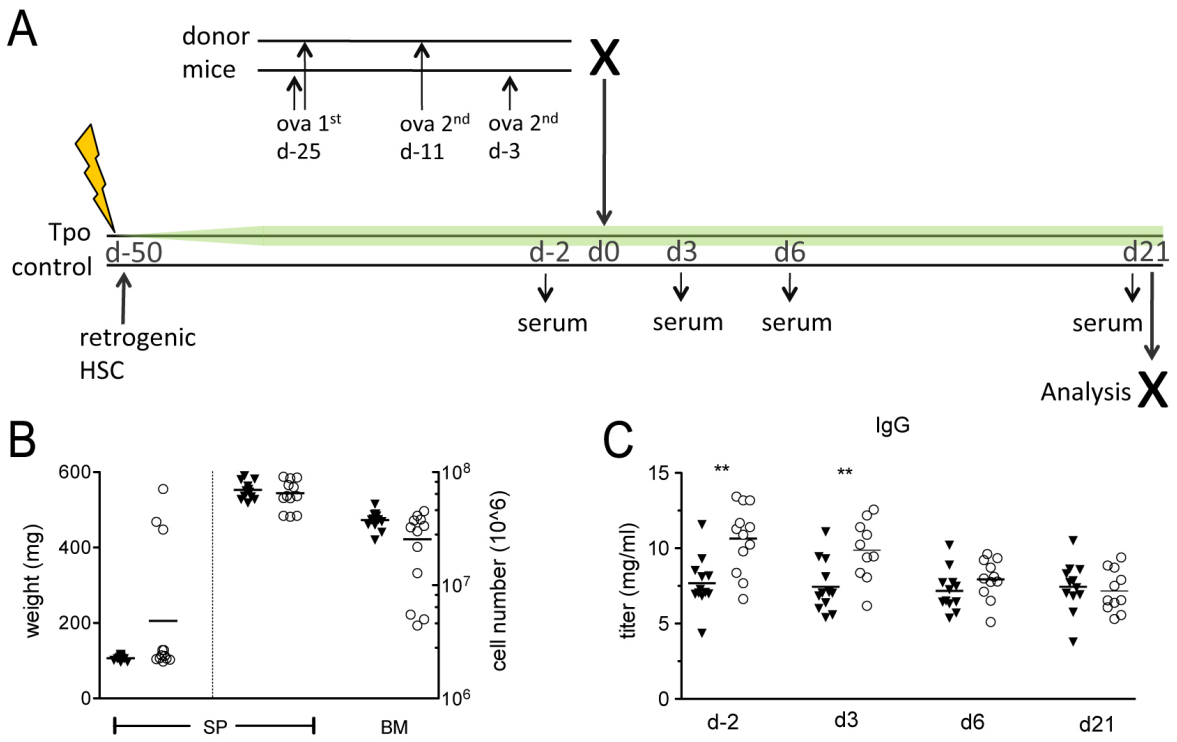

Figure 3.11: *Transfer of Ova-immunized donor splenic cells into TPO-retrogenic mice.* **A** Scheme for Ova transfer experiment as explained in the text. Briefly, donor BALB/c mice were boost immunized with Ova at different time-points prior to transfer of total splenic cells into TPO-retrogenic or GFP-retrogenic (control) recipient mice at day 50 after stem cell transfer. Serum was taken at different time-points before and after spleen cell transfer and mice were sacrificed three weeks after transfer. **B** Spleen weight and total cell number in spleen and bone marrow from sacrificed mice were determined. **C** Serum IgG antibody titers were determined over the time course of the transfer experiment.
n=12; GFP-control(▾); TPO retrogenic(○)

amounts and furthermore isotype-switched plasma cells originating from GC reactions most likely of reactivated memory B cells.

General features of retrogenic mice receiving Ova-transfer

Flow cytometry analysis of cells analyzed directly before the transfer revealed a mild Ova-specific immune response taking place in splenic cells from both immunization groups. Approximately 3000 Ova-specific plasma blasts and plasma cells were transferred *i.v.* along with manyfold more Ova-specific B cells, as computed from total cell counts and population frequencies determined via flow cytometry (data not shown). Mice were frequently controlled throughout the experiment and no obvious difference between TPO and control group could be found. Weight curves showed no striking

difference; TPO mice displayed slightly (mean $\Delta < 0.5$ g) reduced body weight starting around the sixth week after transfer of TPO-retrogenic HSC transfer (data not shown). Mice were sacrificed at day 21 after Ova-immunized splenic cell transfer and organs were inspected for appearance and weight and cell number was determined, as seen in Fig. 3.11B. Of the 12 TPO-retrogenic animals, only 3 displayed features of enlarged spleens as described before. However, splenic cell numbers were only slightly decreased. Similarly, only 3 of the retrogenic mice showed visible signs of bone marrow alterations, as they appeared notably paler and less crimson, which coincided with roughly 60% decreased cell counts in organs of these mice. However, only one mouse had a combined phenotype in both organs, indicating independent regulation of these effects.

Antibody titers of retrogenic mice receiving Ova-transfer

Blood was taken from the recipient mice at different time points before and after the transfer of splenic cells from Ova-boosted donor mice as indicated in Fig. 3.11A. Total IgM titers were similar in both mouse groups throughout the experiment (data not shown). Total IgG antibody levels, however, were significantly increased before and early after Ova-transfer in TPO-retrogenic mice compared to the GFP-control (Fig. 3.11C). No significant difference was detected at later time points for total IgG, possibly caused by an inhibitory effect of immunization on pre-existing antibody levels. Also, no significant increase in total antibody titers was observed after Ova-transfer, suggesting that the transferred immune response lead to a rather weak immune response in the recipient mice that did not significantly add to the pre-existing titers. This is further undermined by the fact that no Ova-specific IgM titers could be measured in either group (data not shown). Ova-specific IgG titers could be detected after Ova-transfer but they only reached levels 5-fold lower than those seen in blood from Ova-boosted mice. Additionally, no difference could be observed in Ova-specific titers between both groups of mice.

Plasma cells in retrogenic mice receiving Ova-transfer

The two groups of retrogenic mice that received cells from Ova-immunized mice were sacrificed three weeks after transfer when the immune reaction was expected to be terminated. Any differences in plasma cells at this time point would originate from different survival of the generated plasma cells rather than their generation as the majority was already generated or driven to expansion and differentiation.
Splenic and bone marrow plasma cells numbers were determined via ELISPOT. No significant difference was observed for total plasma cell numbers of either measured isotype. Only Ova-specific IgG ASCs were slightly reduced in the TPO-retrogenic group. In contrast, Ova-specific IgG secreting cells were significantly increased in bone marrows of TPO-retrogenic mice whereas no difference was observed for Ova-specific IgM secreters. Looking into total ASCs in bone marrow, a highly significant drop (to 40%) of IgM plasma cells was observed in the TPO group.

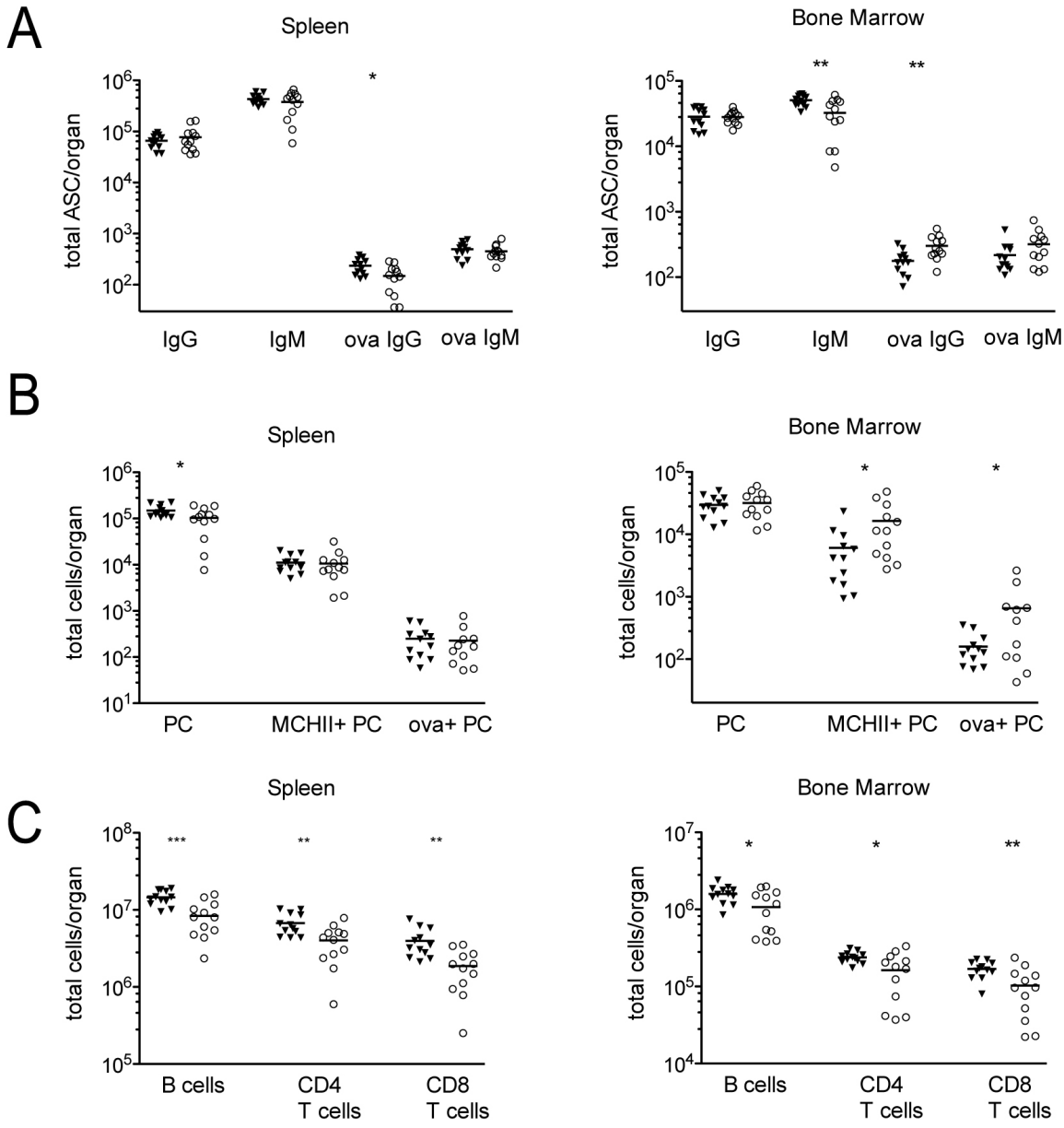

Figure 3.12: *Plasma cell and lymphocyte analysis of TPO-retrogenic mice after transfer of Ova-boosted splenic cells.*
Experiment was performed as delineated in Fig. 3.11 and mice were sacrificed at day 21 after spleen cell transfer into TPO(○)- or GFP(▾)-retrogenic mice. **A** Single cell suspensions from spleen (left panel) and bone marrow (right panel) were analyzed with ELISPOT for numbers of ASCs of IgM and IgG isotypes total and specific for Ova-peptide. **B** Plasma cells ($B220^{-/lo}CD138^{++}$) were identified and counted via flow cytometry and further subdivided according to surface expression of MHCII and intracellular Ova binding. **C** Spleens and bone marrows were analyzed via flow cytometry for prevalence of major lymphocyte populations using the lineage markers B220, CD4 and CD8.
n=12; GFP-control(▾); TPO retrogenic(○); PC, plasma cell.

Comparable results were obtained from respective flow cytometric analysis (Fig. 3.12B). In addition to the analysis of total and Ova-specific plasma cells, the marker MHCII was used to further discriminate between recently generated plasmablasts/ plasma cells (MHC^{++}) and terminally differentiated plasma cells ($MHC^{-/lo}$). A slight reduction of total plasma cells in TPO-mice was observed in the spleen but there was no difference in the plasmablasts or Ova-specific plasma cells.
In the bone marrow, a significant increase in both $MHCII^{+}$plasmablasts/plasma cells and Ova-specific plasma cells was observed in the TPO-retrogenic group compared to control. This indicates a selective advantage in TPO mice not only of the Ova-specific plasma cells but of all recently generated plasma cells.

Alteration of lymphocyte populations in retrogenic mice receiving Ova-transfer

As seen above, increased numbers of recently generated plasma cells were detected in the bone marrow of TPO-retrogenic mice. This could be due to increased survival or migration of plasma cells into the bone marrow of TPO-retrogenic mice or merely reflect an overall inflated lymphocyte population caused by increased levels of TPO. In previous experiments with TPO mice, severely decreased B cell frequencies were observed in TPO mice[13] but the situation might be different in these mice displaying a much weaker phenotype as they were not lethally irradiated.
In Fig. 3.12C, flow cytometry analysis of B and T cell populations is shown. All measured populations (B cells, $CD4^{+}$and $CD8^{+}$T cells) were significantly decreased in TPO mice (20-40% reduction). This reduction was more pronounced in spleens compared to bone marrow. As total cell numbers in spleen were comparable between both groups of mice, this decreased lymphocyte count must have been compensated by a different cell type. These cells can only be assumed to be extramedullary hematopoietic progenitors mobilized and expanded by the high TPO levels prevalent in the bone marrow of TPO-retrogenic mice. However, numbers of HSCs were not determined by flow cytometry.
On the other hand, the lymphocyte reduction seen in the bone marrow of TPO mice was well in line with the observed reduction of total cell counts.

3.2.3 Transfer of retrogenic spleen cells into Ova-immunized mice

So far, titers and plasma cells after immunizations were analyzed in mice with an already altered megakaryocyte compartment. In order to investigate the effects of an acute increase in megakaryopoiesis on an ongoing immune reaction, small amounts of retrogenic cells were transferred into Ova-immunized non-irradiated wild type mice (Fig. 3.13A). Control mice received similar amounts of GFP-retrogenic cells. To differentiate between plasma cells generated prior to the immunization from the ones arising

[13] see Fig. 3.7B

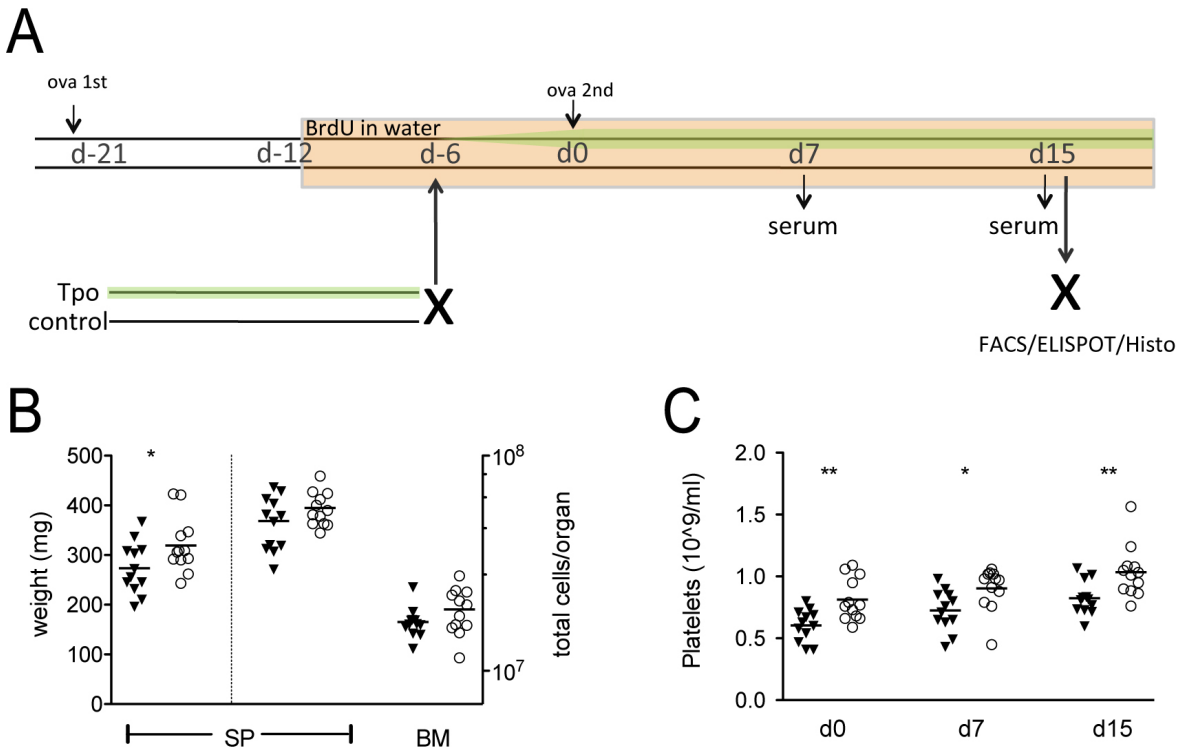

Figure 3.13: *Transfer of TPO-retrogenic splenic cells into Ova-immunized animals.* **A** Scheme for the TPO-transfer experiment as explained in the text. Briefly, recipient mice were *i.p.* immunized with Ova in alum and three weeks later boosted with the same antigen *i.p.* (day 0). 6 days before boost, total splenic cells from TPO- or GFP-retrogenic mice were transferred into recipients for short-term increase in megakaryopoiesis. Serum was taken at the noted time points and mice were sacrificed two weeks after boost. **B** Spleens weight and total cell numbers as assessed via flow cytometry are shown. **B** Defined amounts of blood were taken at the given time points and platelet numbers were determined vial flow cytometry as described in section 2.4.3. n=12; GFP-control(▾); TPO retrogenic(○)

from the immune reaction, mice were continuously fed with BrdU, starting about two weeks before the secondary immunization. Plasma cells negative for BrdU must have been generated and stopped dividing before the first dose of BrdU.
6 days after transfer of retrogenic HSCs, a secondary immune reaction was triggered by *i.p.* Ova injection.
Two weeks after boost immunization, mice were sacrificed and analyzed. The two groups of mice did not display any overt phenotypical differences and weight curves showed no differences (data not shown). Similarly, total cell numbers in spleen and bone marrow were comparable and only a slight increase in spleen size was observed (Fig. 3.13B) between the groups. After visual examination, neither spleen nor bone marrow seemed to be influenced by the TPO levels achieved with this method.

Platelets and megakaryocytes in mice receiving TPO-transfer

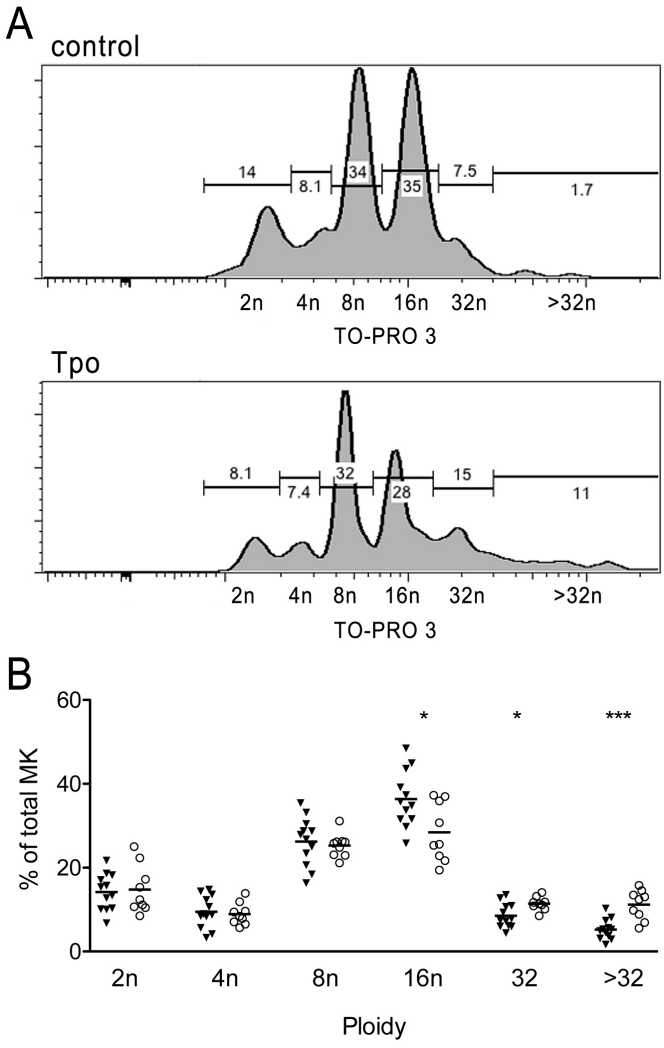

Figure 3.14: *Ploidy analysis of bone marrow megakaryocytes.*
A Representative histograms of bone marrow MKs of GFP-retrogenic control (upper panel) and TPO-retrogenic mice(bottom panel). The ploidy analysis was performed as described in 2.4.4. Histograms show cells gated on MKs ($SSC^{+}CD61^{++}$) and TO-PRO 3 incorporation is determined. Numbers represent percentages of cells in respective ploidy state.
B MK ploidy comparison between GFP- and TPO-retrogenic mice with ploidy distribution analyzed as shown in **B**. Ploidy state on the x-axis is plotted against the respective percentage of megakaryocytes.
n=12; GFP-control(▾); TPO retrogenic(○); MK, Megakaryocyte

In order to confirm that TPO levels were indeed stably increased in mice receiving TPO-retrogenic cells, platelet count analysis[14] was performed using blood drawn at different time points after TPO-transfer. As seen in Fig. 3.13C, platelet counts were significantly increased in the TPO group compared to controls, revealing successful modulation of the megakaryopoietic system by our approach. Only an increase in the number of fully mature megakaryocytes can cause an elevated platelet count as seen in the TPO mice.
In order to further define the impact of increased TPO-levels, flow cytometric ploidy analysis was performed of bone marrow megakaryocytes[15]. A pair of representative histograms of this analysis comparing ploidy states between bone marrow megakaryocytes from one control and one TPO mouse is displayed in Fig. 3.14A. The peaks represent megakaryocyte populations with a common ploidy stage which were statistically assessed as seen in Fig. 3.14B. No difference could be seen in the frequencies of less mature megakaryocytes and progenitors with ploidy stages between 2 and 8. In the 16n population, a decrease is seen in the TPO group. In contrast, megakaryocytes of the highest maturity (32n and higher) are significantly increased in the mice that received TPO-retrogenic cells, revealing a striking shift in favor of highly mature megakaryocytes in these mice. Of note, these large polyploid megakaryocytes were found in contact with bone marrow plasma cells (161).

Antibody titers in mice receiving TPO-transfer

As seen in the previous section, slightly increased levels of TPO caused by a transfer of few TPO-retrogenic cells into immunized mice lead to a notable shift of bone marrow megakaryocytes toward highly mature stages. Next, a possible change in antibody production in these mice was investigated via ELISA.
No difference in total and Ova-specific IgM titers could be observed at any time point (data not shown). In contrast, total IgG titers were significantly increased two weeks after secondary immunization (Fig. 3.15A). More importantly, Ova-specific IgG titers in TPO mice were significantly increased already one week after boost with a tendency to further increase over time. Hence, increased TPO-levels clearly influence the amount of the immune response.

Splenic GC reaction in mice receiving TPO-transfer

Next, the question arose whether these increased antibody titers were caused by a prolonged GC reaction in the spleen and could therefore be attributed mainly to short-lived plasma blasts in the spleen. As seen in Fig. 3.16, B cells were present in comparable numbers in both groups of mice. However, total GC B cells and especially the ones of IgG1-isotype that contain the majority of Ova-specific B cells in these mice (90), were significantly decreased in TPO mice. Switched, post-GC B cells however, were present

[14] see Materials and Methods section 2.4.3 on page 40
[15] see Materials and Methods section 2.4.4 on page 40

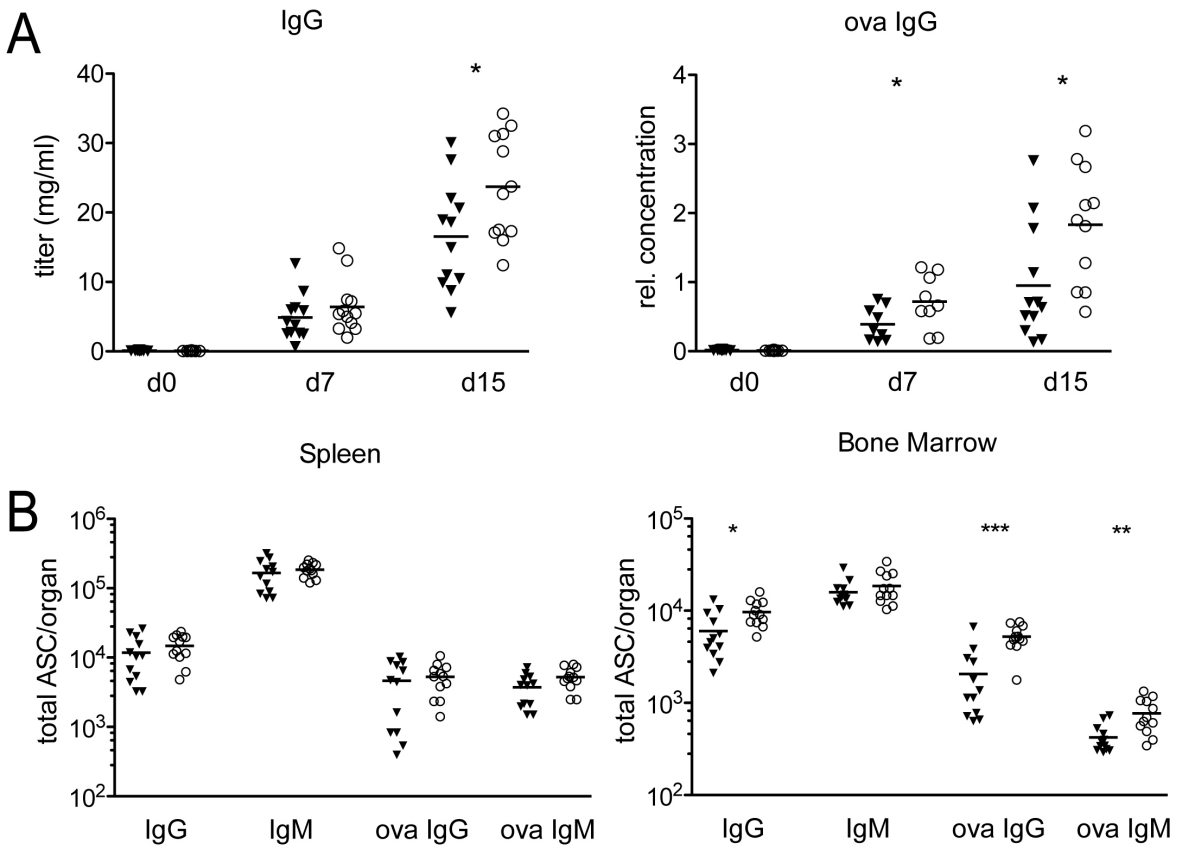

Figure 3.15: *Analysis of antibody titers and antibody producing cells in mice receiving TPO-retrogenic splenic cells*
Mice were treated as explained in the text and depicted in Fig. 3.13A **A** Blood was taken at the time points noted on the x-axis and serum antibody levels were determined via ELISA for total IgG (left panel) and Ova-specific IgG (right panel). **B** Numbers of plasma cells secreting total and Ova-specific IgM and IgG antibodies were determined by ELISPOT.
n=12; GFP-control(▾); TPO retrogenic(○); ASC: antibody secreting cell; d, day

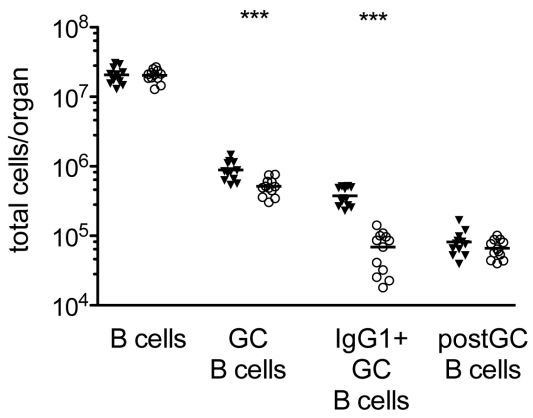

Figure 3.16:
Analysis of GC reaction in mice receiving TPO-retrogenic splenic cells
Splenic cells of control and TPO-retrogenic animals were analyzed via flow cytometry for prevalence of GC reaction. Noted cell populations were defined as follows: B cells: $B220^+CD4/8^-$; GC B cells: as before plus $CD38^+PNA^+$; postGC B cells: $IgG1^+PNA^-$ B cells.
n=12; GFP-control(▾); TPO retrogenic(○)

in similar numbers in both groups. These B cells keep both their isotype and CD38 expression but become negative for the GC specific marker PNA (122).

Plasma cells in mice receiving TPO-retrogenic cells

As the GC response was clearly diminished in the TPO group two weeks after immunization, increased maintenance of plasma cells must account for the higher antibody titers seen in TPO mice. In order to test this assumption, spleen and bone marrow were analyzed with ELISPOT for antibody-secreting cells (Fig. 3.15C). No significant differences in plasma cell numbers between control mice and TPO mice were seen in spleen. In bone marrow of TPO mice, IgG^+plasma cell numbers were significantly increased compared to control. Furthermore, Ova-specific plasma cells of both IgM and IgG isotype were significantly increased in the mice that had received TPO-retrogenic cells. Clearly, the presence of increased numbers of polyploid megakaryocytes strongly favors the survival of antigen-specific plasma cells coming from a recent immune reaction.

3.3 Gene Expression Analysis of Murine Megakaryocytes

In the last section, TPO levels were demonstrated to influence antibody titers as well as plasma cell homeostasis and maintenance. Most likely, this was mediated by megakaryocytes interacting with plasma cells.
Plasma cells require survival signals to prevent apoptosis and several of these factors have already been identified (16). Megakaryocytes could possibly provide these signals. In order to probe this possibility, megakaryocyte mRNA was isolated via LCM for ensuing gene expression studies.

3.3.1 LCM of single bone marrow megakaryocytes for expression analysis

LCM requires a 2-dimensional cell preparation to work properly. For our goal, this could be achieved either by cytospin preparations of bone marrow cells or by cryosections of murine bone marrow.
Cytospins allow for adjustment of cell density as well as enable the user to manipulate cell suspensions prior to the cytospin procedure. Thus, megakaryocytes could be purified via negative MACS-enrichment before the cytospin procedure.
LCM on cryosections is advantageous as it adds structural and co-localization information to cell isolation. Additionally, cryosections are kept at $-20°C$, which reduces RNA degradation by cell-intrinsic degradation pathways.

LCM from Cytospins

Initially, isolation of mature megakaryocytes was attempted from cytospin slides obtained from whole bone marrow cell suspensions (Fig. 3.17). Megakaryocytes were easily identified with the microscopic unit of the LCM device after staining the sections with fluorochrome-coupled antibodies against the megakaryocyte marker CD41. However, LCM of these cells failed due to strong adherence of the cells onto the slide. It was, therefore, necessary to investigate other means of isolating megakaryocytes containing intact RNA from murine tissues.

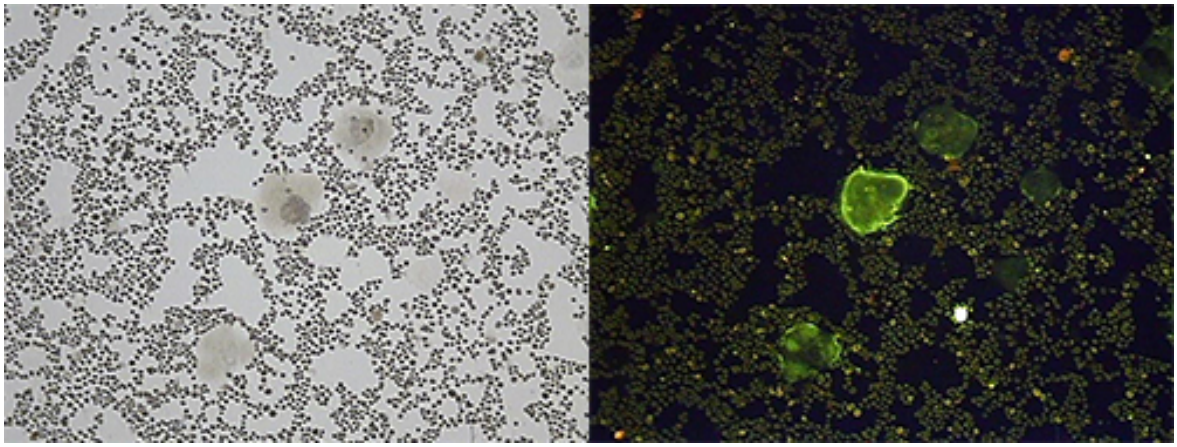

Figure 3.17: *Cytospin of murine bone marrow cells*
Bone marrow cells were prepared from murine femora. Single Cell Suspension was adjusted to $3 \cdot 10^4$ cells were applied to the cytospin device.
A shows the slide in light transmission mode. **B** shows the slide stained against CD41 with a FITC-coupled antibody.

LCM on bone marrow cryosections

mRNA was obtained from cryosections of fresh murine bone marrow under differing fixation conditions. Special focus was put on keeping the RNA as stable as possible for ensuing RT into cDNA. For microarray analysis of isolated RNA to be successful, quality and amount of sample has to be very high. Isolation procedure was performed with strict adherence to the precautionary measures described in section 2.8
Initial LCM experiments were performed with sections from total femora or tibiae. Retaining the bone structure, however, proved to be disadvantageous for the capture, as bone fragments oftentimes became brittle and salient, thereby preventing the cap membrane to align properly with the tissue section. Hence, a method to isolate consummate and intact bone marrow tissue from murine tibia was established in order to circumvent the difficulties with bone (2.8.1).

RNA-quality after LCM

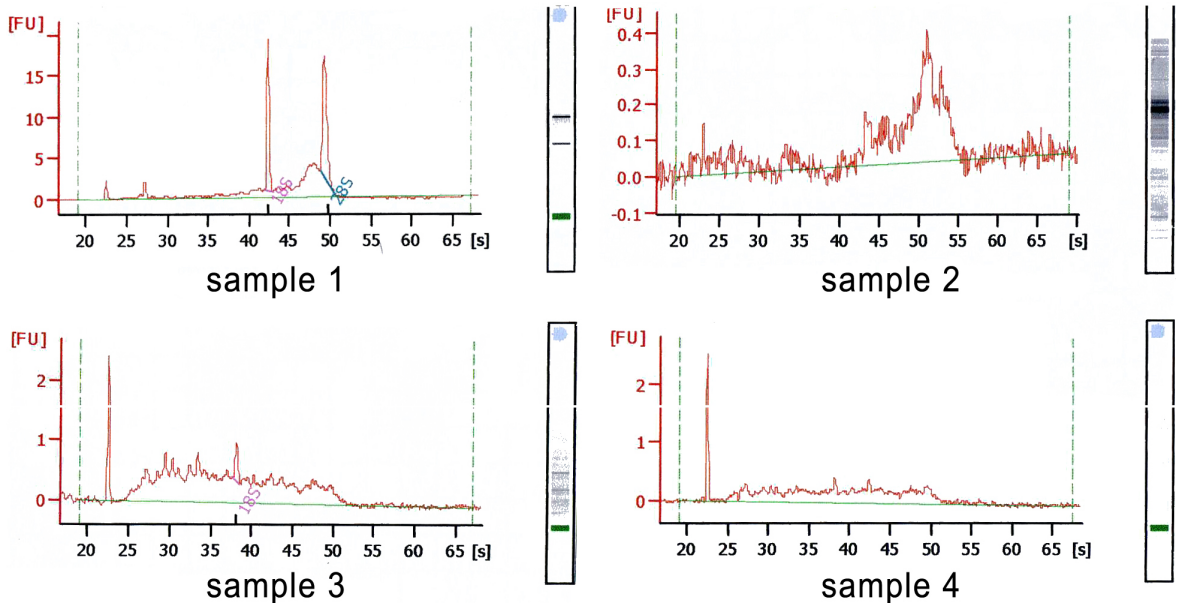

Figure 3.18: *RNA quality after LCM and RNA purification*
Whole bone marrow RNA was extracted as described in the text for each sample and was then subjected to RNA quality analysis with the BioAnalyzer Instrument. According to the peaks of the 18S rRNA and 28S rRNA, quality of purified RNA dramatically decreases along with the number of purification steps applied, resulting in virtually no useable RNA after performing the full procedure.

For an initial assessment of RNA, 4 slides containing consecutive cryosections of BALB/c bone marrow were treated under different conditions as follows:

Sample 1 - control RNA was directly added to elution buffer as a positive control

Sample 2 - control RNA was directly added to extraction buffer for RNA isolation

Sample 3 - Entire tissue was extracted from fresh non-fixed slides

Sample 4 - Tissue was prepared as for LCM and than placed in extraction buffer

Samples 2 to 4 were next subjected to the providers RNA isolation procedure, dissolved in elution buffer and subsequently vacuum dried to 3fold concentration.
After RNA-isolation, RNA was reverse transcribed with 3'-primers against the mRNA sequence of the housekeeping gene hypoxanthine-guanine phosphoribosyl transferase (HPRT). All samples showed comparable cDNA amplification as estimated from gel electrophoresis (data not shown). However, when overall RNA quality was determined, all samples subjected to the RNA-isolation procedure showed strong signs of degradation according to the detectability of 18S and 28S rRNA peaks (see Fig. 3.18). As a counter-measure, yeast rRNA was added from that point on as carrier to the extracted solution.
Nevertheless, RNA quality did not reach the standards required for microarray analysis. As seen in Fig. 3.19, RNA quality was greatly improved after addition of carrier RNA when tissue is extracted right after the fixation procedure (sample 5). However, after an additional waiting period of 3 hours, which would be a rough time estimate for the extraction of 30-50 pure megakaryocytes, RNA shows severe degradation (sample 6), as seen by the diffusion and broadening of the 18S- and 28S-rRNA peaks. Hence, the isolation of the minimum number of megakaryocytes necessary to obtain about 2 μg of RNA required for microarray analysis takes too long with LCM to yield high quality RNA.
Therefore, the RNA extracted from megakaryocytes was analyzed with the less demanding RT-PCR. Reverse transcription and ensuing PCR only require a fraction of the isolated RNA to remain intact. Consequently, expression analysis had to be restricted to a limited set of genes known to be crucial for the maintenance of murine plasma cells.

3.3.2 RT-PCR analysis of LCM-isolated megakaryocytes

We decided to analyze megakaryocytes for expression of the following survival factors:

- IL-6 – is regarded the most potent survival factor for newly generated plasma cells *in vitro* (16)
- SDF-1 (stromal cell-derived factor 1) – acts as both a chemoattractant and a survival factor for plasma cells *in vitro* (48, 16)
- TNFα – has also been shown to be a survival factor for plasma cells in culture (16)

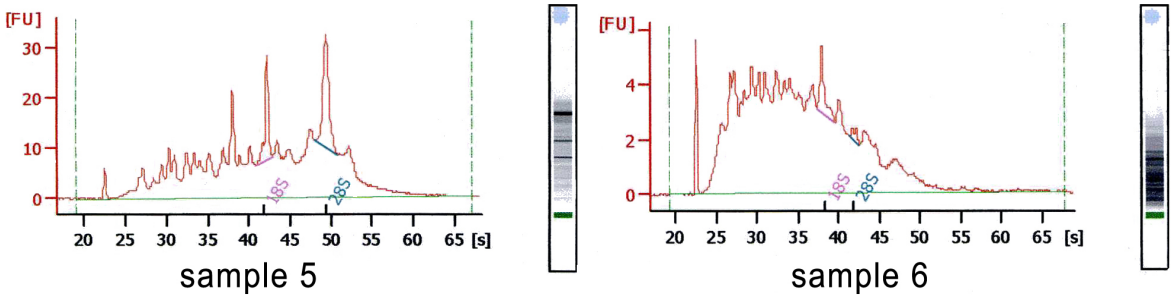

Figure 3.19: *RNA quality after LCM and RNA purification when using carrier RNA* Whole bone marrow RNA was extracted as described for Fig. 3.18. For sample 5, extraction was performed directly after fixation and dehydration. For sample 6, an additional waiting period of 3 hours was included to simulate degradation due to time spent for the capture procedure. rRNA peaks are not detectable after the waiting period. Please note the erroneous identification of rRNA peaks in sample 6.

- APRIL (a proliferation-inducing ligand) – acts via the receptor B cell maturation antigen (BCMA) on plasma cells which is essential for long-lived plasma cell *in vivo* and promotes plasma cell survival *in vitro* (109)
- BAFF (B cell-activating factor belonging to the TNF family) – also acts via the essential receptor BCMA on plasma cells and promotes plasma cell survival *in vitro* and *in vivo* (109, 85)

Additionally, a set of control genes was included into the experiment, in order to estimate purity and specificity of the extraction procedure.

- β-actin and hypoxanthine-guanine phosphoribosyltransferase (HPRT) – ubiquitous housekeeping genes that were used as positive controls in order to exclude failure of the RNA-isolation procedure.
- CD41 – is part of the gpII/gpIII glycoprotein complex on platelets and megakaryocytes and was used to ensure the successful isolation of megakaryocyte RNA.
- CD11b – is a marker for the majority of monocytes and macrophages prevailing in the bone marrow. The marker is used as a contamination control, as a pure megakaryocyte isolation should not contain CD11b RNA.

Establishment of RT-PCR

Primers for all the mentioned genes were designed using the mRNA and genomic sequences[16] and they were tested under various conditions on whole bone marrow template mRNA. A list of utilized primers is shown in Table 2.3 on page 33.

[16] available in online databases

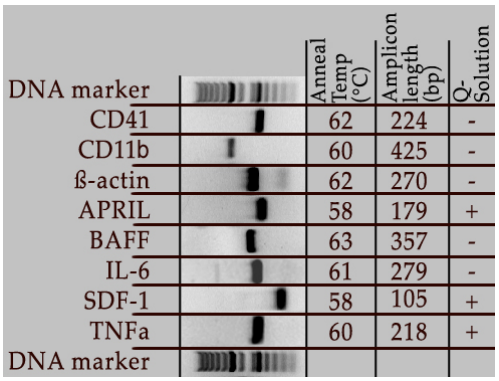

Figure 3.20: *Overview of PCR-products for expression analysis of megakaryocytes*
After optimization of PCR conditions for each primer pair, PCR was performed using whole bone marrow cDNA as template. The figure displays gel bands showing the respective amplicons, their calculated base-pair lengths, annealing temperatures as determined via gradient-PCR, and whether or not Q-solution was required.

Next, different RT-PCR approaches were tested for applicability in this investigation. Real-time RT-PCR offers the greatest sensitivity and allows exact quantification of transcripts. Initial experiments with whole bone marrow RNA from sample 6 (sample list on page 85), however, revealed a large extent of degradation evident in the extracted RNA (data not shown) making a 1-step RT-PCR the method of choice[17] for reasons of suitability. The advantage of this procedure is the inherent cell lysis capability of the RT-PCR mix allowing the user to forgo all RNA-extraction and isolation steps.
After LCM the caps were directly placed on PCR tubes containing the RT-PCR reaction mix. We succeeded in receiving a clear amplification of the housekeeping gene HPRT from as few as 100 pure megakaryocytes attached to a single LCM cap, but only when tRNA as a carrier was added to the RT-PCR mix prior to the amplification reaction (data not shown). However, in order to employ this semi-quantitative RT-PCR for the analysis of up to 8 genes, a multiplex RT-PCR was required. Attempts at establishing suitable primer combinations for the amplification of at least two control genes and two target genes failed due to the formation of excessive unspecific amplicons (primer dimers) or simply no product formation. Finally, RNA was extracted from bone marrow megakaryocytes by a conventional extraction/isolation method[18] using tRNA as a carrier at all times.

RT-PCR analysis of bone marrow megakaryocytes

Ultimately, RNA was extracted from between 180 to 310 murine megakaryocytes attached to a total of 20 caps and pooled for RNA isolation. Furthermore, comparable areas (as computed by the LCM software) of $CD61^-$ tissue were captured as controls. RNA showed immense signs of degradation comparable to that seen in sample 6 of Fig. 3.19. Nevertheless, 1-step RT-PCR was performed successfully with the resulting

[17] This kit uses a proprietary PCR mix additive called *Q-solution*, with every unique primer combination showing different (but oftentimes greatly increased) performance and specificity when *Q-solution* is added, as noted in table 3.20
[18] see Materials and Methods section 2.8.4 on page 51

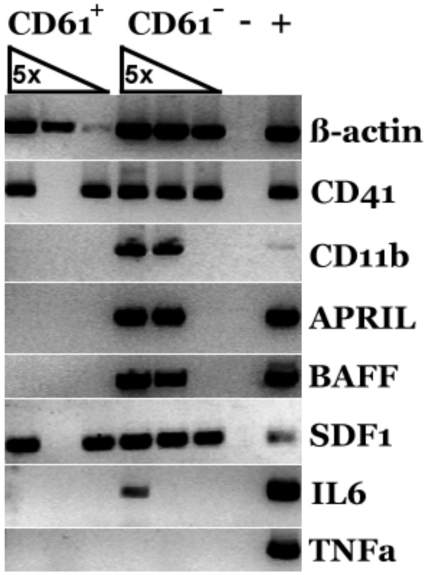

Figure 3.21: *RT-PCR results from LCM experiments*
Cryosections of bone marrow from adult BALB/c mice were stained with CD61-specific antibodies and fixed/dehydrated as described. 310 single megakaryocytes ($CD61^+$) and a comparable $CD61^-$ surface area was transferred to membrane caps using LCM. RNA of pure megakaryocytes and $CD61^-$ bone marrow was isolated after LCM. Both RNA samples were titrated in a 5-fold dilution series and semiquantitative RT-PCR was performed using primers as noted in the figure.
(-) Yeast RNA as a negative control.
(+) whole bone marrow RNA as a positive control.

RNA, as can be seen in Fig. 3.21. 5-fold dilutions of megakaryocyte ($CD61^+$) RNA and $CD61^-$ control tissue were used for the individual RT-PCR reactions for semi-quantitative interpretation of the results[19].
Occasionally, a PCR reaction failed to yield amplicons apparent in gel electrophoresis, as seen in the second lane of the $CD61^+$sample. Due to the low amount of initial mRNA material, degradation seems to behave almost stochastically, even though all measures preventing contamination with degrading RNase were taken. Consequently, in 20 to 30% of samples, RNA degradation led to no apparent product amplification, as exemplified in Fig. 3.21. RNA of 5-fold diluted megakaryocyte RNA contained yet sufficient β-actin mRNA to be amplified but failed to yield products for any of the other target genes, as inherent degradation rendered most of the remaining mRNA sequences too short to be recognized by the primers provided by the RT-PCR mix.

β-actin was detected in most of the $CD61^+$and $CD61^-$ RNA samples, whereas CD11b signals were measured merely in the $CD61^-$ fraction, showing overall success to isolate RNA from the tissues and proving the purity of the megakaryocyte RNA. CD41 gene expression was detected throughout the tissue in both megakaryocyte as well as $CD61^-$ RNA. This was probably due to the prevalence of small megakaryocyte progenitors of later stages that already show weak CD41 expression or due to RNA from $CD41^{++}$platelets that were too small to be detected via histological investigation. Interestingly, stromal cell-derived factor 1 (SDF-1) expression was reproducibly found in the megakaryocyte samples at levels comparable to that seen in total bone marrow RNA. However, no signals for either a proliferation-inducing ligand (APRIL), IL-6 or tumor necrosis factor (TNF)-α could be detected in any of the megakaryocyte RNA

[19]see Materials and Methods section 2.2.2 on page 26

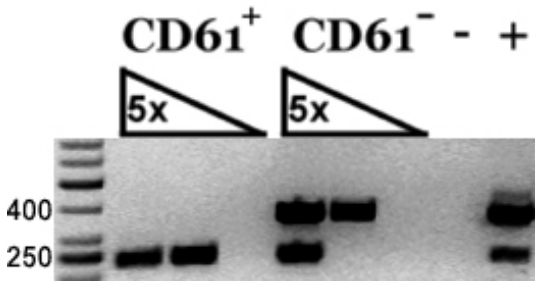

Figure 3.22: *MK RNA shows atypical product in RT-PCR specific for BAFF.*
RNA was isolated and diluted as explained in the text and in Fig. 3.21 and RT-PCR was performed with BAFF-specific primers. All CD61$^-$ samples show the predicted amplicon at 357bp. megakaryocyte-samples show only a band of ≈230bp.
(-) Yeast RNA; (+) Whole bone marrow RNA.

preparations. However, signals for these markers were also in very low abundance in the CD61$^-$ fractions as seen by the fact that products could rarely be detected even in the least diluted samples (see missing bands in Fig. 3.21). Especially IL-6 proved to be very unstable. On the other hand, the positive controls used with whole bone marrow RNA always showed strong signals.
The RT-PCR product for BAFF showed amplification in the higher concentrations of CD61$^-$ RNA preparations but no products of the predicted length of 357bp where detected in the megakaryocyte RNA. However, a smaller product was reproducibly obtained in all megakaryocyte samples and occasionally in the highest CD61$^-$ concentrations (not visible in the small gel cut-out in Fig. 3.21, but seen in Fig. 3.22). The primers for BAFF transcripts were designed to amplify a sequence spanning from exon 5 to exon 7 of the BAFF gene thereby encompassing the complete exon 6 with a length of 151bp. Thus it was possible, that the observed smaller product would be the result of a so far unreported alternative splicing event excising exon 6 and leading to a 206 bp fragment.
Following that assumption, the respective BAFF band was excised from the gel, cloned into the pCR2.1-Topo cloning vector (Invitrogen, US) and sent for sequencing. The resulting sequence failed to identify as an alternative splicing event and was furthermore barely recognized by any online alignment software. The only distant alignment originated from a structural protein of an algae, a result dwhich must be interpreted as highly inconclusive.
In summary, RNA was successfully isolated from pure megakaryocytes, albeit with low quality that did not allow us to use the obtained RNA for global expression profiling (GEP). We could show megakaryocytes to be rather high producers of the chemokine and survival factor SDF-1 on the transcription level but could neither show nor definitively exclude production of BAFF, APRIL, IL-6 or TNF-α by murine megakaryocytes. Low amounts of isolated RNA from megakaryocytes and degradation inherent to the method did not allow for definitive statement concerning the expression levels of mentioned sequences.

4. Discussion

4.1 Introduction

In the past, terminally differentiated, resting plasma cells with long half-lives were found to reside in the bone marrow (52,91) and to provide long-term antibody titers (5, 136,135). These protective antibody titers, essentially representing the humoral memory, provide the first line of defense against many re-encountered pathogens by facilitating complement activation, opsonization, and neutralization. Later, it was shown that long-lived plasma cells can contribute to autoimmune disease by facilitating chronic inflammation via constitutive autoantibody titers (111, 118). Additionally, they are resistent to conventional therapy (56).
What determines whether a plasma cell becomes long-lived?
For once, intrinsic factors like origin, affinity to antigen (36, 114) and isotype (138, 6) influence fate decision of plasma cells for entrance into the long-lived compartment. Soon, microenvironments in the bone marrow (88), and later also in the spleen (144), were shown to provide unique conditions essential for the survival of plasma cells and the name plasma cell niche was coined. Defining and manipulating these niches is of paramount importance for the clinical modulation of humoral memory. Vaccination strategies could be vastly improved by specifically triggering the establishment of an antigen-specific long-lived plasma cell compartment. Furthermore, disrupting the long-lived plasma cell survival niche could be a promising treatment for autoimmune diseases involving a humoral component like systemic lupus erythematosus (SLE).
Several soluble and matrix factors have been identified on the way toward a clear definition of the niche, including interleucin (IL)-6, tumor necrosis factor (TNF)-α (16) as well as signals transduced by the plasma cell receptors B cell maturation antigen (BCMA) and CD44 (109, 16). However, its cellular components are still ill-defined.
Recently, Winter et al could show (161) that megakaryocytes co-localize with and impact the survival of plasma cells. Additionally, a strongly inflated megakaryocyte population in the lupus-prone (New Zealand Black x New Zealand White)F1 (NZB/W) mice directly correlates with similarly increased plasma cell numbers in that organ (100), further underlining the importance of megakaryocytes for the plasma cell compartment.
The aim of this work was to further define the role of megakaryocytes for the generation and maintenance of plasma cells under homeostatic conditions and their impact on immune responses.

4.2 Methods Used in this Work

Different technical approaches were used for investigating the role of megakaryocytes in plasma cell niches. A brief discussion of the used methods and their applicability and caveats follows.

4.2.1 Working with mouse models

Immunological experiments with mice are well established and have been used for many centuries. Mice can be rapidly bred and easily be maintained due to their small size. As mammals they closely resemble the human immune system at least in terms of the used modalities, making them an invaluable tool not only in the field of immunology. Most experiments feasible in mice, e.g. immunization, disease induction, cell transfer, transgenes, comparison of clonally identical mice, as well as analysis of inner organs, cannot be performed in humans.
However, in the evolutionary course that separates humans and mice, several signaling cascades have been fine-tuned to fulfill the specific needs of the respective species. Factors like life span and available organ space e.g. in the bone marrow can greatly affect the way biological problems posed by the environment are solved evolutionarily. Hence, results obtained from mouse do not necessarily translate directly into the human immune system but give a general idea about the way evolution solved specific problems posed by the constant threat by pathogens.
Additionally, experimental mice are without any exception inbred strains that show only an individual facet of the murine immune system.

4.2.2 Induction of Megakaryopoiesis by retrovirally transgenic TPO

The systemic thrombopoietin (TPO)-levels are tightly regulated by blood platelets that bind most free TPO via the TPO-receptor c-Mpl[1]. Hence, even repeated injections of TPO only lead to a transient increase in megakaryocytes, as most TPO is bound and neutralized by the excess platelets generated as a consequence of the initial TPO-injection.
Only a few transgenic models for increased megakaryopoiesis are available as of yet. GATA-1low mice (155) express greatly increased megakaryocyte numbers. However, reduced platelet counts suggest these megakaryocytes to be functionally impaired. Furthermore, eosinophils are also affected by GATA-1 expression. As eosinophils have been shown to impact the establishment of the bone marrow plasma cell niche (20), interpretations of the results obtained from experiments with GATA-1low mice would be complicated.

[1] see Introduction section 1.4.2 on page 17

Ectopic expression of TPO, on the other hand, has been shown to increase megakaryocytes. TPO also affects hematopoietic stem cell (HSC) differentiation which is, nevertheless, unlikely to influence plasma cells in the bone marrow.
In the study described here, TPO was ectopically overexpressed in bone marrow resident HSC via retrogenic[2] transduction (84, 54) in order to constitutively increase megakaryocyte numbers. As shown in murine culture experiments (161), plasma cells are irresponsive to TPO signaling and do not express the receptor c-Mpl. Therefore, any alterations of plasma cell homeostasis would be attributable to TPO acting on megakaryocytes and their progenitors. However, several developmental stages upstream of megakaryopoiesis, e.g. proliferation of early hematopoietic progenitors, are also affected by TPO levels. Therefore, indirect effects have to be taken into account when interpreting the data. Furthermore, megakaryocytes are known to produce growth factors involved in bone remodeling and myelopoiesis. Consequently, drastically increased megakaryocyte numbers could also increase local concentrations of the respective growth factors leading to additional indirect effects.
Nevertheless, retroviral transduction was the method of choice to test this influence of TPO provision on plasma cell homeostasis, due to the ease of use and quick generation time compared to a conventional transgenic approach involving germ-line transmission of microinjected oocytes. So far, retroviral transduction cannot be used for lineage-specific gene expression, because the promoter regulating the gene of interest is fixed on the viral genome irrespective of the site of insertion into the host genome. TPO, however, is mainly produced systemically in the liver (71) and although local production in the bone marrow has been detected (143), its source and regulation remain elusive. Therefore, overexpression of TPO by all hematopoietic cells in the bone marrow appeared a suitable approach.
In the two-step protocol used (54), the first step was the generation of virus producer cell lines (92) that stably and safely produce high titers of retrovirus particles. By these means, retroviral transduction of murine cells was more reproducible as virus titers were not depending on transient expression in triple-transfected HEK 293 cells. Retroviral transduction has been used for many years as an easy and reliable means of gene transfer (84). In this work, retroviral transduction of mice with TPO was used for the manipulation of megakaryopoiesis in spleen and bone marrow in order to investigate the influence of megakaryocytes on plasma cell biology.
Finally, a TPO-dependent cell line was generated in order to show biological activity of TPO produced and secreted by TPO-retrogenic cells.

4.2.3 The cell line 32D-Mpl displays high sensitivity for TPO

The 32D cell line has been used for long in functional essays for the detection of cytokines. The original cell line 32D-clone3 has been derived from mouse long-term bone marrow cultures and is strictly dependent on IL-3 in the culture medium (44).

[2] retrogenic: neologism for retrovirally transgenic

The cytokine IL-3 causes 32D cells to proliferate in a concentration-dependent manner, whereas IL-3 levels below a certain threshold lead to cell arrest and apoptosis. Later, a number of 32D subclones were described that showed sensitivity to a range of different cytokines. They have been generated via selection in cell culture (133, 1) or transgenic expression of the respective receptor (153).
Using the established method of retroviral transduction, a cell line was generated that overexpressed the TPO-receptor c-Mpl (32D-Mpl). Selection via decreasing levels of TPO led to cells highly dependent on the cytokine TPO. Indeed, a striking correlation between the levels of TPO and the cell numbers (Fig. 3.3) was observed which closely resembled Michaelis-Menten-kinetics (97). It describes the kinetics of chemical reactions as a function of the concentration of the substrate that is being used up during the reaction. Similarly, the "substrate" TPO is used up by the 32D cell transforming the received signal into proliferation. TPO is bound on the cells by the receptor c-Mpl, after which the c-Mpl-TPO complex is rapidly internalized and degraded via lysosomal and proteasomal pathways (128). The cells were highly sensitive to soluble TPO in a concentration range from around 40 pg/ml up to 90 ng/ml. However, sensitivity was not sufficient for detecting differences in the TPO levels of mice. Human serum levels of unbound TPO have been found to be around 95 pg/ml (26) and this number might well be lower in mice, making detection with 32D-Mpl cells impossible. Nevertheless, the established essay is suitable for the reliable determination of functional TPO in a wide range of concentrations.
Applying this TPO essay, functional TPO was detected at high concentrations in the supernatant of cells transduced with the TPO-retrovirus (Fig. 3.3C) but not in cells transduced with the empty vector. This showed that TPO-retrogenic cells indeed produce and secrete functional TPO.

4.2.4 Laser capture microdissection

Megakaryocytes were found to be co-localized with plasma cells in the bone marrow under both homeostatic and inflammatory conditions, making them an obvious candidate for the production of plasma cell survival factors. Thus, megakaryocytes were investigated for production of one or more of these factors.
The analysis of the proteome (or the secretome) of a cell type is generally restricted by the numbers of protein markers that can successfully be identified with specific antibodies. Transcriptome analysis on the other hand, is greatly facilitated by the fact that the mere knowledge of the nucleotide sequence of a given marker suffices to identify its expression via reverse transcription (RT)-PCR or microarray analysis. However, gene expression analysis does not take into account the possibility for post-translational modifications or the mode of secretion which could be constitutive or inducible via storage vesicles.
The use fluorescence activated cell sorting (FACS) for the isolation of fully mature megakaryocytes was not successful, as the large, highly mature megakaryocytes did

not withstand the harsh physical conditions[3] prevailing during that procedure.
Consequently, laser capture microdissection (LCM) from bone marrow cryosections was established as a means to isolate highly pure megakaryocytes for RNA isolation. This method allows for fluorescent microscopy-aided isolation of defined cells. Possible applications would be the specific isolation of megakaryocytes found in contact with plasma cells.

4.3 Discussion of Results

Long-term survival of plasma cells in appropriate niches is the prerequisite for protective antibody titers with a long half-life and without the need for B cell re-stimulation, making these microenvironments attractive targets for new vaccination strategies (126). However, the same niches can also contribute to constitutive autoantibody titers in an autoimmune setting (56). Defining the molecular and cellular components of this niche is of paramount importance for future therapies and vaccination strategies.
Co-localization studies previously performed in our lab identified large multi-nucleated megakaryocytes as promising candidates for more in-depth investigation (161). Therefore, these results were furthered by analyzing the humoral immune response in mice displaying elevated megakaryocyte numbers. Therefore, a TPO-retrogenic mouse model (54) was used by which a clear connection between antibody production and levels of the megakaryocyte growth factor TPO could be shown.

4.3.1 Effects of increased TPO-levels by retrogenic cell transfer

Tpo-retrogenic mice show increased megakaryopoiesis

The retroviral transduction of mice with Thpo, the coding sequence for the protein TPO, for elevation of megakaryopoiesis proved successful, as can be seen by increased numbers of megakaryocytes in the spleens of TPO-retrogenic mice compared to control mice (Fig. 3.5). Increased platelet numbers in blood (Fig. 3.13C) and an enlarged polyploid megakaryocyte compartment in bone marrow (Fig. 3.14) could be detected even at the mildest retrogenic dosage (without irradiation prior to retrogenic transfer), which shows the high efficiency of the method. Elevated platelet counts were stably detected throughout the experiment, suggesting that transgenic TPO production directly at the site of megakaryopoiesis overcomes the negative feedback that inversely correlates platelet numbers in blood to megakaryocyte numbers in the bone marrow (129, 72).
However, undesired side-effects were also observed. Several mice died of septic shock as a consequence of HSC transfer. This only occurred when the HSCs were co-cultured with the virus producer cells suggesting contaminating producer cells as the powerful

[3] Steep gradients in flow velocity at the nozzle create high pressures

immunogenic source. In follow-up experiments, this was prevented by refraining from direct co-cultures between virus producers and HSCs.

Effects of ectopic TPO on megakaryopoiesis are multilayered and time-dependent

Megakaryopoiesis is a fine-balanced biological system involving the three tissues liver, blood and bone marrow and the principal regulatory cytokine TPO[4]. This growth factor is constitutively and systemically produced by liver hepatocytes and the levels produced are maintained constant except during immune reactions (70). TPO travels through the blood stream and most of it is taken up and removed by the roughly 10^{11} platelets in circulation. The fraction of TPO arriving in the bone marrow acts on early and intermediate progenitors as well as on fully mature megakaryocytes (26). Proplatelet formation seems to be rapidly induced by peak levels of TPO on mature megakaryocytes resulting in a rapid drop in the numbers of highly polyploid megakaryocytes in the first hours of increased megakaryopoiesis. Simultaneously, increased stimulation of progenitor cells results in elevated hematopoiesis and new generation of megakaryocyte progenitors. Replenishment and hyper-compensation of the lost megakaryocytes follows after a few days. Soon, elevated platelet numbers in the blood dramatically decrease concentrations of available TPO (82) and megakaryopoiesis is halted.
Consequently, manipulation of this balance by *i.v.*-injection of TPO leads to a gradual increase in mature megakaryocyte progenitors at 4 and 8 days after injection (161). At day 10 after injection, megakaryocyte numbers are decreased most likely due to decreased TPO-concentrations reaching the bone marrow.
Similarly, the effects of increased TPO by retrogenic overexpression are highly dose- and time-dependent and not easy to predict.
At high concentrations, as seen in mice lethally irradiated prior to HSC-transfer (Fig. 3.1.5, 3.7), platelet counts in blood are high and numbers of megakaryocytes are elevated in the spleen. This is accompanied by severe side effects like osteoporosis and myelofibrosis. As seen by the weight curves reflecting overall fitness, severe effects only start to manifest late after retrogenic cell transfer (approx. after 7 weeks; Fig. 3.7B). Bone marrow of these mice could not be analyzed after 10 weeks because of excessive trabecular bone content but very high megakaryocyte frequencies can be assumed in this organ. Follicular structure in the spleen was disrupted and lymphocyte populations were offset. Hence, systemic immune reactions can be expected to be severely impaired in these mice, which would lead to decreased plasma cell generation.
At lower concentrations of TPO, threshold levels for osteopetrosis and myelofibrosis were not exceeded and consequently neither weight loss nor cell numbers were greatly affected in these mice. Alternatively, lower levels of initial TPO result in slower kinet-

[4]Other factors like granulocyte monocyte colony-stimulating factor (GM-CSF), IL-3, and IL-6 have also been shown to mediate megakaryocyte growth (152, 13, 25) but assert their effect rather on early progenitors than on mature megakaryocytes.

ics and delayed onset of side effects.
These milder effects notwithstanding, platelet counts were elevated and mature megakaryocyte numbers were significantly higher in the bone marrow of these TPO-retrogenic mice. Splenic megakaryocyte numbers were not investigated in these mice but are probably not significantly increased as elevated megakaryocyte numbers would result in myelofibrosis. The constitutively increased TPO-levels expressed by bone marrow HSCs did not tip the balance for a limited time but rather shifted the equilibrium of the megakaryopoietic system.
The half-life of megakaryocytes has not been established yet in certainty but it is widely assumed to be limited and to end in the consummate disintegration into proplatelets. Therefore, increased numbers of megakaryocytes must result in greater megakaryocyte turnover, i.e. the frequency of megakaryocyte disintegration and replenishment are increased. However, this remains speculative as clear data is still missing.

Osteopetrosis occurs late after increase of TPO-levels

The organs of TPO-retrogenic mice receiving lethal irradiation showed clear signs of altered cellularity and architecture at later time points after retrogenic cell transfer. The bone marrow of these mice appeared very pale and showed signs of osteopetrosis identified by decreased medullary space and greater content of trabecular bone, which greatly hampered analysis via flow cytometry or histology of these organs.
Increased levels of TPO possibly caused an imbalance in bone remodeling. Osteoblasts of non-hematopoietic origin build up new bone material whereas osteoclasts of hematopoietic origin resorb it (147). TPO has not only been shown to be the main growth factor for mature megakaryocytes and their progenitors, but it has also been identified as a major cytokine regulating hematopoiesis (24). TPO drives differentiation of hematopoietic progenitors towards megakaryopoiesis, which could indirectly reduce numbers of other hematopoietic lineages including osteoclasts. A decreased osteoclast department cannot resorb sufficient amounts of bone material which leads to excessive bone formation by osteoblasts. This would explain the osteopetrotic phenotype of mice with high levels of TPO in the bone marrow.
Furthermore, a direct link between megakaryocytes and bone remodeling has been established recently (69, 68). Megakaryocytes were shown to express several factors directly or indirectly involved in bone metabolism. Production of osteocalcin (148) or osteonectin (119, 12) by megakaryocytes could directly lead to increased bone formation if these cells were prevailing at highly elevated numbers.
On the other hand, osteoblasts can possibly be elicited to proliferate and form new bone material by still ill-defined mechanisms involving megakaryocytes expressing estrogen and calcium-sensing receptors (10, 55).

Additionally, osteoblasts can be stimulated in cultures by megakaryocytes to down-regulate osteoclastogenic receptor activator of NF-κB ligand (RANKL) and to express higher levels of the respective antagonistic decoy receptor osteoprotegerin (OPG), revealing an indirect pathway for increased bone formation (9). Finally, megakaryocytes have been found to directly inhibit osteoclastogenesis and thereby bone resorption in culture via thus far unidentified factors (69).
Mice receiving lower dosages of TPO-retrogenic cells showed only marginal or no signs of osteoporosis, suggesting that kinetics of osteoporosis are regulated by retrogenic TPO-levels. Side effects could have been manifested much later (and after the time point of analysis) in these mice. Alternatively, development of side effects depends on a threshold concentration of TPO that was not met in mice that had not been lethally irradiated before retrogenic cell transfer.

Anemia and splenic myelofibrosis are a late consequence of increased megakaryopoiesis

The medullary space of highly TPO-retrogenic mice did not only display symptoms of osteopetrosis but also appeared much paler than in control mice. Additionally, the spleens of TPO-retrogenic mice displayed increased size, smaller total cell counts and a disturbed follicular structure, all symptoms of severe myelofibrosis (96). These negative effects of higher TPO levels in bone marrow and spleen were partly linked and caused by the effects of TPO on hematopoietic progenitors. TPO boosts HSC proliferation and shifts the ratios of developing cell types toward the megakaryocyte lineage and away from erythroblasts and other cell types.
Increased levels of transgenic TPO specifically in murine HSCs has previously been found to cause fatal myelofibrosis (157). It is still argued whether this aberrant behavior is directly accountable to TPO acting on hematopoietic progenitors or caused indirectly by factors expressed by elevated numbers of megakaryocytes. However, circumstantial evidence strongly suggests megakaryocytes to be causative for myelofibrosis. Support for this comes from GATA-1 low mice that display high megakaryocyte levels accompanied by myelofibrosis and anemia (155). Coherently, megakaryocytes have been found to produce several growth factors involved in hematopoiesis and myeloproliferative disorders including transforming growth factor (TGF-β) (159), platelet-derived growth factor (PDGF) and vascular endothelial growth factor (VEGF). In line with that, myelofibrosis is abolished in TPO transgenic TGF-$\beta^{-/-}$ mice (18), revealing TGF-β as indispensable for pathogenesis.
We performed weight curves in order to monitor the health status of the mice roughly reflecting the development of fatal myelofibrosis. At high dosage of TPO, mice started to show signs of pathology around 7 weeks after TPO-transfer, whereas in the lower dosage models no such effects were visible. This indicates the existence of a threshold level for TPO leading to these aberrant effects that is only reached after the TPO-retrogenic HSC compartment has sufficiently expanded. Side effects might manifest much later (after the time point of analysis) in these mice.

In summary, retrogenic TPO clearly leads to increased megakaryopoiesis. Side effects were observed only in mice receiving lethal irradiation prior to retrogenic HSC-transfer.

4.3.2 Antibody titers in TPO-retrogenic mice

Antibody titers reflect plasma cell numbers under the observed conditions

Antibody levels in the blood are tightly regulated by several distinct mechanisms affecting both their generation and systemic half-life (89).
Plasma cells and plasma blasts constitutively secrete antibodies into the blood stream and the interstitial tissue space, where they are positioned to neutralize pathogens and to activate effector mechanisms. Secretion levels of individual antibody secreting cells (ASCs) are not assumed to be regulated externally and thus antibody titers are mainly a function of plasma cell numbers.
Antibody half-life is unlikely to be affected by TPO as neither megakaryocytes nor platelets express Fc-receptors (FcRs) and the cells expressing immunoglobulin (Ig)G recycling receptor FcRn like endothelial cells are not affected by TPO-treatment.
Therefore, changes in antibody levels caused by altered TPO levels are accountable mainly to differences in plasma cell numbers under these conditions. Plasma cells are generated mainly in secondary lymphoid organs. These involve intestinal peyer's patches of the mucosal immune system expressing IgA isotype, lymph nodes of the lymphatic system and the spleen as the lymphatic organ in charge of systemic immune responses. The latter two organs mainly produce plasma cells of the isotypes IgM and IgG.
After being generated, plasma cells undergo apoptosis after a few days unless they are rescued via survival signals expressed in respective plasma cell niches located in bone marrow (91) and to a certain extent in the splenic red pulp (144). Thus, antibody titers under non-inflamed conditions are informative of the overall size of the collective plasma cell survival niche since only plasma cells protected from apoptosis can sustain antibody levels that would otherwise decline only a few days after the immune reaction, depending on the antibody-half-life.
Antibody titers during immune reactions are influenced by both the generation and survival of newly generated plasma cells as well as the underlying homeostatic antibody levels. Here, detection of antigen-specific antibody levels (and plasma cells) allowed us to investigate the influence of altered megakaryopoiesis on plasma cell generation and maintenance of plasma cells in the long-lived plasma cell niche.
In summary, changes of IgM and IgG antibody titers are directly accountable to plasma cell numbers in secondary lymphatic organs and bone marrow.

Homeostatic IgG titers are elevated in mice with increased megakaryopoiesis

Increased megakaryopoiesis by TPO-retrogenic HSC-transfer had different outcomes depending on strength and duration of the retrogenic approach, differently impacted

antibody levels. At high HSC transfer efficiencies, retrogenic TPO led to massively disturbed bone marrow architecture and splenic myelofibrosis accompanied by severely decreased cell counts. This was confirmed by following the weight of these mice which declined around week 7. Coherently, IgM antibody titers in these mice were largely decreased compared to control mice (Fig. 3.9B), indicating a massive defect in the immune response in these animals.
IgG-titers, on the other hand, were comparable or even slightly increased in these mice, hinting at a distinct impact of megakaryopoiesis on IgG plasma cells. Any overt positive effect mediated by increased megakaryopoiesis in spleen and bone marrow, however, was most likely outweighed by the defective generation of any kind of B lineage cell (Fig. 3.7C, 3.12).
In contrast, mice receiving a milder dosage of TPO-retrogenic HSCs did not show such severe signs of aberrant organ development as in the previous experiments. In these mice, IgG titers were significantly increased compared to control animals, albeit only within a narrow time-frame depending on the conditions of the respective experiment:

- In the experiment using sub-lethally irradiated mice that received retrogenic HSC-transfer 7 weeks before transfer of ovalbumin (Ova)-immunized splenic cells, (Fig. 3.11C), TPO-levels gradually increased due to a positive auto-feedback loop between TPO-susceptible HSCs and the production of TPO by these very cells. This probably resulted in the observed side-effects at later time-points.

- When small numbers of TPO-retrogenic cells were transferred into non-irradiated mice (3.13) shortly before secondary Ova immunization, the TPO-retrogenic compartment had to establish itself in the target organs in order to exert its impact on plasma cells, which explains the increase in IgG titers only at the late time point.

The impact of aberrant splenic megakaryopoiesis on homeostatic antibody titers could not be clarified in this mouse model due to the strong side effects accompanying strongly TPO-retrogenic mice. Splenic myelofibrosis, disrupted follicular structure and highly decreased total cell counts observed in these mice adversely affected antibody generation and masked any favoring effects possibly conveyed by the inflated megakaryocyte population.
However, plasma cell frequencies were increased at early time points in mice with increased splenic megakaryocytes before exacerbation of side effects (Fig. 3.10) which was not reflected in titers due to the decreased cell numbers. Further, significantly increased IgG titers in mice that received Ova-specific donor cells (Fig. 3.11C) might be at least partly attributable to increased plasma cell survival in spleens displaying elevated TPO-levels.
Lupus-prone NZB/W mice show an autoimmune phenotype characterized by increased total and autoreactive antibody titers that ultimately cause fatal glumerulonephritis (56). These mice display both a greatly enlarged long-lived plasma cell compartment in spleen and highly elevated numbers of splenic megkaryocytes, strongly suggesting

a link between the two cell types (100). Possibly, survival signals provided by splenic megakaryocytes favor the maintenance of potentially autoreactive plasma cells originating from primary foci which results in autoantibody titers. Interestingly, Sle2, one of the major lupus susceptibility loci derived from NZB/W mice, maps into a region comprising the gene for the TPO-receptor c-Mpl (98, 164). Importantly, the Sle2 locus, increased megakaryopoiesis and elavated splenic plasma cell numbers are all genetically contributed by the parental New Zealand Black (NZB) strain further hinting at a crucial role for TPO-c-Mpl signaling in plasma cell homeostasis and possibly the development of humoral autoreactivity.
Nevertheless, further interpretations on the role of splenic megakaryocytes in plasma cell homeostasis remain speculative with the retrogenic approach.
In summary, these data clearly show that increased TPO-levels result in increased IgG antibody titers, strongly indicating a beneficial effect of megakaryocytes on plasma cell survival and therefore on the size of the plasma cell niche. This effect seems to be specific for IgG plasma cells originating mainly from germinal center reactions rather than from extrafollicular immune responses, as IgM titers are not affected by increased TPO-levels.

Antigen-specific antibody titers are specifically protected by increased megakaryopoiesis

Secondary immunization with the T-cell-dependent antigen Ova of mice that received retrogenic HSC after lethal irradiation (Fig. 3.7A; from here on referred to as *lethally irradiated mice*) rapidly led to increased Ova IgM titers in control mice but only a slight increase in the Ova-specific IgG titers (Fig. 3.9B) when compared with Ova titers in non-irradiated mice after secondary immunization. This indicates that the primary immunization performed in these mice two weeks after lethal irradiation did not trigger a complete immune response and thus the secondary immunization set three weeks later was more characteristic of a a primary response. In addition, these TPO-retrogenic mice started displaying symptoms of disturbed immunity around the time point of secondary immunization, which would explain the failure to properly respond with Ova-specific IgM titers. In line with total IgG titers, antigen-specific titers of IgG isotype were much less decreased compared to the IgM titers that remained below the detection limit of ELISA. Possibly, the few antigen-specific IgG-secreting plasma cells were protected from apoptosis by larger numbers of megakaryocytes in these mice.
Accordingly, Ova-specific antibodies specifically of the IgG isotype were significantly increased in mice that received secondary Ova-immunization along with a TPO-retrogenic cell transfer (Fig. 3.15A), whereas IgM antibodies were comparable in both groups.
This preferential increase (or markedly less decrease) in IgG titers specific for Ova could have been caused by a stronger germinal center response in TPO-retrogenic animals, as class switched plasma cells originate predominantly in germinal centers (120). However, splenic germinal center B cells were markedly decreased in these mice (Fig. 3.16), which excludes this possibility. Alternatively, the extrafollicular immune response that

precedes germinal center generation could be impaired in TPO-retrogenic mice leading to faster development of germinal centers as well as a shift in isotype distribution towards IgG, as IgM^+short-lived plasmablasts are the predominant outcome of the extrafollicular response (144). No data is available, however, to solidify the latter hypothesis.
Hence, only improved survival of IgG^+plasma cells could account for the increased titers.

4.3.3 Plasma cells in TPO-retrogenic mice

Theoretically, two important steps determine the longevity of plasma cells within the confines of a limited-niche concept:

1. In order to become long-lived, plasma cells have to enter the respective survival niche which might be occupied by pre-existing plasma cells from earlier immune responses. Thus far, no selection mechanism has been discovered for the entrance into the long-lived plasma cell niche in bone marrow or spleen, favoring a certain type of plasma cell over others. Rather, a stochastic model has been proposed that argues for a dynamic niche maintaining constant cell numbers via an equilibrium between entrance of plasma cells bearing novel specificities and depletion of tiny fractions of pre-existing plasma cells with various specificities (53). In a niche of constant size (i.e. supporting survival of a fixed number of cells), the number of depleted cells would directly translate into available free spaces to be occupied by the newly generated cells.

2. Independent of the entrance phase, the overall size of the niche directly affects the number of plasma cells that can be supported by the niche. Assuming a fixed fraction of the entire niche be depleted during each immune response, greater niche size would also result in a greater number of plasma that could enter the vacancies.

It is difficult to conclusively decipher which of the two possibilities causes the increased antibody titers with both plasma cells and megakaryocytes partaking in a highly dynamic regulatory circuit. However, the analysis of different plasma cell compartments reveals distinct aspects of the proposed niche:

- Total plasma cell numbers in the bone marrow and spleen after a declined immune reaction (under homeostatic conditions) indicate the size of the respective plasma cell niche.

- Antigen-specific plasma cell numbers at different time points after immunization reflect entrance into the plasma cell niche, i.e. the extent to which newly-formed plasma cells can enter the niche compartment.

Megakaryopoiesis influences plasma cell homeostasis in the bone marrow

Further analysis of plasma cell populations in spleen and bone marrow revealed a striking difference between the two organs as far as plasma cell alterations were concerned. In TPO-retrogenic mice that received high dosage retrogenic cell transfer after lethal irradiation, total splenic plasma cell frequencies were severely decreased three weeks after immunization (Fig. 3.10). In bone marrow, however, plasma cell frequencies were significantly increased despite the profound decrease in total cell numbers in that organ.

Bone marrow versus spleen The distinction between the two organs might lie in the different prerequisites for plasma cell survival in these two organs. Whereas the general prevalence of megakaryocytes in the bone marrow argues for a possible supportive role for plasma cells there, spleens do not contain significant numbers of megakaryocytes under normal conditions, making their involvement in niche formation in the spleen less likely. The spleen has been shown to have limited plasma cell survival capacity (20-100 plasma cells per mm^2 as determined in histological sections; (144)) with long-lived plasma cells dispersed in the red pulp.
The relative absence of megakaryocytes makes other cell types like basophils (39) and dendritic cells (87) likely candidates for - or facilitators of entrance into - the splenic plasma cell niche, respectively. Furthermore, massive infiltration of megakaryocytes along with other mobilized cells of hematopoietic origin into an environment usually void of these cells - ultimately leading to the observed myelofibrotic symptoms - is likely to destabilize the existing plasma cell niche.
Accordingly, only marginal differences were observed with regard to plasma cell numbers in spleens of TPO-retrogenic mice generated without lethal irradiation. It can be assumed from the absence of splenomegaly and fibrotic symptoms, that no HSC mobilization took place eventually expand the megakaryocyte population there. And even under conditions of increased megakaryopoiesis, consequences for resident plasma cells might be unpredictable, as megakaryocytes may be different in that organ compared to bone marrow (134).
Naturally, increased megakaryopoiesis was mainly observed in the bone marrow showing an increase in the most mature megakaryocyte populations in this organ (Fig. 3.14). This was expected, as bone marrow is the primary site of megakaryopoiesis and is supposed to be sensitive to changes in TPO-levels (67). In contrast to the spleen, the majority of plasma cells in the bone marrow are isotype switched (161) and most have undergone somatic hypermutation of their antibody variable regions (138), reflecting the importance of this organ for the support of the humoral memory. Increased plasma cell frequencies under conditions of increased megakaryopoiesis reveal a connection between megakaryocytes and the bone marrow plasma cell niche. Thus, it has has to be assumed that alterations in the size of the respective plasma cell niche mediated by increased numbers of megakaryocytes were responsible for the increased IgG titers in TPO-retrogenic mice.

Newly generated, antigen-specific plasma cells are favored in TPO-retrogenic mice

Furthermore, transfer of small numbers of splenic cells from Ova immunized donors into TPO-retrogenic mice (Fig. 3.12) led to increased Ova-specific IgG^+plasma cells in bone marrow but a decrease in spleen when compared to control mice, underlining the difference between spleen and bone marrow.
The increased fraction of antigen-specific plasma cells in the bone marrow hints at a regulatory function of megakaryocytes for the entrance of plasma cells into the plasma cell niche. Further evidence for that is provided by the fact that total plasma cell numbers remained unchanged whereas newly generated major histocompatibility complex (MHC)$II^+$and Ova^+plasma cells were elevated in the bone marrow of TPO retrogenic mice[5] (Fig. 3.12B).
Accordingly, Ova-specific bone marrow plasma cell numbers were again significantly increased in mice displaying significantly increased fractions of highly polyploid megakaryocytes (Fig. 3.15B), whereas total plasma cell numbers remained more or less unchanged. These differences were not observed in spleen.

IgG vs. IgM In all experiments, the changes in antigen-specific IgG plasma cells were more prominent than those observed for the IgM isotype, which was also reflected by the measured antibody titers. Possibly, IgM plasma cells are less prone to enter the bone marrow niche due to insufficient homing or survival capacity. However, intrinsic advantages of IgG^+in contrast to IgM^+plasma cells have not been established yet.
Alternatively, IgM plasma cells might settle in the bone marrow primarily under homeostatic conditions in the absence of adaptive immune responses or after a primary immune response. If depletion of pre-existing niches were favored during increased megakaryopoiesis, this would indeed lead to decreased total IgM^+plasma cell numbers (or Ova-specific IgM^+) in change for higher antigen-specific plasma cells of predominantly IgG isotype when compared to control mice.

4.3.4 The germinal center reaction in TPO-retrogenic mice

Beside the increased support of newly generated plasma cells in the bone marrow of TPO-retrogenic mice compared to control, the analysis of the splenic germinal center reaction revealed additional alterations in the immune response of TPO-retrogenic mice.
Total and especially $IgG1^+$germinal center (GC) B cells associated with an Ova response (90), were highly decreased in mice that had received a mild dose of TPO-retrogenic cells with prior irradiation. In contrast, switched, post-GC B cells (140) were present in similar numbers in both groups, indicating an undisturbed memory B cell response in the TPO group.This indicates either a strong impairment of the splenic

[5]This could not have been a consequence of altered plasma cell generation, as splenic subpopulations were comparable in both groups.

GC reaction in the TPO-retrogenic mice or a drastically hastened secondary immune response in mice with elevated TPO-levels.
Differences in the number and frequency of T cells as observed in the blood of TPO-retrogenic mice (Fig. 3.12C) hint at a possibly offset B cell - T cell ratio resulting in a compromised GC reaction.
Following the alternative scenario, the potentially faster immune reaction in the TPO group could have already led to a contraction of the GC reaction, possibly mediated by the elevated Ova-specific antibody titers seen in these mice. This would also explain the smaller numbers of Ova IgG plasma cells in the spleens of TPO-retrogenic mice that received a transfer Ova-immunized splenic cells. Higher numbers of Ova IgG titers in bone marrow could have resulted in a more rapid abortion of the GC reaction.

4.3.5 Gene expression analysis of murine megakaryocytes

In order to investigate in which way megakaryocytes contribute mechanistically to the maintenance of plasma cells in the bone marrow, it was attempted to isolate megakaryocyte mRNA for expression analysis.

Megakaryocyte mRNA isolated with LCM is not suitable for microarray analysis

The analysis of thousands of genes in parallel called global expression profiling (GEP) allows for data-driven research such that interesting genes can be selected from the usually vast pool of putatively expressed genes according to the questions that need to be answered. In this work, the focus was laid on factors expressed by megakaryocytes that might influence plasma cell biology. Therefore, any data set obtained from GEP of *ex-vivo* megakaryocytes using microarray technology would be screened for secreted and adhesion molecules.
As seen in Fig. 3.18, RNA stability after LCM was not suitable for microarray analysis. Even after addition of yeast carrier RNA in order to prevent RNA degradation, the time necessary to dissect sufficient amounts of megakaryocytes from bone marrow tissue was enough for degradation to proceed too far (Fig. 3.19). Microarray analysis is a very sensitive quantitative method and therefore depends on high quality RNA in order to exceed the high detection limit of the method. With such advanced degradation as seen in our samples, many false-negatives would be obtained and possibly important information be lost.
Consequently, no GEP was performed and selected survival factors were analyzed for the expression in megakaryocytes.

Megakaryocytes express the chemokine SDF-1

The plasma cell survival factors shown in histology to be expressed by $CD41^+$megakaryocytes (161) could not be confirmed via LCM. This might be due to the advanced

RNA-degradation observed in our samples. Alternatively, these signals might have been falsely attributed to megakaryocytes because of unspecific binding or insufficient subtraction of the high autofluorescence shown by megakaryocytes.
However, stromal cell-derived factor 1 (SDF-1) was shown for the first time to be expressed by bone marrow megakaryocytes via RT-PCR. This is a very interesting finding as this chemokine plays a twofold role in plasma cell homeostasis. First, SDF-1 is the major chemokine directing plasma cells into the respective niche in the bone marrow or other tissues (47). Secondly, plasma cells lose chemotactic responsiveness toward SDF-1 shortly after entering the bone marrow while expression of the cognate receptor CXCR4 remains intact. Signals transduced via SDF-1–CXCR4 now promote survival of plasma cells (16).
SDF-1 has been found to be expressed by several additional cell types in the bone marrow, the most prominent among these being stromal cells of mesenchymal origin (150). In that context it has been shown that megakaryocytes migrate towards SDF-1 (45) and interact with stromal cells producing SDF-1 in an $\alpha_4\beta_1$-integrin-dependent manner (34).
Therefore, it is tempting to regard megakaryocytes as part of a multicellular niche together with SDF-1$^+$stromal cells. Megakaryocytes could be attracted by SDF-1 gradients originating from stromal cells to facilitate encounter between the two cell types and plasma cells moving toward the same gradient. In that niche, megakaryocytes increase local SDF-1 concentrations and potentially provide additional plasma cell survival signals. This idea is further supported by findings that stromal cells themselves produce local TPO and may stabilize megakaryocytes by suppressing platelet formation (101, 103).

4.3.6 Proposed interplay between immune response and megakaryopoiesis

The results of the transfer of splenic cells from previously Ova-immunized mice into TPO-retrogenic mice clearly showed an impact of TPO levels and therefore of increased megakaryopoiesis on the maintenance of antibody titers and the numbers of recently generated plasma cells in the bone marrow. In that experimental setup, megakaryocyte numbers had already been elevated prior to the immune reaction.
It was shown previously that an increase in TPO levels via *i.v.* injection initially leads to an increase in total megakaryocytes accompanied by a drop in the number of highly polyploid megakaryocytes (160), a situation most likely resembling the initial stage of retrogenic HSC transfer. However, megakaryocyte numbers rapidly recovered and not even repeated TPO-injections were able to increase megakaryocyte numbers again. This is due to a negative feedback between megakaryocytes in the bone marrow and platelet counts in blood[6] resulting in a quick return of megakaryocytes to equilibrium numbers. In TPO-retrogenic mice, constitutively elevated TPO-levels led to an equilib-

[6]Please see Introduction section 1.4.2 on page 17

rium between megakaryocytes and platelets in the blood at much higher megakaryocyte numbers because TPO levels had been uncoupled from blood platelet numbers.
It is possible that the initial tipping of the TPO equilibrium leading to a rapid drop in highly mature megakaryocytes immediately followed by a quick compensatory boost in megakaryocytes of more immature stages indeed regulates the entry phase of plasma cells migrating to the bone marrow plasma cell niche. In other words, depletion of highly mature megakaryocytes as a result of an ongoing immune response might lead to depletion (or mobilization) of pre-existing plasma cells followed soon by the re-establishment of vacant niche-forming megakaryocytes (110). Newly generated plasma cells that enter the bone marrow favorably occupy these niche vacancies and become part of the long-lived plasma cell compartment.
This hypothesis is solidified by the fact that the coincidence of immune reaction and tipping of megakaryopoietic equilibrium is the common scenario during injury. Blood loss, wound healing and blood vessel coagulation lead to a drop in platelet numbers causing more TPO to reach megakaryocyte progenitors in the bone marrow. Also, systemic TPO levels are coupled to inflammation via IL-6 expressed by many immune cells early in inflamed tissues. Interleucin-6 leads to increased systemic TPO-production by hepatocytes (70, 132) also resulting in increased megakaryopoiesis. A few days later, pathogens entering the blood stream via the wound have proliferated sufficiently to elicit a systemic immune reaction. Facilitating plasma cell entry into the bone marrow niche under these circumstances would be an efficient mechanism to ensure long-term protection via long-lived plasma cells constitutively producing antibodies against the encountered pathogen.
So far, the half-life of megakaryocytes under homeostatic conditions has not been determined, albeit the existence of long-lived megakaryocytes appears to be a precondition for this hypothesis. In an alternative dynamic niche model, plasma cells might require only occasional contact with plasma cells.
Whether megakaryocytes indeed have no influence on the actual niche capacity but rather regulate solely the depletion of pre-existing specificities remains elusive.

4.4 Outlook

A clear link between TPO-levels and the plasma cell compartment could be shown. Megakaryocytes are strongly indicated to be the mediators of this interaction. However, undesirable side effects and insufficient data about certain aspects of megakaryopoiesis like half-life or immediate response to changes in TPO-levels preclude further investigation with the retrogenic mouse model. Especially, the role of an inflated megakaryocyte compartment in spleen remains unresolved.
More sophisticated models like megakaryocyte-specific inducible transgenics could further enlighten the importance of megakaryocytes by e.g. targeted disruption of putative survival factors specifically on megakaryocytes. Thereby, the possibility to modify vaccination strategies by targeted modulation of the megakaryocyte populations will be

scrutinized in appropriate mouse models of immunization.
Future lines of research will focus on the impact of increased splenic megakaryopoiesis in lupus-prone NZB/W mice on the development of autoantibody titers. Interestingly, the gene for the TPO-receptor c-Mpl is located within the SLE-susceptibility locus Sle2 on chromosome 4 (99, 98), which raises the possibility that indeed the TPO-cMpl axis is important for establishment of the autoimmune lupus phenotype. To that end, it will be investigated whether crossing mice carrying the Sle2 locus with cMpl $^{-/-}$ mice abolishes or at least ameliorates the autoimmune phenotype observed in these animals. This would shed more light on novel approaches for the treatment of autoimmune diseases with contribution from humoral memory.
Finally, intravital microscopy of bone marrow in homeostasis and after immunization will shed more light on the life cycle of megakaryocytes and the time-resolved interaction with plasma cells. A refined view on the impact of megakaryocytes and other involved cell types in entry and maintenance of plasma cells will help to further characterize the dynamics of the plasma cell niche (60).

5. Summary

Long-lived plasma cells constitutively produce protective antibody titers and persist in survival niches in the bone marrow and spleen. Identification of the cellular microenvironment in these niches would allow improvement of vaccination protocols and facilitate treatment of autoimmune disease. Megakaryocytes have been shown to colocalize with plasma cells and both cell types are concomitantly increased in the spleens of lupus-prone NZB/W mice, strongly indicating a mutual interaction within a shared niche.

Therefore, the role of megakaryocytes in plasma cell maintenance in the bone marrow and splenic microenvironment was further investigated in this work. Mice retrovirally transgenic for TPO were established as a model for increased megakaryopoiesis.

Elevated megakaryopoiesis was correlated with a significant increase in IgG antibody titers under homeostatic conditions. In an immune reaction against Ova, increased megakaryopoiesis led to larger antigen-specific plasma cell numbers in bone marrow, suggesting an impact of megakaryocytes on the shaping of the long-lived plasma cell niche there. Elevated plasma cell numbers in bone marrow were caused by increased survival of plasma cells and not by increased generation because the germinal center reaction was impaired in TPO-transgenic mice. A dose and time-dependent effect of TPO on both splenic architecture and bone remodeling was also observed, highlighting additional effects of increased megakaryopoiesis.

These experiments showed that increased TPO-signaling resulted in improved plasma cell survival and elevated antibody titers. This suggests a role for the TPO-cMpl axis in the establishment of humoral memory and the maintenance of autoimmune diseases.

For the analysis of a possible molecular mechanism, gene expression analysis was performed of bone marrow megakaryocytes isolated via LCM. They were found to express SDF-1, a major chemoattractant and survival factor for plasma cells. Megakaryocytes might attract plasma cells and provide survival signals to plasma cells upon contact via SDF-1 and other factors. Alternatively, they could orchestrate plasma cell migration into a niche mutually shared with other cells like stromal cells that could provide additional survival factors.

In future studies, the impact of megakaryopoiesis will be investigated in more sophisticated transgenic models in order to shed more light on the impact of megakaryopoiesis on humoral immunity in health and disease. The contribution of megakaryopoiesis to the establishment of autoimmunity will be further elucidated in the NZB/W model for SLE.

Zusammenfassung

Langlebige Plasmazellen produzieren in ihren Überlebensnischen in Knochenmark und Milz kontinuierlich protektive Antikörper. Die Identifizierung der an der Nische beteiligten Zelltypen würde über deren gezielte Manipulation neue Therapien für Autoimmunerkrankungen sowie verbesserte Impfprotokolle ermöglichen. Es wurde gezeigt, dass Megakaryocyten mit Plasmazellen kolokalisiert sind und das beide Zellarten in den Milzen von NZB/W-Mäusen, einem Modell für SLE, stark vermehrt auftreten. Beides zusammen legt eine Beteiligung von Megakaryozyten an der Plasmazellnische nahe.
Daher wurde in dieser Arbeit die Rolle der Megakaryozyten für das Plasmazellüberleben in Milz und Knochenmark näher untersucht. Zu diesem Zweck wurden Mäuse generiert, die retroviral transgen für TPO sind. In diesen Mäusen ging eine verstärkte Megakaryopoese unter homöostatischen Bedingungen einher mit einem signifikanten Anstieg der IgG Antikörpertiter. Infolge einer Immunreaktion gegen Ovalbumin führten größere Megakaryozytenzahlen zu einer Erhöhung der antigen-spezifischen Plasmazellzahlen im Knochenmark, was die Vermutung nahelegt, dass Megakaryozyten in diesem Organ einen Anteil an der Öffnung der Plasmazellnische für neue Spezifitäten haben. Da die Keimzentrumsreaktion in TPO-retrogenen Mäusen vermindert war, lässt sich schließen, dass die erhöhten Plasmazellzahlen im Knochenmark durch verbessertes Überleben als durch verstärke Nachbildung von Plasmazellen verursacht wurde. Zusätzlich wurde in diesen Mäusen ein zeit- und dosisabhängiger Effekt der erhöhten TPO-level auf die Milzarchitektur und die Knochenneubildung festgestellt, der auf weitergehende Effekte der erhöhten Megakaryopoiese hindeutet.
Diese Experimente haben gezeigt, das sich die von TPO vermittelten Signale in höheren Plasmazellzahlen und Antikörpertitern äußern. Damit lässt sich eine Rolle für die TPO-cMpl-Achse im Aufbau des humoralen Gedächtnisses sowie der Etablierung von Autoimmunkrankheiten vermuten. Um einen möglichen molekularen Mechanismus zu ergründen, wurden Megakaryozyten mit LCM aus dem Knochenmark isoliert und ihre Genexpression untersucht. Dabei wurde herausgefunden, das sie das Chemokin SDF-1 expremieren, welches sowohl die Migration als auch das Überleben von Plasmazellen fördert. Damit könnten Megakaryozyten Plasmazellen anziehen und daraufhin deren Überleben mittels SDF-1 und zusätzlicher Faktoren gewährleisten. Alternativ könnten sie Plasmazellen in eine gemeinsame Nische locken, die sie mit Zellen teilen, welche wiederum Plasmazellüberlebensfaktoren produzieren.

In weiterführenden Studien soll die festgestellte Rolle der Megakaryozyten im humoralen Gedächtnis und ihre Beteiligung an Autoimmunerkrankungen unter besser kontrollierbaren Bedingungen überprüft werden. Dazu sollen induzierbare Transgen-Modelle sowie gezielte Kreuzungen in Wildtyp- und NZB/W durchgeführt werden.

References

[1] G. Amabile, A. D. Noia, E. Alfani, A. M. Vannucchi, M. Sanchez, D. Bosco, A. R. Migliaccio, and G. Migliaccio. Isolation of TPO-dependent subclones from the multipotent 32D cell line. *Blood Cells, Molecules, and Diseases*, 35(2):241–252, 2005. 94

[2] D. Avery, S. L. Kalled, J. I. Ellyard, M. Thien, R. Brink, F. Mackay, P. D. Hodgkin, and S. G. Tangye. BAFF selectively enhances the survival and effector function of $CD38^+$ plasmablasts generated from activated human memory B cells. *Journal of Clinical Investigation*, 112:286–297, 2003. 12

[3] T. D. Bartley, J. Bogenberger, P. Hunt, Y. S. Li, H. S. Lu, F. Martin, M. S. Chang, B. Samal, J. L. Nichol, and S. Swift. Identification and cloning of a megakaryocyte growth and development factor that is a ligand for the cytokine receptor mpl. *Cell*, 77(7):1117–1124, 1994. 16

[4] E. Belnoue, M. Pihlgren, T. L. McGaha, C. Tougne, A. F. Rochat, C. Bossen, P. Schneider, B. Huard, P. H. Lambert, and C. A. Siegrist. APRIL is critical for plasmablast survival in the bone marrow and poorly expressed by early-life bone marrow stromal cells. *Blood*, 111(5):2755, 2008. 12

[5] R. Benner, W. Hijmans, and J. J. Haaijman. The bone marrow: the major source of serum immunoglobulins, but still a neglected site of antibody formation. *Clinical and Experimental Immunology*, 46(1):1–8, 1981. 91

[6] M. J. Benson, L. D. Erickson, M. W. Gleeson, and R. J. Noelle. Affinity of antigen encounter and other early B-cell signals determine B-cell fate. *Current Opinion in Immunology*, 19(3):275–280, 2007. 91

[7] N. L. Bernasconi, E. Traggiai, and A. Lanzavecchia. Maintenance of serological memory by polyclonal activation of human memory B cells. *Science*, 298(5601):2199–2202, 2002. 7

[8] M. Bopst, C. Haas, B. Car, and H. P. Eugster. The combined inactivation of tumor necrosis factor and interleukin-6 prevents induction of the major acute phase proteins by endotoxin. *European Journal of Immunology*, 28(12):4130–4137, 1998. 2

[9] S. Bord, E. Frith, D. Ireland, M. Scott, J. Craig, and J. Compston. Megakaryocytes modulate osteoblast synthesis of type-I collagen, osteoprotegerin, and RANKL. *Bone*, 36(5):812–819, 2005. 98

[10] S. Bord, S. Vedi, S. R. Beavan, A. Horner, and J. E. Compston. Megakaryocyte population in human bone marrow increases with estrogen treatment: a role in bone remodeling? *Bone*, 27(3):397–401, 2000. 97

[11] F. W. Brambell, W. A. Hemmings, and I. G. Morris. A theoretical model of Gamma-Globulin catabolism. *Nature*, 203:1352–1354, 1964. 6

[12] J. Breton-Gorius, P. Clezardin, J. Guichard, N. Debili, L. Malaval, W. Vainchenker, E. M. Cramer, and P. D. Delmas. Localization of platelet osteonectin at the internal face of the alpha-granule membranes in platelets and megakaryocytes. *Blood*, 79(4):936–941, 1992. 97

[13] V. C. Broudy and K. Kaushansky. Thrombopoietin, the c-mpl ligand, is a major regulator of platelet production. *Journal of Leukocyte Biology*, 57(5):719–725, 1995. 96

[14] K. L. Calame. Plasma cells: finding new light at the end of B cell development. *Nature Immunology*, 2(12):1103–1108, 2001. 5

[15] L. M. Calvi, G. B. Adams, K. W. Weibrecht, J. M. Weber, D. P. Olson, M. C. Knight, R. P. Martin, E. Schipani, P. Divieti, F. R. Bringhurst, L. A. Milner, H. M. Kronenberg, and D. T. Scadden. Osteoblastic cells regulate the haematopoietic stem cell niche. *Nature*, 425(6960):841–846, 2003. 9, 10

[16] G. Cassese, S. Arce, A. E. Hauser, K. Lehnert, B. Moewes, M. Mostarac, G. Muehlinghaus, M. Szyska, A. Radbruch, and R. A. Manz. Plasma cell survival is mediated by synergistic effects of cytokines and adhesion-dependent signals. *The Journal of Immunology*, 171(4):1684–1690, 2003. 12, 13, 83, 86, 91, 106

[17] F. Ceciliani, A. Giordano, and V. Spagnolo. The systemic reaction during inflammation: the acute-phase proteins. *Protein and Peptide Letters*, 9(3):211–223, 2002. 2

[18] H. Chagraoui, E. Komura, M. Tulliez, S. Giraudier, W. Vainchenker, and F. Wendling. Prominent role of TGF-β1 in thrombopoietin-induced myelofibrosis in mice. *Blood*, 100(10):3495 –3503, 2002. 98

[19] S. Chevrier, C. Genton, A. Kallies, A. Karnowski, L. A. Otten, B. Malissen, M. Malissen, M. Botto, L. M. Corcoran, S. L. Nutt, and H. Acha-Orbea. CD93 is required for maintenance of antibody secretion and persistence of plasma cells in the bone marrow niche. *Proc Natl Acad Sci U S A*, 106(10):3895–3900, 2009. 13

[20] V. T. Chu, A. Frohlich, G. Steinhauser, T. Scheel, T. Roch, S. Fillatreau, J. J. Lee, M. Lohning, and C. Berek. Eosinophils are required for the maintenance of plasma cells in the bone marrow. *Nature Immunology*, 12(2):151–159, 2011. 14, 92

[21] B. R. Clark, J. T. Gallagher, and T. M. Dexter. Cell adhesion in the stromal regulation of haemopoiesis. *Baillière's Clinical Haematology*, 5(3):619–652, 1992. 14

[22] F. J. de Sauvage, P. E. Hass, S. D. Spencer, B. E. Malloy, A. L. Gurney, S. A. Spencer, W. C. Darbonne, W. J. Henzel, S. C. Wong, W. Kuang, K. J. Oles, B. Hultgren, L. A. Solberg, D. V. Goeddel, and D. L. Eaton. Stimulation of megakaryocytopoiesis and thrombopoiesis by the c-Mpl ligand. *Nature*, 369(6481):533–538, 1994. 16

[23] C. G. de Vinuesa, A. Gulbranson-Judge, M. Khan, P. O'Leary, M. Cascalho, M. Wabl, G. G. B. Klaus, M. J. Owen, and I. C. M. MacLennan. Dendritic cells associated with plasmablast survival. *European Journal of Immunology*, 29(11):3712–3721, 1999. 14

[24] N. Debili, F. Wendling, D. Cosman, M. Titeux, C. Florindo, I. Dusanter-Fourt, K. Schooley, N. Methia, M. Charon, and R. Nador. The mpl receptor is expressed in the megakaryocytic lineage from late progenitors to platelets. *Blood*, 85(2):391–401, 1995. 97

[25] V. R. Deutsch, T. A. Olson, A. Nagler, S. Slavin, R. F. Levine, and A. Eldor. The response of cord blood megakaryocyte progenitors to IL-3, IL-6 and aplastic canine serum varies with gestational age. *British Journal of Haematology*, 89(1):8–16, 1995. 96

[26] V. R. Deutsch and A. Tomer. Megakaryocyte development and platelet production. *British Journal of Haematology*, 134(5):453–466, 2006. 16, 94, 96

[27] M. A. Duchosal. B cell development and differentiation. *Semin Hematol*, 34:2–12, 1997. 5

[28] A. Ehrlich and R. Kuppers. Analysis of immunoglobulin gene rearrangements in single B cells. *Current Opinion in Immunology*, 7:281–284, 1995. 3

[29] B. D. Elzey, J. Tian, R. J. Jensen, A. K. Swanson, J. R. Lees, S. R. Lentz, C. S. Stein, B. Nieswandt, Y. Wang, B. L. Davidson, and T. L. Ratliff. Platelet-mediated modulation of adaptive immunity: A communication link between innate and adaptive immune compartments. *Immunity*, 19(1):9–19, 2003. 15

[30] N. Emi, T. Friedmann, and J. K. Yee. Pseudotype formation of murine leukemia virus with the g protein of vesicular stomatitis virus. *Journal of Virology*, 65(3):1202–1207, 1991. 22

[31] I. Ertenli, S. Kiraz, M. A. Öztürk, I. C. Haznedaroğlu, I. Çelik, and M. Çalgüneri. Pathologic thrombopoiesis of rheumatoid arthritis. *Rheumatology International*, 23(2):49–60, 2003. 17

[32] R. Ettinger, G. P. Sims, R. Robbins, D. Withers, R. T. Fischer, A. C. Grammer, S. Kuchen, and P. E. Lipsky. IL-21 and BAFF/BLyS synergize in stimulating plasma cell differentiation from a unique population of human splenic memory B cells. *The Journal of Immunology*, 178(5):2872, 2007. 12

[33] A. J. Ferraro, M. T. Drayson, C. O. S. Savage, and I. C. M. MacLennan. Levels of autoantibodies, unlike antibodies to all extrinsic antigen groups, fall following B cell depletion with rituximab. *European Journal of Immunology*, 38(1):292–298, 2008. 7

[34] N. E. Fox and K. Kaushansky. Engagement of integrin $\alpha 4\beta 1$ enhances thrombopoietin-induced megakaryopoiesis. *Experimental Hematology*, 33(1):94–99, 2005. 106

[35] J. N. Gass, N. M. Gifford, and J. W. Brewer. Activation of an unfolded protein response during differentiation of antibody-secreting B cells. *Journal of Biological Chemistry*, 277(50):49047 –49054, 2002. 12

[36] D. Gatto, T. Pfister, A. Jegerlehner, S. W. Martin, M. Kopf, and M. F. Bachmann. Complement receptors regulate differentiation of bone marrow plasma cell precursors expressing transcription factors Blimp-1 and XBP-1. *The Journal of Experimental Medicine*, 201(6):993–1005, 2005. 91

[37] A. Geffroy-Luseau, G. Jégo, R. Bataille, L. Campion, and C. Pellat-Deceunynck. Osteoclasts support the survival of human plasma cells. *International Immunology*, 20(6):775 –782, 2008. 13

[38] L. Genestier, M. Taillardet, P. Mondiere, H. Gheit, C. Bella, and T. Defrance. TLR agonists selectively promote terminal plasma cell differentiation of B cell subsets specialized in thymus-independent responses. *The Journal of Immunology*, 178(12):7779–7786, 2007. 4

[39] M. R. Gomez, Y. Talke, N. Goebel, F. Hermann, B. Reich, and M. Mack. Basophils support the survival of plasma cells in mice. *The Journal of Immunology*, 185(12):7180 –7185, 2010. 14, 103

[40] S. Gompertz and R. A. Stockley. Inflammation–role of the neutrophil and the eosinophil. *Seminars in Respiratory Infections*, 15(1):14–23, 2000. 1

[41] I. Gonzalez-Garcia, B. Rodriguez-Bayona, F. Mora-Lopez, A. Campos-Caro, and J. A. Brieva. Increased survival is a selective feature of human circulating antigen-induced plasma cells synthesizing high-affinity antibodies. *Blood*, 111(2):741–749, 2008. 13

[42] C. C. Goodnow, J. Sprent, B. F. de St Groth, and C. G. Vinuesa. Cellular and genetic mechanisms of self tolerance and autoimmunity. *Nature*, 435(7042):590–597, 2005. 8

[43] F. L. Graham, J. Smiley, W. C. Russell, and R. Nairn. Characteristics of a human cell line transformed by DNA from human adenovirus type 5. *Journal of General Virology*, 36(1):59–72, 1977. 32

[44] J. S. Greenberger, M. A. Sakakeeny, R. K. Humphries, C. J. Eaves, and R. J. Eckner. Demonstration of permanent factor-dependent multipotential (erythroid/neutrophil/basophil) hematopoietic progenitor cell lines. *Proc Natl Acad Sci USA*, 80(10):2931–2935, 1983. 93

[45] T. Hamada, R. Möhle, J. Hesselgesser, J. Hoxie, R. L. Nachman, M. A. Moore, and S. Rafii. Transendothelial migration of megakaryocytes in response to stromal cell-derived factor 1 (SDF-1) enhances platelet formation. *The Journal of Experimental Medicine*, 188(3):539 –548, 1998. 106

[46] R. R. Hardy, C. E. Carmack, S. A. Shinton, J. D. Kemp, and K. Hayakawa. Resolution and characterization of pro-B and pre-pro-B cell stages in normal mouse bone marrow. *The Journal of Experimental Medicine*, 173:1231, 1991. 3

[47] D. C. Hargreaves, P. L. Hyman, T. T. Lu, V. N. Ngo, A. Bidgol, G. Suzuki, Y. Zou, D. R. Littman, and J. G. Cyster. A coordinated change in chemokine responsiveness guides plasma cell movements. *The Journal of Experimental Medicine*, 194(1):45–56, 2001. 106

[48] A. E. Hauser, G. F. Debes, S. Arce, G. Cassese, A. Hamann, A. Radbruch, and R. A. Manz. Chemotactic responsiveness toward ligands for CXCR3 and CXCR4 is regulated on plasma blasts during the time course of a memory immune response. *The Journal of Immunology*, 169(3):1277–1282, 2002. 6, 11, 12, 68, 86

[49] U. Heider, L. C. Hofbauer, I. Zavrski, M. Kaiser, C. Jakob, and O. Sezer. Novel aspects of osteoclast activation and osteoblast inhibition in myeloma bone disease. *Biochemical and biophysical research communications*, 338(2):687–693, 2005. 13

[50] J. Hendriks, L. Planelles, J. de Jong-Odding, G. Hardenberg, S. T. Pals, M. Hahne, M. Spaargaren, and J. P. Medema. Heparan sulfate proteoglycan binding promotes APRIL-induced tumor cell proliferation. *Cell Death Differ*, 12(6):637–648, 2005. 12

[51] L. A. Herzenberg, J. Tung, W. A. Moore, L. A. Herzenberg, and D. R. Parks. Interpreting flow cytometry data: a guide for the perplexed. *Nature Immunology*, 7(7):681, 2006. 42

[52] F. Ho, J. E. Lortan, I. C. M. MaClennan, and M. Khan. Distinct short-lived and long-lived antibody-producing cell populations. *European Journal of Immunology*, 16(10):1297–1301, 1986. 91

[53] T. Hoefer, G. Muehlinghaus, K. Moser, T. Yoshida, H. E. Mei, K. Hebel, A. Hauser, B. Hoyer, E. O. Luger, T. Dörner, et al. Adaptation of humoral memory. *Immunological Reviews*, 211(1):295–302, 2006. 14, 102

[54] J. Holst, A. L. Szymczak-Workman, K. M. Vignali, A. R. Burton, C. J. Workman, and D. A. A. Vignali. Generation of T-cell receptor retrogenic mice. *Nature Protocols*, 1(1):406–417, 2006. 20, 93, 95

[55] M. G. House, L. Kohlmeier, N. Chattopadhyay, O. Kifor, T. Yamaguchi, M. S. Leboff, J. Glowacki, and E. M. Brown. Expression of an extracellular calcium-sensing receptor in human and mouse bone marrow cells. *Journal of Bone and Mineral Research*, 12(12):1959–1970, 1997. 97

[56] B. F. Hoyer. Short-lived plasmablasts and long-lived plasma cells contribute to chronic humoral autoimmunity in NZB/W mice. *Journal of Experimental Medicine*, 199(11):1577–1584, 2004. 66, 68, 91, 95, 100

[57] B. Huard, T. McKee, C. Bosshard, S. Durual, T. Matthes, S. Myit, O. Donze, C. Frossard, C. Chizzolini, C. Favre, R. Zubler, J. P. Guyot, P. Schneider, and E. Roosnek. APRIL secreted by neutrophils binds to heparan sulfate proteoglycans to create plasma cell niches in human mucosa. *Journal of Clinical Investigation*, 2008. 12

[58] G. Hutchinson. Concluding remarks, cold spring harbor symposium. In *Cold Spring Harbor Symposia on Quantitative Biology*, volume 22 of *2*, pages 415–427. Quant. Biol., 1957. 11

[59] K. Ingold, A. Zumsteg, A. Tardivel, B. Huard, Q. Steiner, T. G. Cachero, F. Qiang, L. Gorelik, S. L. Kalled, H. Acha-Orbea, P. D. Rennert, J. Tschopp, and P. Schneider. Identification of proteoglycans as the APRIL-specific binding partners. *The Journal of Experimental Medicine*, 201(9):1375–1383, 2005. 12

[60] T. Ishii and M. Ishii. Intravital two-photon imaging: a versatile tool for dissecting the immune system. *Annals of the Rheumatic Diseases*, 70 Suppl 1:i113–115, 2011. 108

[61] J. Jacob, G. Kelsoe, K. Rajewsky, and U. Weiss. Intraclonal generation of antibody mutants in germinal centres. *Nature*, 354(6352):389–392, 1991. 5

[62] H. Jasin. Scientific overview of systemic lupus erythematosus (SLE). *Prog Clin Biol Res*, 106:65–80, 1982. 1

[63] S. Jiang, J. D. Levine, Y. Fu, B. Deng, R. London, J. E. Groopman, and H. Avraham. Cytokine production by primary bone marrow megakaryocytes. *Blood*, 84(12):4151, 1994. 15

[64] K. Jöhrer, K. Janke, J. Krugmann, M. Fiegl, and R. Greil. Transendothelial migration of myeloma cells is increased by tumor necrosis factor (TNF)-β via TNF receptor 2 and autocrine up-Regulation of MCP-1. *Clinical Cancer Research*, 10(6):1901 –1910, 2004. 12

[65] R. P. Junghans and C. L. Anderson. The protection receptor for IgG catabolism is the beta2-microglobulin-containing neonatal intestinal transport receptor. *Proc Natl Acad Sci USA*, 93(11):5512–5516, 1996. 6

[66] T. Junt, H. Schulze, Z. Chen, S. Massberg, T. Goerge, A. Krueger, D. D. Wagner, T. Graf, J. E. Italiano, R. A. Shivdasani, and U. H. von Andrian. Dynamic visualization of thrombopoiesis within bone marrow. *Science*, 317(5845):1767–1770, 2007. 17

[67] M. K. Kaushansky. Thrombopoietin: Understanding and manipulating platelet production. *Annual Review of Medicine*, 48(1):1–11, 1997. 103

[68] M. A. Kacena, C. M. Gundberg, and M. C. Horowitz. A reciprocal regulatory interaction between megakaryocytes, bone cells, and hematopoietic stem cells. *Bone*, 39(5):978–984, 2006. 97

[69] M. A. Kacena, T. Nelson, M. E. Clough, S. Lee, J. A. Lorenzo, C. M. Gundberg, and M. C. Horowitz. Megakaryocyte-mediated inhibition of osteoclast development. *Bone*, 39(5):991–999, 2006. 97, 98

[70] A. Kaser, G. Brandacher, W. Steurer, S. Kaser, F. A. Offner, H. Zoller, I. Theurl, W. Widder, C. Molnar, O. Ludwiczek, M. B. Atkins, J. W. Mier, and H. Tilg. Interleukin-6 stimulates thrombopoiesis through thrombopoietin: role in inflammatory thrombocytosis. *Blood*, 98(9):2720–2725, 2001. 2, 96, 107

[71] K. Kaushansky. Thrombopoietin: the primary regulator of platelet production. *Blood*, 86(2):419–431, 1995. 93

[72] K. Kaushansky. The molecular mechanisms that control thrombopoiesis. *Journal of Clinical Investigation*, 115(12):3339–3347, 2005. 95

[73] K. Kaushansky, S. Lok, R. D. Holly, V. C. Broudy, N. Lin, M. C. Bailey, J. W. Forstrom, M. M. Buddle, P. J. Oort, F. S. Hagen, G. J. Roth, T. Papayannopoulou, and D. C. Foster. Promotion of megakaryocyte progenitor expansion and differentiation by the c-Mpl ligand thrombopoietin. *Nature*, 369(6481):568–571, 1994. 16, 18

[74] M. J. Kiel and S. J. Morrison. Uncertainty in the niches that maintain haematopoietic stem cells. *Nature Reviews Immunology*, 8(4):290–301, 2008. 10

[75] M. J. Kiel, O. H. Yilmaz, T. Iwashita, O. H. Yilmaz, C. Terhorst, and S. J. Morrison. SLAM family receptors distinguish hematopoietic stem and progenitor cells and reveal endothelial niches for stem cells. *Cell*, 121(7):1109–1121, 2005. 10

[76] H. J. Kim, V. Krenn, G. Steinhauser, and C. Berek. Plasma cell development in synovial germinal centers in patients with rheumatoid and reactive arthritis. *Journal of Immunology*, 162(5):3053–3062, 1999. 15

[77] R. Kim, M. Emi, K. Tanabe, and S. Murakami. Role of the unfolded protein response in cell death. *Apoptosis*, 11(1):5–13, 2006. 12

[78] M. H. Klinger and W. Jelkmann. Review: Role of blood platelets in infection and inflammation. *Journal of Interferon & Cytokine Research*, 22(9):913–922, 2002. 15

[79] M. Kozak. An analysis of 5'-noncoding sequences from 699 vertebrate messenger RNAs. *Nucleic Acids Research*, 15(20):8125–8148, 1987. 57

[80] M. Kozak. At least six nucleotides preceding the AUG initiator codon enhance translation in mammalian cells. *Journal of Molecular Biology*, 196(4):947–950, 1987. 57

[81] E. J. Kunkel and E. C. Butcher. Plasma-cell homing. *Nature Reviews Immunology*, 3(10):822–829, 2003. 6

[82] D. J. Kuter and R. D. Rosenberg. The reciprocal relationship of thrombopoietin (c-Mpl ligand) to changes in the platelet mass during busulfan-induced thrombocytopenia in the rabbit. *Blood*, 85(10):2720–2730, 1995. 96

[83] P. A. Lalor, G. J. Nossal, R. D. Sanderson, and M. G. McHeyzer-Williams. Functional and molecular characterization of single, (4-hydroxy-3-nitrophenyl)acetyl (NP)-specific, IgG1+ B cells from antibody-secreting and memory B cell pathways in the C57BL/6 immune response to NP. *European Journal of Immunology*, 22(11):3001–3011, 1992. 66

[84] Z. Li, M. Schwieger, C. Lange, J. Kraunus, H. Sun, E. van den Akker, U. Modlich, E. Serinsöz, E. Will, D. von Laer, et al. Predictable and efficient retroviral gene transfer into murine bone marrow repopulating cells using a defined vector dose. *Experimental hematology*, 31(12):1206–1214, 2003. 20, 93

[85] F. Mackay and P. Schneider. Cracking the BAFF code. *Nature Reviews Immunology*, 9(7):491–502, 2009. 87

[86] I. C. MacLennan. Germinal centers. *Annu Rev Immunol*, 12:117–131, 1994. 5

[87] I. C. MacLennan and C. G. Vinuesa. Dendritic cells, BAFF, and APRIL: innate players in adaptive antibody responses. *Immunity*, 17(3):235–238, 2002. 14, 103

[88] R. A. Manz, S. Arce, G. Cassese, A. E. Hauser, F. Hiepe, and A. Radbruch. Humoral immunity and long-lived plasma cells. *Current Opinion in Immunology*, 14(4):517–521, 2002. 7, 91

[89] R. A. Manz, A. E. Hauser, F. Hiepe, and A. Radbruch. Maintenance of antibody levels. *Annual Review of Immunology*, 23(1):367–386, 2005. 99

[90] R. A. Manz, M. Löhning, G. Cassese, A. Thiel, and A. Radbruch. Survival of long-lived plasma cells is independent of antigen. *International Immunology*, 10(11):1703–1711, 1998. 7, 66, 81, 104

[91] R. A. Manz, A. Thiel, and A. Radbruch. Lifetime of plasma cells in the bone marrow. *Nature*, 388(6638):133–134, 1997. 91, 99

[92] D. Markowitz, C. Hesdorffer, M. Ward, S. Goff, and A. Bank. Retroviral gene transfer using safe and efficient packaging cell lines. *Annals of the New York Academy of Sciences*, 612:407–414, 1990. 20, 36, 93

[93] M. G. McHeyzer-Williams and R. Ahmed. B cell memory and the long-lived plasma cell. *Current Opinion in Immunology*, 11:172–181, 1999. 6, 72

[94] R. McMillan, R. L. Longmire, R. Yelenosky, J. E. Lang, V. Heath, and C. G. Craddock. Immunoglobulin synthesis by human lymphoid tissues: Normal bone marrow as a major site of IgG production. *The Journal of Immunology*, 109(6):1386–1394, 1972. 11

[95] S. Meister, U. Schubert, K. Neubert, K. Herrmann, R. Burger, M. Gramatzki, S. Hahn, S. Schreiber, S. Wilhelm, M. Herrmann, et al. Extensive immunoglobulin production sensitizes myeloma cells for proteasome inhibition. *Cancer research*, 67(4):1783, 2007. 12, 13

[96] R. A. Mesa. How I treat symptomatic splenomegaly in patients with myelofibrosis. *Blood*, 113(22):5394 –5400, 2009. 98

[97] L. Michaelis and M. Menten. Die Kinetik der Invertinwirkung. *Biochemische Zeitung*, 49:333, 1913. 60, 94

[98] C. Mohan, L. Morel, P. Yang, and E. K. Wakeland. Genetic dissection of systemic lupus erythematosus pathogenesis: Sle2 on murine chromosome 4 leads to B cell hyperactivity. *The Journal of Immunology*, 159(1):454, 1997. 101, 108

[99] L. Morel, U. H. Rudofsky, J. A. Longmate, J. Schiffenbauer, and E. K. Wakeland. Polygenic control of susceptibility to murine systemic lupus erythematosus. *Immunity*, 1(3):219–229, 1994. 108

[100] K. Moser. *Grundlagen des Überlebens von Plasmazellen im autoimmunen (NZBxNZW)F1 Mausmodell des Systemischen Lupus Erythematodes*. Dissertation, Freie Universität Berlin, Berlin, 2008. 17, 66, 91, 101

[101] H. Nagahisa, Y. Nagata, T. Ohnuki, M. Osada, T. Nagasawa, T. Abe, and K. Todokoro. Bone marrow stromal cells produce thrombopoietin and stimulate megakaryocyte growth and maturation but suppress proplatelet formation. *Blood*, 87(4):1309–1316, 1996. 106

[102] T. Nagasawa. Microenvironmental niches in the bone marrow required for B-cell development. *Nature Reviews Immunology*, 6(2):107–116, 2006. 10

[103] Y. Nagata, H. Nagahisa, T. Nagasawa, and K. Todokoro. Regulation of megakaryocytopoiesis by thrombopoietin and stromal cells. *Leukemia*, 11 Suppl 3:435–438, 1997. 106

[104] X. Nie, S. Basu, and J. Cerny. Immunization with immune complex alters the repertoire of antigen-reactive B cells in the germinal centers. *European Journal of Immunology*, 27(12):3517–3525, 1997. 7

[105] Y. Nie, J. Waite, F. Brewer, M. Sunshine, D. R. Littman, and Y. Zou. The role of CXCR4 in maintaining peripheral B cell compartments and humoral immunity. *The Journal of Experimental Medicine*, 200(9):1145–1156, 2004. 11

[106] F. Nimmerjahn and J. V. Ravetch. Fcγ receptors as regulators of immune responses. *Nature Reviews Immunology*, 8(1):34–47, 2008. 6

[107] S. L. Nutt, D. Metcalf, A. D'Amico, M. Polli, and L. Wu. Dynamic regulation of PU.1 expression in multipotent hematopoietic progenitors. *The Journal of Experimental Medicine*, 201(2):221 –231, 2005. 16

[108] E. A. Obeng, L. M. Carlson, D. M. Gutman, W. J. Harrington, K. P. Lee, and L. H. Boise. Proteasome inhibitors induce a terminal unfolded protein response in multiple myeloma cells. *Blood*, 107(12):4907 –4916, 2006. 12

[109] B. P. O'Connor, M. W. Gleeson, R. J. Noelle, and L. D. Erickson. The rise and fall of long-lived humoral immunity: terminal differentiation of plasma cells in health and disease. *Immunological Reviews*, 194:61–76, 2003. 12, 87, 91

[110] M. Odendahl. Generation of migratory antigen-specific plasma blasts and mobilization of resident plasma cells in a secondary immune response. *Blood*, 105(4):1614–1621, 2005. 14, 107

[111] M. Odendahl, A. Jacobi, A. Hansen, E. Feist, F. Hiepe, G. R. Burmester, P. E. Lipsky, A. Radbruch, and T. Dörner. Disturbed peripheral B lymphocyte homeostasis in systemic lupus erythematosus. *The Journal of Immunology*, 165(10):5970 –5979, 2000. 91

[112] L. Pang, M. J. Weiss, and M. Poncz. Megakaryocyte biology and related disorders. *Journal of Clinical Investigation*, 115(12):3332–3338, 2005. 16, 17

[113] C. Patil and P. Walter. Intracellular signaling from the endoplasmic reticulum to the nucleus: the unfolded protein response in yeast and mammals. *Current Opinion in Cell Biology*, 13(3):349–355, 2001. 11

[114] D. Paus, T. G. Phan, T. D. Chan, S. Gardam, A. Basten, and R. Brink. Antigen recognition strength regulates the choice between extrafollicular plasma cell and germinal center B cell differentiation. *The Journal of Experimental Medicine*, 203(4):1081 –1091, 2006. 91

[115] N. Pelletier, M. Casamayor-Palleja, K. D. Luca, P. Mondiere, F. Saltel, P. Jurdic, C. Bella, L. Genestier, and T. Defrance. The endoplasmic reticulum is a key component of the plasma cell death pathway. *The Journal of Immunology*, 176(3):1340, 2006. 12, 13

[116] N. Pelletier, L. J. McHeyzer-Williams, K. A. Wong, E. Urich, N. Fazilleau, and M. G. McHeyzer-Williams. Plasma cells negatively regulate the follicular helper T cell program. *Nature Immunology*, 11(12):1110–1118, 2010. 6

[117] J. Przylepa, C. Himes, and G. Kelsoe. Lymphocyte developmente and selection in germinal centers. *Curr Top Microbiol Immunol*, 229:85–97, 1998. 8

[118] C. Putterman, B. Deocharan, and B. Diamond. Molecular analysis of the autoantibody response in peptide-induced autoimmunity. *The Journal of Immunology*, 164(5):2542 –2549, 2000. 91

[119] J. K. R J, G. A. Hair, K. G. Mann, and B. W. Grant. Characterization of human osteoblast and megakaryocyte-derived osteonectin (SPARC). *Blood*, 80(12):3112–3119, 1992. 97

[120] K. Rajewsky. Clonal selection and learning in the antibody system. *Nature*, 381(6585):751–758, 1996. 101

[121] J. V. Ravetch and M. Nussenzweig. Killing some to make way for others. *Nature Immunology*, 8(4):337–339, 2007. 14

[122] A. Ridderstad and D. M. Tarlinton. Kinetics of establishing the memory B cell population as revealed by CD38 expression. *The Journal of Immunology*, 160(10):4688 –4695, 1998. 83

[123] M. Roederer, A. Treister, W. Moore, and L. A. Herzenberg. Probability binning comparison: a metric for quantitating univariate distribution differences. *Cytometry*, 45(1):37–46, 2001. 42

[124] E. Roldán, A. García-Pardo, and J. A. Brieva. VLA-4-fibronectin interaction is required for the terminal differentiation of human bone marrow cells capable of spontaneous and high rate immunoglobulin secretion. *The Journal of Experimental Medicine*, 175(6):1739–1747, 1992. 13, 14

[125] M. L. Rose, M. S. Birbeck, V. J. Wallis, J. A. Forrester, and A. J. Davies. Peanut lectin binding properties of germinal centres of mouse lymphoid tissue. *Nature*, 284(5754):364–366, 1980. 40

[126] F. Sallusto, A. Lanzavecchia, K. Araki, and R. Ahmed. From vaccines to memory and back. *Immunity*, 33(4):451–463, 2010. 95

[127] A. Sapoznikov, Y. Pewzner-Jung, V. Kalchenko, R. Krauthgamer, I. Shachar, and S. Jung. Perivascular clusters of dendritic cells provide critical survival signals to B cells in bone marrow niches. *Nature Immunology*, 9(4):388–395, 2008. 11

[128] S. J. Saur, V. Sangkhae, A. E. Geddis, K. Kaushansky, and I. S. Hitchcock. Ubiquitination and degradation of the thrombopoietin receptor c-Mpl. *Blood*, 115(6):1254–1263, 2010. 94

[129] S. Scheding, M. Bergmann, A. Shimosaka, P. Wolff, C. Driessen, G. Rathke, K. Jaschonek, W. Brugger, and L. Kanz. Human plasma thrombopoietin levels are regulated by binding to platelet thrombopoietin receptors in vivo. *Transfusion*, 42(3):321–327, 2002. 95

[130] B. Schittek and K. Rajewsky. Maintenance of B-cell memory by long-lived cells generated from proliferating precursors. *Nature*, 346(6286):749–751, 1990. 7

[131] M. Shapiro-Shelef and K. Calame. Regulation of plasma-cell development. *Nature Reviews Immunology*, 5(3):230–242, 2005. 5

[132] K. Sheth and P. Bankey. The liver as an immune organ. *Current Opinion in Critical Care*, 7(2):99–104, 2001. 2, 107

[133] Y. Shimada, G. Migliaccio, H. Ralph, A. R. Migliaccio, and H. Shaw. Erythropoietin-specific cell cycle progression in erythroid subclones of the interleukin-3-dependent cell line 32D. *Blood*, 81(4):935–941, 1993. 94

[134] W. B. Slayton, D. A. Wainman, X. M. Li, Z. Hu, A. Jotwani, C. R. Cogle, D. Walker, R. C. Fisher, J. R. Wingard, E. W. Scott, and M. C. Sola. Developmental differences in megakaryocyte maturation are determined by the microenvironment. *Stem Cells*, 23(9):1400–1408, 2005. 103

[135] M. K. Slifka and R. Ahmed. Long-lived plasma cells: a mechanism for maintaining persistent antibody production. *Current Opinion in Immunology*, 10(3):252–258, 1998. 91

[136] M. K. Slifka, R. Antia, J. K. Whitmire, and R. Ahmed. Humoral immunity due to Long-Lived plasma cells. *Immunity*, 8(3):363–372, 1998. 91

[137] J. P. Smith, G. F. Burton, J. G. Tew, and A. K. Szakal. Tingible body macrophages in regulation of germinal center reactions. *Developmental Immunology*, 6(3-4):285–294, 1998. 6

[138] K. G. Smith, A. Light, G. J. Nossal, and D. M. Tarlinton. The extent of affinity maturation differs between the memory and antibody-forming cell compartments in the primary immune response. *The EMBO Journal*, 16(11):2996–3006, 1997. 91, 103

[139] K. G. C. Smith, T. D. Hewitson, G. J. V. Nossal, and D. M. Tarlinton. The phenotype and fate of the antibody-forming cells of the splenic foci. *European Journal of Immunology*, 26(2):444–448, 1996. 4

[140] K. E. Stein. Thymus-independent and thymus-dependent responses to polysaccharide antigens. *The Journal of Infectious Diseases*, 165 Suppl 1:S49–52, 1992. 5, 104

[141] S. Suematsu, T. Matsuda, K. Aozasa, S. Akira, N. Nakano, S. Ohno, J. Miyazaki, K. Yamamura, T. Hirano, and T. Kishimoto. IgG1 plasmacytosis in interleukin 6 transgenic mice. *Proc Natl Acad Sci USA*, 86(19):7547–7551, 1989. 12

[142] T. Sugiyama, H. Kohara, M. Noda, and T. Nagasawa. Maintenance of the hematopoietic stem cell pool by CXCL12-CXCR4 chemokine signaling in bone marrow stromal cell niches. *Immunity*, 25(6):977–988, 2006. 10

[143] R. Sungaran, B. Markovic, and B. Chong. Localization and regulation of thrombopoietin mRNA expression in human kidney, liver, bone marrow, and spleen using in situ hybridization. *Blood*, 89(1):101–107, 1997. 93

[144] D. M. Sze, K. Toellner, C. G. de Vinuesa, D. R. Taylor, and I. C. MacLennan. Intrinsic constraint on plasmablast growth and extrinsic limits of plasma cell survival. *The Journal of Experimental Medicine*, 192(6):813–822, 2000. 15, 66, 91, 99, 102, 103

[145] Y. Takahashi, H. Ohta, and T. Takemori. Fas is required for clonal selection in germinal centers and the subsequent establishment of the memory B cell repertoire. *Immunity*, 14(2):181–192, 2001. 7

[146] S. G. Tangye and D. M. Tarlinton. Memory B cells: Effectors of long-lived immune responses. *European Journal of Immunology*, 39(8):2065–2075, 2009. 7

[147] S. L. Teitelbaum. Bone resorption by osteoclasts. *Science*, 289(5484):1504 –1508, 2000. 97

[148] M. A. Thiede, S. L. Smock, D. N. Petersen, W. A. Grasser, D. D. Thompson, and S. K. Nishimoto. Presence of messenger ribonucleic acid encoding osteocalcin, a marker of bone turnover, in bone marrow megakaryocytes and peripheral blood platelets. *Endocrinology*, 135(3):929–937, 1994. 97

[149] G. J. Todaro and H. Green. Quantitative studies of the growth of mouse embryo cells in culture and their development into established lines. *The Journal of Cell Biology*, 17(2):299 –313, 1963. 32

[150] K. Tokoyoda, T. Egawa, T. Sugiyama, B. Choi, and T. Nagasawa. Cellular niches controlling B lymphocyte behavior within bone marrow during development. *Immunity*, 20(6):707–718, 2004. 10, 14, 106

[151] K. Tokoyoda, A. E. Hauser, T. Nakayama, and A. Radbruch. Organization of immunological memory by bone marrow stroma. *Nature Reviews Immunology*, 10(3):193–200, 2010. 10

[152] A. Tomer, L. A. Harker, and S. A. Burstein. Purification of human megakaryocytes by fluorescence-activated cell sorting. *Blood*, 70(6):1735–1742, 1987. 96

[153] W. Tong and H. F. Lodish. Lnk inhibits tpo–mpl signaling and tpo-mediated megakaryocytopoiesis. *The Journal of Experimental Medicine*, 200(5):569 –580, 2004. 94

[154] M. Tsuiji, S. Yurasov, K. Velinzon, S. Thomas, M. C. Nussenzweig, and H. Wardemann. A checkpoint for autoreactivity in human IgM+ memory B cell development. *The Journal of Experimental Medicine*, 203(2):393–400, 2006. 8

[155] A. M. Vannucchi, L. Bianchi, C. Cellai, F. Paoletti, R. A. Rana, R. Lorenzini, G. Migliaccio, and A. R. Migliaccio. Development of myelofibrosis in mice genetically impaired for GATA-1 expression (GATA-1low mice). *Blood*, 100(4):1123 –1132, 2002. 92, 98

[156] P. Vieira and K. Rajewsky. The half-lives of serum immunoglobulins in adult mice. *European Journal of Immunology*, 18(2):313–316, 1988. 6

[157] J. Villeval, K. Cohen-Solal, M. Tulliez, S. Giraudier, J. Guichard, S. A. Burstein, E. M. Cramer, W. Vainchenker, and F. Wendling. High thrombopoietin production by hematopoietic cells induces a fatal myeloproliferative syndrome in mice. *Blood*, 90(11):4369 –4383, 1997. 98

[158] C. G. Vinuesa, S. G. Tangye, B. Moser, and C. R. Mackay. Follicular B helper T cells in antibody responses and autoimmunity. *Nature Reviews Immunology*, 5(11):853–865, 2005. 6

[159] C. Wickenhauser, J. Lorenzen, J. Thiele, A. Hillienhof, K. Jungheim, B. Schmitz, M. L. Hansmann, and R. Fischer. Secretion of cytokines (interleukins-1 alpha, -3, and -6 and granulocyte-macrophage colony-stimulating factor) by normal human bone marrow megakaryocytes. *Blood*, 85(3):685–691, 1995. 15, 98

[160] O. Winter. *Megakaryozyten bilden eine funktionelle Komponente der Plasmazellnische im Knochenmark*. Dissertation, Technische Universität Berlin, Berlin, 2010. 106

[161] O. Winter, K. Moser, E. Mohr, D. Zotos, H. Kaminski, M. Szyska, K. Roth, D. M. Wong, C. Dame, D. M. Tarlinton, et al. Megakaryocytes constitute a functional component of a plasma cell niche in the bone marrow. *Blood*, 116(11):1867, 2010. 14, 19, 55, 81, 91, 93, 95, 96, 103, 105

[162] H. A. M. Wols, G. H. Underhill, G. S. Kansas, and P. L. Witte. The role of bone Marrow-Derived stromal cells in the maintenance of plasma cell longevity. *The Journal of Immunology*, 169(8):4213–4221, 2002. 14

[163] Z. Xiang, A. J. Cutler, R. J. Brownlie, K. Fairfax, K. E. Lawlor, E. Severinson, E. U. Walker, R. A. Manz, D. M. Tarlinton, and K. G. C. Smith. Fc?RIIb controls bone marrow plasma cell persistence and apoptosis. *Nature Immunology*, 8(4):419–429, 2007. 4, 12

[164] Z. Xu, B. Duan, B. P. Croker, E. K. Wakeland, and L. Morel. Genetic dissection of the murine lupus susceptibility locus Sle2: contributions to increased peritoneal B-1a cells and lupus nephritis map to different loci. *The Journal of Immunology*, 175(2):936, 2005. 101

[165] X. Q. Yan, D. Lacey, D. Hill, Y. Chen, F. Fletcher, R. G. Hawley, and I. K. McNiece. A model of myelofibrosis and osteosclerosis in mice induced by overexpressing thrombopoietin (mpl ligand): reversal of disease by bone marrow transplantation. *Blood*, 88(2):402–409, 1996. 18

[166] J. Zhang, C. Niu, L. Ye, H. Huang, X. He, W. Tong, J. Ross, J. Haug, T. Johnson, J. Q. Feng, S. Harris, L. M. Wiedemann, Y. Mishina, and L. Li. Identification of the haematopoietic stem cell niche and control of the niche size. *Nature*, 425(6960):836–841, 2003. 9

[167] M. Ziegner, G. Steinhauser, and C. Berek. Development of antibody diversity in single germinal centers: selective expansion of high-affinity variants. *European Journal of Immunology*, 24(10):2393–2400, 1994. 5

6. Appendix

Publications

- O. Winter, K. Moser, E. Mohr, D. Zotos, H. Kaminski, **M. Szyska**, K. Roth, D.M. Wong, C. Dame, D.M. Tarlinton, et al. Megakaryocytes constitute a functional component of a plasma cell niche in the bone marrow. *Blood*, 116(11):1867, 2010.

- G. Cassese, S. Arce, A.E. Hauser, K. Lehnert, B. Moewes, M. Mostarac, G. Mühlinghaus, **M. Szyska**, A. Radbruch, and R.A. Manz. Plasma cell survival is mediated by synergistic effects of cytokines and adhesion-dependent signals. *The Journal of Immunology*, 171(4):1684-1690, 2003

Posters

- M. Szyska, et al. Interplay between megakaryopoiesis and plasma cell homeostasis. *2^{nd} European Congress of Immunology*, Berlin, September 2009

- M. Szyska et al. Long-lived Plasma Cells in the Bone Marrow Niche. *Joint Annual Meeting of Immunology, ÖGAI, Wien, September 2008*

- M. Szyska et al. Long-lived Plasma Cells in the Bone Marrow Niche. *3^{rd} ENII–MUGEN Summer School in Advanced Immunology*, Sardinia, May 2008

Danksagung

Ich möchte hiermit allen Personen danken, die mich über all diese Jahre unterstützt haben und daran geglaubt haben, dass diese Arbeit einmal fertig sein wird.

Zuallererst gilt es, meinem Betreuer Rudi Manz zu danken, der mich stets unterstützt hat und der mir viele Jahre ein wissenschaftliches Zuhause geboten hat und dies auch aus der Ferne.

Weiterhin gilt mein Dank allen Mitarbeitern der AG Orphan, die mich unterstützt, ausgehalten und zum Lachen gebracht haben. Vor allem danke ich Katrin, mit der ich einen langen Weg zusammen gegangen bin und die all meine zahlreichen Fragen gerne beantwortet hat.

Ferner danke ich allen Mitarbeitern, Diplomanden und Doktoranden, die zusammen diese einmalige DRFZ-Atmosphäre erzeugt haben, die ich wohl vermissen werde.

Für Korrekturen und Anmerkungen danke ich Rudi, Katrin und Arthur.

Und zu guter letzt gilt mein größter Dank meiner Franzi. Du warst sehr tapfer und hast mir viel Kraft gegeben!

Erklärung

Berlin, den 28.04.2011

Ich, Martin Szyska, versichere an Eides statt, dass ich die vorliegende Dissertation selbstständig verfasst und keine anderen als die angegebenen Hilfsmittel verwendet habe. Wörtlich oder inhaltlich entnommene Stellen sowie Abbildungen aus benutzten Quellen wurden als solche gekennzeichnet. Die Arbeit wurde in dieser oder ähnlicher Form noch keiner Prüfungskommission vorgelegt.

Martin Szyska

Abbreviations

APRIL	a proliferation-inducing ligand; also known as TNFSF13
ASC	antibody secreting cell
BAFF	B cell-activating factor belonging to the TNF family; also known as BLyS, TALL-1, zTNF4, THANK, and TNFSF13B
BCMA	B cell maturation antigen; also known as TNF receptor superfamily member 17 (TNFRSF17)
BCR	B-cell receptor
BMEC	bone marrow endothelial cell
BrdU	5-bromodeoxyuridine
BSA	bovine serum albumin
CD	cluster of differentiation
cDM	conditioned DMEM (see composition here)
CLP	common lymphoid progenitor
CMP	common myeloid progenitor
CSR	class switch recombination
DAPI	4',6-diamidino-2-phenylindole
DNA	deoxyribonucleic acid
EDTA	ethylenediaminetetraacetic acid
eGFP	enhanced GFP
ELISA	enzyme-linked immunosorbent assay
ELISPOT	enzyme-linked immunosorbent spot
FACS	fluorescence activated cell sorting (also used as a synonym for flow cytometry)
5-FU	5-fluorouracil
FcγR	Fcγ-receptor

FcR	Fc-receptor
FCS	fetal calf serum
FDC	follicular dendritic cell
GC	germinal center
GEP	global expression profiling
GFP	green fluorescent protein
GM-CSF	granulocyte monocyte colony-stimulating factor
HPRT	hypoxanthine-guanine phosphoribosyltransferase
HSC	hematopoietic stem cell
Ig	immunoglobulin
Ig κ	Ig kappa light chain
IL	interleucin
LCM	laser capture microdissection
LTR	long terminal repeat
MEP	MK-erythroid progenitor
MHC	major histocompatibility complex
MM	multiple myeloma
MMLV	Moloney murine leukemia virus
MSC	multiple cloning site
NZB	New Zealand Black
NZB/W	(New Zealand Black x New Zealand White)F1
OPG	osteoprotegerin
Ova	ovalbumin
PAMP	pathogen-associated molecular pattern
PBS	phosphate buffered saline
PCR	polymerase chain reaction

PDGF	platelet-derived growth factor
PNA	peanut agglutinin
PRR	pattern recognition receptor
RANKL	osteoclastogenic receptor activator of NF-κB ligand
rt	room temperature
RT	reverse transcription
SA-AP	streptavidine coupled to alkaline phospatase
SCF	stem cell factor; also known as steel factor
SDF-1	stromal cell-derived factor 1; also known as CXCR12
SFM	serum-free medium
SHM	somatic hypermutation
SLE	systemic lupus erythematosus
TACI	transmembrane activator and CAML interactor; also known as TNF receptor superfamily member 13B (TNFRSF)
TCR	T-cell receptor
T_{FH}	T follicular helper cell
TGF-β	transforming growth factor
TLR	Toll-like receptor
TNF	tumor necrosis factor
TPO	thrombopoietin
UPR	unfolded protein response
VCAM-1	vascular cell adhesion molecule 1; also known as CD106
VEGF	vascular endothelial growth factor
VLA-4	very late antigen 4; also known as integrin $\alpha_4\beta_1$

List of Figures

List of Tables